2013-11-21

Masonry Walls Strengthened with Fabric-Reinforced Cementitious Matrix Composite Subjected to In-Plane and Out-of-Plane Load

Saman Babaeidarabad
University of Miami, sbaba005@fiu.edu

UNIVERSITY OF MIAMI

MASONRY WALLS STRENGTHENED WITH FABRIC-REINFORCED CEMENTITIOUS MATRIX COMPOSITE SUBJECTED TO IN-PLANE AND OUT-OF-PLANE LOAD

By

Saman Babaeidarabad

A DISSERTATION

Submitted to the Faculty
of the University of Miami
in partial fulfillment of the requirements for
the degree of Doctor of Philosophy

Coral Gables, Florida

December 2013

UNIVERSITY OF MIAMI

A dissertation submitted in partial fulfillment of
the requirements for the degree of
Doctor of Philosophy

MASONRY WALLS STRENGTHENED WITH FABRIC-REINFORCED CEMENTITIOUS MATRIX COMPOSITE SUBJECTED TO IN-PLANE AND OUT-OF-PLANE LOAD

Saman Babaeidarabad

Approved:

_____ Antonio Nanni, Ph.D. Professor and Chair of Civil, Architectural & Environmental Engineering	_____ Amir Rahmani, Ph.D. Assistant Professor of Mechanical & Aerospace Engineering
_____ Carol Hays, Ph.D. Associate Profesor in Practice of Civil, Architectural & Environmental Engineering	_____ Matthew Jacob Trussoni, Ph.D. Assistant Professor in Practice Civil, Architectural & Environmental Engineering
_____ Francisco J. De Caso y Basalo, Ph.D. Lecturer of Civil, Architectural & Environmental Engineering	_____ M. Brian Blake, Ph.D. Dean of the Graduate School

BABAEIDARABAD, SAMAN (Ph.D., Civil Engineering)
Masonry Walls Strengthened with (December 2013)
Fabric-Reinforced Cementitious Matrix
Composite Subjected to In-Plane and Out-of-Plane Load

Abstract of a dissertation at the University of Miami.

Dissertation supervised by Professor Antonio Nanni.
No. of pages in text. (134)

A natural evolution of ferrocement has been the replacement of the reinforcing steel with new composite materials. Not only has this addressed the issue of possible durability problems associated with steel corrosion, but has opened the possibility of using thin-section cementitious products as repair materials. Fabric-reinforced cementitious matrix (FRCM) is a class of composite systems that has recently emerged as an alternative to traditional retrofitting methods like fiber-reinforced polymers (FRP), steel plate bonding, section enlargement, and external post-tensioning for repairing and strengthening reinforced concrete (RC) and masonry structures. FRCM consists of a reinforcing phase (fabrics) embedded into a matrix (cementitious mortar) adhered to concrete or masonry structural members and acts as supplemental, externally-bonded reinforcement.

The goal of this dissertation is to experimentally and analytically investigate the effectiveness of FRCM to retrofit existing masonry structures; to evaluate the flexural and shear capacity of FRCM walls; to develop structural design procedures; and, to compare FRCM and FRP externally strengthened masonry walls.

The dissertation is articulated in three studies. The first study (Study 1) investigates masonry walls externally strengthened with FRCM subjected to diagonal compression; the second (Study 2) focuses on FRCM strengthened walls subjected to out-of-plane loading; and the third (Study 3) presents a comparison between experimental results in this research program and other research programs using FRP systems when the normalized shear or flexural capacity is related to a calibrated reinforcement ratio.

To my Mom and Dad
for their unconditional love,
support and guidance

To my Brother and Sisters
for their real friendship

To Professor Nanni
who gave me this chance
and opportunity

ACKNOWLEDGEMENTS

Throughout the journey of this research, I have been accompanied by numerous individuals. These few lines are not enough to thank to those who gave me the support and cooperation to complete this research project.

First of all, I would like to thank my advisor, Dr. Antonio Nanni, whose continuous support, encouragement and guidance made this voyage possible and a worthwhile experience. I can only hope one day to be for someone what he has been for me.

Many thanks go to Dr. Carol Hays, Dr. Francisco De Caso, and Dr. Amir Rahmani for their kindness of being on my committee.

Special thanks go to Dr. Francisco De Caso who helped me throughout of this project, and Dr. Carol Hays whose experience and knowledge contributed to make this work much better.

I gratefully acknowledge the National Science Foundation (NSF) for the support provided to the Industry/University Center for Integration of Composites into Infrastructure (CICI) at the University of Miami under grant IIP-0933537 and its industrial member Ruredil S.p.A., San Donato Milanese, Italy. I also thank Titan America Inc., Medley, FL for their support to this research. I hope my research has been worthy of their investment.

Last, I am greatly indebted to my Parents, Shakour and Fooroogh, to my Brother, Soheil, to my sisters, Nasim and Sharareh, for their unconditional love and guidance without which I would never have made it through.

TABLE OF CONTENTS

LIST OF FIGURES

LIST OF TABLES

CHAPTER I
INTRODUCTION

Masonry is one of the oldest construction materials. For thousands of years masonry was the predominant building material until modern materials such as concrete and steel appeared in the nineteenth century. Un-reinforced masonry (URM) structures comprise a large portion of the world's built stock; as such, it is an important target for new repair and rehabilitation methods aimed at conservation and structural life extension. Masonry is a building technology that meets many of the attributes of sustainable construction; therefore, efforts devoted to the improvements of existing masonry structures in terms of safety and performance can help practitioners and ultimately society in meeting the goals of a cultural shift towards economical, environmentally-sound and socially-acceptable building solutions.

Overloading, dynamic vibrations, settlement, and in-plane and out-of-plane deformations generally caused by earthquakes or wind can cause failure of masonry structures. Organizations such as The Masonry Society (TMS) and the Federal Emergency

Management Agency (FEMA) have identified that collapse of URM walls during earthquakes is a leading cause of property damage and loss of human life more than any other type of structural failure (Tumialan et al. 2003). URM walls are not well-suited to withstand in-plane and out-of-plane loading and may exhibit brittle failure mode followed by scattering of debris; therefore, retrofitting of these structures is urgently needed to ensure their continued working and safe conditions. Over the past two decades, in the United States and Europe, large investments have been directed to retrofitting projects. Conventional strengthening techniques were often time-consuming, costly, and added significant weight to the structure.

By the late 1980s, fiber-reinforced polymer (FRP) systems were researched and developed worldwide by the construction industry for infrastructure strengthening and repair due to deterioration from lack of maintenance, poor design, and more stringent code provisions (Bakis et al. 2002). Retrofitting of URM masonry walls with FRP is one of the most recent and common techniques. The use of FRP composites of various organic matrices and fiber compositions have proven to be highly effective in enhancing the shear and flexural strength, and pseudo-ductility of masonry structures (Tinazzi 2000; Tumialan et al. 2001; Morbin 2002; Nanni et al. 2003; Grando et al. 2003; Li et al. 2005; Hrynyk 2006; Yu et al. 2007; Silva et al. 2008; Petersen 2009; Myers 2011). The popularity of FRP reinforcement is due to its effectiveness, lightweight, ease of application, and availability in different forms such as laminates, sheets, grids, and bars. FRP reinforcement does not experience the common corrosion problems which are

typically associated with conventional steel reinforcement (fib bulletin 2001; Al-Salloum et al. 2012).

Although the use of epoxy has proven to give excellent performances both in terms of bonding and durability, externally-bonded FRP with epoxy has some drawbacks, such as: inability of applying FRP to a damp substrate; poor behavior of the resin at temperatures above the glass transition temperature; poorfire resistance, low reversibility; and, lack of vapor permeability (Triantafillou 2006; Papanicolaou et al. 2007; D'Ambrisi and Focacci 2011; Ombres 2011; Al-Salloum et al. 2012; ACI 549 2013). Since these limitations are mainly related to the organic binder, one solution is to replace the organic binder (e.g., epoxy) with an inorganic one (e.g., cementitious matrix). Accordingly, a composite made of cement-based matrix reinforced by continuous dry-fiber fabric termed fiber-reinforced-cementitious matrix (FRCM) was proposed to address these disadvantages. FRCM like reinforced concrete (RC) depends on composition, specific constituent, curing, and many other parameters. FRCM has been presented in the technical literature for both new construction and repair using different acronyms: textile reinforced mortar (TRM) (Bisby et al. 2009; Triantafillou and Papanicolau 2006; Al-Salloum et al. 2012); textile-reinforced concrete (TRC) (Banholzer et al. 2006; Brückner et al. 2006; Hartig et al. 2008; Hegger et al. 2006; Peled 2007; Wiberg 2003; Zastrau et al. 2008), mineral-based composites (MBC) (Blanksvärd et al. 2009); or fiber-reinforced cement (FRC) (Wu and Sun 2005).

Specifically, previous studies have addressed the use of externally-bonded FRCM composites to retrofit reinforced-concrete (RC) elements and masonry walls to improve flexural and shear capacity (Faella et al. 2004; Prota et al. 2006; Papanicolaou et al. 2007; D'Ambrisi 2011; Ombres 2011; Al-Salloum et al. 2012; Babaeidarabad et al. 2013; Loreto et al. 2013).

DISSERTATION OUTLINE

Articulated in three studies, this dissertation investigates the in-plane and out-of-plane structural behavior of concrete masonry unit (CMU) and clay brick masonry walls retrofitted externally with two levels of FRCM. A comparison with results available in the literature for FRP strengthening is also presented. The three studies resulted in nine papers submitted to peer reviewed journals or presented at conferences, as reported in **Figure 1**. The first study, *Study 1*, assesses the structural performance of 18 concrete and clay masonry walls strengthened with FRCM on both faces of the wall when subjected to an in-plane diagonal force; the second study, *Study 2*, is devoted to out-of-plane behavior of concrete and clay masonry walls strengthened by applying extreme amounts of FRCM suggested by Acceptance Criteria for masonry and RC concrete structures (AC434) using one and four plies on the tension side; and *Study 3*, compares the effectiveness of FRCM strengthening technique with traditional FRP systems when experimental results are normalized and related to a calibrated reinforcement ratio.

Study 1 titled "URM walls strengthened with FRCM subjected to diagonal compression" produces new experimental evidence by testing under diagonal compression 18 masonry

walls of which nine are made of clay bricks and nine of CMU blocks. This setup is referred to as in-plane loading. For each set of walls, three are control specimens, three are strengthened with 1-ply FRCM on both sides, and three are strengthened with 4-ply FRCM in the same fashion. The effect of FRCM on the shear capacity, pseudo-ductility, and failure mode are discussed.

Study 2 titled “Out-of-plane behavior of URM walls strengthened with FRCM” describes an experimental campaign on a total of 18 CMU and clay brick masonry walls strengthened with 1-ply and 4-ply FRCM applied to the tension side only. The same test matrix of Study 1 is used here for walls subjected to lateral uniformly-distributed pressure. This setup is referred to as out-of-plane loading. The effects of FRCM on the flexural capacity and failure mode are analyzed.

Study 3 titled “Comparison between FRCM and FRP strengthened walls” demonstrates the similarity of FRCM and FRP systems on improving the flexural and shear capacity of CMU and clay walls based on the results of this project and other research programs. It is shown that these two retrofitting systems provide similar enhancements if normalized against the calibrated reinforcement ratio.

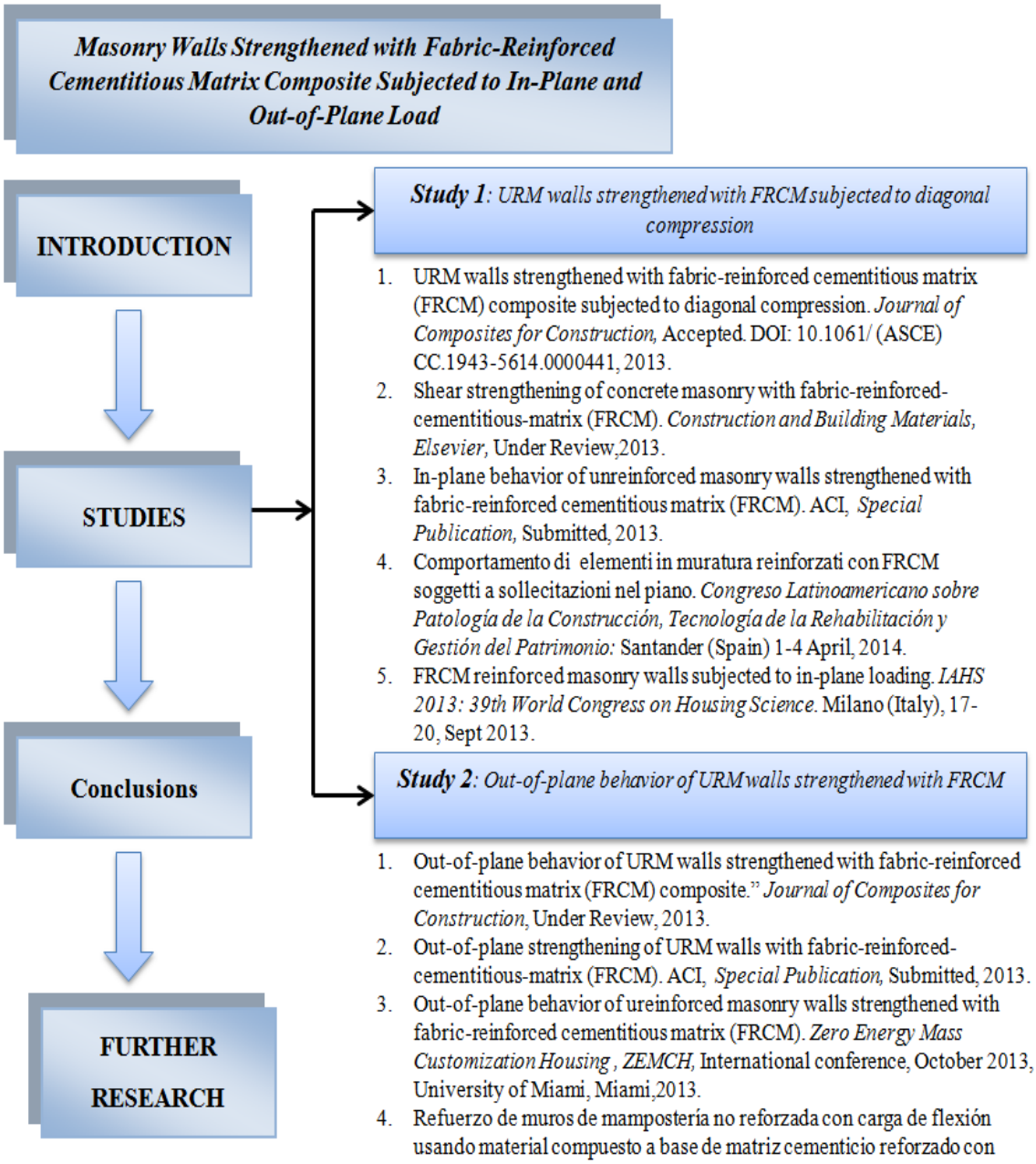

Figure 1- Dissertation and outcomes

OBJECTIVES

Study 1 aims to:

(a) describe specimen fabrication, FRCM installation, in-plane test setup, and test procedures;

(b) interpret the experimental test results and failure mechanisms;

(c) understand the contribution of FRCM on improving the shear strength, stiffness, and pseudo-ductility of masonry walls; and,

(d) develop an analytical model based on ACI 549 (2013) to compute shear capacity of retrofitted masonry walls and compare its results with the experimental database.

Study 2 aims to:

(a) illustrate the specimen construction, FRCM installation, out-of-plane test setup, and test methods;

(b) explore the effectiveness of the externally-bonded FRCM to retrofit masonry walls under out-of-plane load;

(c) evaluate whether the FRCM is able to increase flexural capacity and deformability of masonry walls;

(d) analyze the test results and failure mechanisms of the failure mode; and,

(e) develop an analytical model as per ACI 549 (2013) to predict flexural strength of the walls and compare its results with experimental results.

Study 3 aims to:

(a) report experimental test results under out-of-plane and in-plane loading of CMU and clay walls retrofitted with FRP systems from other research programs; and,

(b) compare the effectiveness of FRCM and FRP on shear and flexural capacity in CMU and clay brick masonry walls vs. the calibrated reinforcement ratio index.

RESEARCH SIGNIFICANCE

Although masonry is one of the oldest construction materials, its behavior has not been investigated as extensively as other construction materials. Masonry is a building technology that meets many of the attributes of sustainable construction. An economical alternative solution rather than demolish-rebuild culture for the masonry stock is to retrofit with novel composite strengthening systems. From the sustainability prospective, a newly developed rehabilitation technology improves existing masonry structure in terms of safety and performance by addressing economic, technological, and environmental issues. Recent world events have demonstrated that safety of masonry subject to extreme in-plane and out-of-plane loads are an ever growing concern. Un-reinforced masonry (URM) walls have shown to have low shear and flexural strength to withstand in-plane and out-of-plane loads generally caused by earthquakes and wind.

During the past two decades, the use of FRP reinforcement was particularly attractive for retrofitting of RC members and masonry structures (Sharif et al. 1994; Arduini 1997; Spadea et al. 1998; El-Mihilmy 2000; Tinazzi 2000; fib bulletin 2001; Tumialan et al. 2001; Morbin 2002; Grando et al. 2003; Nanni et al. 2003; El-Hacha 2004; Li et al. 2005;

Toutanji 2007; Yu et al. 2007; Silva et al. 2008; Myers 2011; Al-Salloum et al. 2012). Despite of all of its benefits in terms of increasing the strength and deformability, the use of FRP composites of various organic matrices and fiber compositions has shown some limitations, namely: inability to install FRP on damp substrate; poor behavior of the resin at temperatures above its glass transition temperature; and, lack of vapor permeability (Triantafillou 2006; Papanicolaou et al. 2007; Al-Salloum et al. 2012; ACI 549 2013).

FRCM has emerged as an alternative external retrofit technology to address these draw backs. The potential of externally-bonded FRCM composites is to solve some limitations attributed to FRP while improving the structural performance of masonry walls (Babaeidarabad et al. 2013).

Many studies have addressed in-plane and out-of-plane performance of masonry walls strengthened with FRP (Essaway 1986; Ehsani et al. 1994; Velazquez-Dimas 1998; Tinazzi 2000; Tumialan et al. 2001; Morbin 2002; Nanni et al. 2003; Grando et al. 2003; Li et al. 2005; Yu et al. 2007; Silva et al. 2008; Petersen 2009; Myers 2011; Dizhur et al. 2013), while limited research has explored alternative rehabilitation systems such as fabric embedded within inorganic matrices (Faella et al. 2004; Prota et al. 2006; Papanicolaou et al. 2007).

Based on the experimental and analytical outcomes, this project will contribute to the efforts of the worldwide research community by providing a deeper understanding of the behavior of FRCM, in particular its ability to increase the shear and flexural capacity of

the masonry wall. The interest and funding of private and government agencies, such as the National Science Foundation (NSF) through the support provided to the Industry/University Center for Integration of Composites into Infrastructure (CICI), reflect the significance of the work presented herein.

CHAPTER II

*STUDY 1_* URM WALLS STRENGTHNED WITH FRCM SUBJECTED TO DIAGONAL COMPRESSION

In this study, the FRCM system is applied to URM walls to determine its feasibility as an alternative external strengthening technology. The experimental program consists of testing a total of eighteen CMU and clay brick walls under diagonal compression. Two FRCM strengthening reinforcement schemes are applied, namely: one and four plies of reinforcement fabrics. An analytical model as per ACI 549 (2013) is used to calculate the shear capacity of strengthened URM walls and compare its results with the experimental database. The effect of limitations according to ACI 549 (2013) in design approach on shear capacity of strengthened walls is discussed.

BACKGROUND

URM walls exhibit vulnerability when subjected to in-plane loading. In-plane resistance of URM walls is based on the mortar strength and CMU/brick properties. If the loads are high enough to exceed the in-plane strength capacity of the wall, a failure will occur. The failure mode is generally identified by brittle tensile cracking through the mortar and the masonry unit. **Figure 2** shows in-plane failures of load-bearing walls resulted from an earthquake in Umbria, Italy on September 1997.

Depending on the masonry physical and mechanical properties, the failure modes of URM walls subjected to in-plane diagonal compression as identified by previous tests (Li et al. 2005; Silva et al. 2008; Parisi et al. 2012) and ACI 440.7R (2010), are: diagonal tensile cracking, joint sliding, and toe crushing. Diagonal tensile cracking typically occurs with the formation of a single diagonal crack through concrete masonry units. Shear sliding can form along a single mortar bed joint or along multi-bed and head joints in a step format. Toe crushing failure consists of masonry crushing at the compressed corners.

Since most masonry structures are not in compliance with recent building code provisions, retrofit of existing URM walls is urgently needed to ensure their continued safe working conditions. The use of fiber-reinforced polymer (FRP) composites of various organic matrices and fiber compositions have proven to be highly effective in enhancing the shear resistance and pseudo-ductility of masonry structures (Tinazzi 2000;

Tumialan et al. 2001; Morbin 2002; Nanni et al. 2003; Grando et al. 2003; Li et al. 2005; Yu et al. 2007; Silva et al. 2008; Myers 2011).

Tinazzi (2000) and Morbin (2002) carried out an experimental program applying diagonal compression to clay brick walls retrofitted by embedding glass FRP (GFRP) bars in the mortar joints, known as near-surface mounted (NSM) technique, and adhering external GFRP laminates. These strengthening systems resulted in significantly improved in-plane behavior in terms of load carrying capacity and pseudo-ductility. Likewise, Tumialan (2001) and Li et al. (2005) performed experimental testing under in-plane diagonal compression on concrete masonry walls after strengthening with different schemes of GFRP NSM bars and externally-bonded GFRP strips. Test results showed that FRP effectively increased shear capacity of masonry walls. Similarly, Grando et al. (2003) tested CMU and clay brick masonry walls strengthened with GFRP NSM bars, GFRP and carbon FRP (CFRP) laminates under diagonal compression. These two retrofit systems improved URM structural performance. Yu et al. (2007) tested CMU and clay brick URM walls strengthened with GFRP grid reinforced polyurea with different strengthening schemes subjected to diagonal compression. The results showed significant gain of shear capacity in the strengthened masonry walls.

The popularity of FRP reinforcement is due to its effectiveness, lightweight, ease of application, and availability in different forms such as pre-cured laminates, sheets, grids, and bars (see **Figure 3)**. FRP reinforcement does not experience the common corrosion

problems which are typically associated with conventional steel reinforcement (fib bulletin 2001; Al-Salloum et al. 2012).

Prota et al. (2006) and Parisi et al. (2012) carried out comprehensive experimental testing on tuff masonry walls strengthened externally with different layouts of FRCM under in-plane diagonal compression. Experimental evidence showed that significant improvements on strength and pseudo-ductility were achieved. Papanicolaou et al. (2007) studied the effectiveness of carbon-FRCM to retrofit perforated fired clay brick or solid stone block walls under in-plane lateral and out-of-plane cyclic loading. Test results again showed that FRCM provided a substantial gain in strength and pseudo-ductility.

Notwithstanding studies carried out to investigate the effectiveness of FRCM for masonry strengthening (Prota et al. 2006; Papanicolaou et al. 2007; Parisi et al. 2012), experimental and analytical research is still needed to fully characterize FRCM and quantify its contribution to strength and pseudo-ductility enhancements as a function of fiber type, cementitious matrix type and quality and conditions of the substrate.

This study is an attempt to contribute to the existing knowledge for the case of CMU and clay masonry strengthened with FRCM and subject to diagonal compression. The FRCM consists of a sequence of one or four layers of carbon fabric applied to both faces of a wall using a cementitious mortar reinforced with short zirconium fibers. Finally, ACI 549 (2013) is used to compute shear capacity and considerations are offered on its applicability.

EXPERIMENTAL PROGRAM

URM Specimens

The experimental test matrix for this study consisted of 18 URM walls made of concrete block and clay brick with dimension of 1220 x 1220 x 92 mm (48 x 48 x 3.63 in) and 1145 x 1220 x 92 mm (45 x 48 x 3.63 in), respectively. URM walls were fabricated in a running bond pattern by a professional mason to ensure quality and consistency of workmanship. The retrofitted URM walls were externally strengthened by applying two amounts of FRCM: 1-ply and 4-ply reinforcements with full coverage of both faces of the wall. The strengthening system installation procedure involved the following steps: a first layer of mortar with the thickness of 5 mm (0.2 in) was applied to the masonry. 1-ply FRCM of pre-cut carbon fabric was laid next, and the second layer of mortar with the same thickness was applied and finished. The fabric was applied in two pre-cut size with dimension of 1016 mm (40 in) and 356 mm (14 in), having 152 mm (6 in) overlap (see **Figure 4**).

The identification system used for the test specimens describes each set of specimens in the experimental program. The specimen code is made up of two parts: masonry material (CMU for concrete block and CL for clay brick) and amount of reinforcement (control, 1, and 4). Three repetitions are tested for each set of walls. **Table 1** consists of four columns: Column (1) identifies the specimen code. Columns (2) and (3) identify the strengthening material and the masonry type, respectively. Column (4) identifies the number of replicates used for each set of walls.

Material Characterization

The nominal dimensions of concrete block and clay brick units used in the construction of the walls were 102 x 203 x 406 mm (4 by 8 by 16 in) with a net area of 24,322 mm^2 (38 in^2) and 203x 68 x102 mm (8 x 2 2/3 x 4 in) with a net area of 13,548 mm^2 (21 in^2), respectively (**Figure 5**). A type M mortar was used to build all the walls with a nominal mortar thickness between units of about 10 mm (0.38 in). Mortar compressive strength was obtained by testing 50-mm (2-in) mortar cubes according to ASTM C109 (2012). After 28 days, the average strength of the mortar was found to be 22 MPa (3,193 psi) with a coefficient of variation (C.O.V.) equal to 5.2% (Babaeidarabad et al. 2013). The failure of cube mortar is shown in **Figure 6**. Masonry prisms were constructed with three standard concrete blocks or clay bricks. The prisms were match-cured with the wall specimens and were tested in accordance with ASTM C1314 (2012). The average compressive strength of the CMU and clay brick prism was found to be 19 MPa (2,823psi) with C.O.V. equal to 5.9%, and 24 MPa (3,553 psi) with C.O.V. equal to 3.4%, respectively (Babaeidarabad et al. 2013). **Figure 7** (a) and (b) illustrate CMU and clay brick prisms at the failure, respectively.

FRCM was composed of a sequence of one or four layers of cement-based matrix reinforced with dry-fiber fabrics. The cementitious mortar was composed of Portland cement, silica fume, short zirconium fiber, and fly ash acting as the inorganic binder. The fabric consisted of a balanced network of carbon fiber toes disposed along two orthogonal directions at a nominal spacing of 10 mm (0.394 in). The equivalent nominal fiber thickness was 0.048 mm (0.0019 in) in both primary and secondary directions, as

shown in **Figure 8.** Arboleda (2012) tested FRCM coupons to characterize the tensile properties of this composite as follows:

- Coupons having dimensions of 410 x 51x 10 mm (16 x 2 x 0.4 in) were cut from FRCM panels with a nominal surface area of 410 x 560 mm (16 x 22 in). 152 mm (6 in) steel metal tabs with clevis openings were bonded with glue to both ends of the coupon.

- Panels were made in a flat mold by applying the first layer of mortar at a nominal thickness of 5 mm (0.2 in). A ply of pre-cut carbon fabric was laid next, and later matrix was applied on top of the fabric and the surface troweled to ensure consistent thickness. Panels were left to cure for 28 days.

- Uniaxial, monotonically-increasing, tensile load was applied to each coupon gripped with a clevis-type anchor at its ends to allow for fiber slippage to control failure. Axial deformation was measured using a clip-on extensometer with a 100 mm (4 in) gauge length attached at the specimen mid-height (**Figure 9** (a))**.**

- Specimens were tested in accordance with Annex A of AC434 (2013). Coupon testing results are presented in **Table 2** where Columns (1), (2), and (3) list the FRCM properties of relevance, while Columns (4), (5), and (6) show mean, standard deviation, and C.O.V., respectively.

The idealized tensile stress-strain curve for a FRCM coupon is presented by a simple bilinear curve with a bend-over point corresponding to the intersection point (**Figure 9** (b)). The first linear phase is the un-cracked linear-elastic behaviour characterized by the un-cracked elastic modulus, E^*_f, and the second linear phase is the cracked behaviour characterized by the cracked elastic modulus, E_f. **Figure 10** shows the crack pattern of FRCM coupon at failure. The mechanical properties of both the masonry prisms and the FRCM coupons reported above were used as the basis of the analysis and design of the walls.

Test Setup

Figure 11 illustrates the in-plane test setup configuration. In this experiment, compression was applied diagonally through two 299 kN (67 kip) capacity hollow-plunger cylinders symmetrically mounted at the top corner, activated by a manual pump. Steel shoes were placed on diagonally-opposite corners of the wall. Two steel Dywidag rods went through the shoes and tied them in order to transmit the load. Two load cells were set on the bottom corner of the wall to measure the applied load. Two strain gauges were installed at the center of the strengthened walls on each face. Also, two strain gauges were attached on each Dywidag rod (front and back) in order to verify the load measured by the load cells. Two linear variable displacement transducers (LVDT's) were used to measure the wall shortening and elongation. One LVDT was set parallel to the line of compression on one face, while the other was set on the other face, perpendicular to the line of compression. The load was applied in three stepped cycles of loading and unloading using a hand pump, where the last cycle was continued till failure. All data

were collected by using a National Instruments data acquisition system operating LabVIEW™ software at a frequency of 10 Hz. Diagonal compression is being widely used by the international community to develop knowledge on the in-plane behavior of masonry. It is recognized that diagonal compression does not necessarily reproduce a field condition. However, it is more conservative because of the limited value of the vertical load and is standardized in accordance to ASTM E519/ E519M (2010). In the test setup according to ASTM E 519, weight of the masonry wall is assumed to be disregarded compared to failure loads. Therefore, two test setups, used in this project and ASTM E 519, are comparable.

TEST RESULTS AND DISCUSSION

Experimental test results in terms of maximum load capacity, average maximum load for each set, and failure mode are presented in Columns (1), (2) and (3) of **Table 3**, respectively. Column (2) shows that for the three control CMU walls, the average peak load was 109.4 kN (24.6 kip), while for the clay ones it was 69.7 kN (15.7 kip). The average peak load for three 1-ply FRCM CMU walls was 212.9 kN (47.9 kip) which was about two times that of the control walls. For three 1-ply FRCM clay walls, average peak load was 169.7 kN (38.2 kip) about 2.5 times higher that of control clay walls. The three 4-ply FRCM CMU walls experienced the highest peak load with an average of 257.6 kN (57.9 kip) only 17 % higher than 1-ply concrete walls, while for three 4-ply clay walls average peak load was 329.7 kN (74.1 kip) which was about twice that of the 1-ply FRCM clay wall. It should be noted that the experimental loads reported in the **Table 3** refer to the values measured along the diagonal, which correspond to 1.4 times that of the

shear capacity of the walls along the horizontal direction. **Figure 12** geometrically shows the relation between the maximum diagonal load, P_u measured by the load cells and the horizontal shear component, V_u simply obtained by multiplying the peak load, P_u, by the cosine of 45^o.

A strength enhancement index is defined as the ratio between the average maximum applied load for each set of walls and the control one, and is found to be 1.95 and 2.36 for CMU walls and 2.43 and 4.73 for clay walls, using 1-ply and 4-ply, respectively.

Crack Pattern and Failure Modes

Un-reinforced masonry— The results showed that the three CMU walls failed in a brittle manner with cracking starting in the upper masonry unit, and progressing diagonally in the blocks along direction parallel to the applied load. Diagonal tension failure resulted from the principal tension stress reaching the tensile strength of the CMU (**Figure 13** (a)). The three clay brick walls showed a brittle failure caused by the loss of bond between the mortar and clay bricks. As the load increased, the cracks developed in a stair-stepped shape in the head and bed joints when the principal tensile stresses exceeded the tensile strength at interface mortar-brick. Ultimately, the applied load caused crack growth and joint sliding. This stepped cracking progressed parallel to the direction of the applied load (**Figure 13** (d)).

Masonry wall Strengthened with 1-ply FRCM— The three CMU wall strengthened with 1-ply FRCM failed due to toe crushing, when the compressive stress

reached the compressive strength of CMU (**Figure 13** (b)). Conversely, the three clay walls strengthened with 1-ply FRCM failed by the FRCM failure. The FRCM failure mechanism was characterized by carbon-fabric slippage within the matrix and reflected by horizontal hairline cracks along the bed joints (**Figure 13** (e)). FRCM reinforcement effectively constrained the diagonal stepped cracking and transferred tensile stresses across the diagonal cracks, making the strengthened walls achieve higher shear capacity.

Masonry wall Strengthened with 4-ply FRCM— All walls strengthened with 4-ply FRCM failed due to toe crushing at the loading ends. Toe crushing failure preceded shear failure indicating that the level of strengthening was excessive compared with the capacity of the substrate (**Figure 13** (c) and (f)). **Figure 13** (a) to (f) illustrate the typical crack patterns of the three sets in both concrete block and clay brick masonry walls at failure.

Shear Stress-Shear Strain Diagrams

ASTM E519/ E519M (2010) assumes that a uniform shear stress flow, τ, takes place along the loaded diagonal of a square wall when subjected to diagonal compression. The Mohr's circle corresponding to this condition is shown in **Figure 12**, where the shear stress is equal to both tensile and compressive principal stresses, representing a pure shear stress state (Parisi et al. 2012). The shear stress of any value of P is calculated as $\tau=0.707\ P/A_n$, where P and A_n are the diagonal applied load and net cross-sectional area of the un-cracked section of the wall panels, respectively (A_n= 72903 mm^2 (113 in^2) for CMU walls, and A_n= 81290 mm^2 (126 in^2) for clay brick walls).

The shear strain is defined as $\gamma=\varepsilon_v+\varepsilon_h$, where ε_v and ε_h are the average strains along the compressive and tensile diagonals of the panel measured by two strain gauges. For the control walls, the average strains are calculated by dividing the displacement measured by the two LVDTs along the compression and tension diagonals. **Figure 14** (a) **to** (f) shows shear stress versus shear strain diagrams for each set of walls. Each graph displays three curves representing the three replicates. The horizontal lines correspond to the values obtained by analysis (dash line) and design (solid line) according to ACI 549 (2013).

The test outcomes show a clear and consistent pattern. The walls behave almost in a linear-elastic manner until first crack. In strengthened walls, initial cracking is delayed by the presence of the FRCM reinforcement. The graphs show that shear strength is enhanced by increasing the amount of FRCM layer.

From a shear stress-shear strain curve, the shear modulus of rigidity, G, (see Column (5) in **Table 4**) is computed as the ratio τ_{cr}/γ_{cr} which corresponds to the secant modulus between the origin and the shear stress at cracking point (ASTM E519/ E519M 2010; Parisi et al. 2012; Dizhur et al. 2013). FRCM strengthening substantially increases the shear rigidity of masonry.

Pseudo-Ductility

The wall pseudo-ductility, μ, (see Column (6) in **Table 4**) is defined as the ratio γ_u/γ_{cr} where γ_u is the ultimate shear strain corresponding to the largest strain experienced

during the test (ultimate strain) or the strain at a level of shear stress 20% below the peak, if the shear stress-strain diagram continues with a descending branch (Park 1989; Secondin 2003; Grando et al. 2003; Li et al. 2005; Petersen 2009) (**Figure 15**).

There is no consensus in establishing the value of shear strain at cracking, $\gamma_{cr,}$ in strengthened walls. Some authors (Tumialan et al. 2001; Secondin 2003; Grando et al. 2003; Li et al. 2005) define γ_{cr} as the bend-over point where the in-plane shear stress versus strain curve tends to become flat, other authors (Park 1989; Petersen 2009) define γ_{cr} as the shear strain corresponding to the shear stress taken at 75% of the maximum shear stress, and others use 70% (Parisi et al. 2012; Dizhur et al. 2013). In this paper γ_{cr} is defined as the shear strain corresponding to the shear stress at cracking, τ_{cr}, assumed as 70% of the maximum shear stress. Columns (1), (2), (3), (4), (5) and (6) in **Table 4** show the shear stress and shear strain at ultimate and cracking, shear modulus and pseudo-ductility, respectively.

The masonry wall with higher pseudo-ductility index experiences in-elastic deformation without substantial reduction in the load-carrying capacity. The amount of energy absorption to failure is defined as the total area under shear stress-strain curves (Hrynyk 2006; Dizhur et al. 2013). FRCM makes the strengthened wall achieve higher shear stress and pseudo-ductility, and absorb more energy; however, in the case of 1-ply FRCM, higher pseudo-ductility and energy absorption were attained since in 4-ply FRCM failure was controlled by toe crushing.

Analytical Approach

The in-plane shear capacity of strengthened walls is the sum of the contribution of masonry and the FRCM reinforcement, where the effectiveness of FRCM is considered only after occurrence of masonry cracking (Li et al. 2005; ACI 440.7R 2010; AC434 2013; ACI 549 2013). The design shear strength is calculated in accordance with **Equation 1**:

$$\phi_v V_n = \phi_v \left(V_m + V_f \right) \quad \textbf{(1)}$$

where V_n is the nominal shear strength, and V_m and V_f are the contribution of the masonry and FRCM reinforcement, respectively. In the analysis, the strength reduction factor ϕ_v is assumed equal to be 1.0.

Masonry Contribution (V_m)

Masonry is a non-homogeneous and anisotropic composite structural material, consisting of masonry unit and mortar. The behavior of masonry is complex. The accurate prediction of shear capacity of URM walls is difficult because of the complex brick-block mortar interaction behavior.

Researchers (Li et al. 2005; Silva et al. 2008; Parisi et al. 2012) have shown that the four possible failure modes depend on the URM wall physical and mechanical properties, and these modes have been validated by experimental results. A wall fails when the value of the applied shear force reaches the minimum shear capacity V_m (Li et al. 2005; Silva et

al. 2008; ACI 440.7R 2010). URM shear capacity is calculated in accordance with **Equation 2**:

$$V_m = Min(V_{ss};\ V_{sf};\ V_{dt};\ V_c) \quad (2)$$

In Equation 2, V_m depends on shear sliding (V_{ss}), shear friction (V_{sf}), diagonal tension (V_{dt}), and compression (V_c) failures.

Shear sliding. Shear sliding along a single bed joint can be caused by bond failure between block/ or (brick) and mortar (Secondin 2003; Petersen 2009), modeled by Mohr-Coulomb failure criterion (Li et al. 2005; Silva et al. 2008) and is expressed with **Equation 3**.

$$V_{ss} = \frac{\tau_0}{1 - \mu_0\ tan\theta}\ A_n \quad (3)$$

τ_0 is the bond strength of the mortar joint and is estimated to be 3% of the masonry compressive strength (Paulay 1992; Li et al. 2005; Silva et al. 2008), the coefficient of shear friction, μ_0, is assumed to be equal to 0.3 (Li et al. 2005), and θ is the inclined angle between horizontal and main diagonal of the wall.

Shear friction. Based on Mohr-Coulomb failure criteria, Mann and Müller (1982) proposed a failure theory to explain shear friction behavior between mortar and block/ or (brick) resulting in stepped-stair-mode shear sliding failure considering a more realistic

distribution of normal and shear stress. Normal and shear stress acting on a block/ or (brick) is assumed to be distributed uniformly and no shear stress is transferred through head joints. Crisafulli et al. (1995) modified the Mann and Müller theory by considering linear distribution of normal stress with zero value at the block/ or (brick) center and maximum at the edges. Shear friction capacity is calculated based on Crisafulli et al. and presented with **Equation 4**:

$$V_{sf} = \frac{\tau_{0,m}}{1 - \mu_m \, tan\theta} \, A_n \qquad \textbf{(4)}$$

where:

$$\tau_{0,m} = \frac{\tau_0}{1 + 1.5 \, \mu_0 \, \frac{h}{w}} \qquad \textbf{(4-a)}$$

and

$$\mu_m = \frac{\mu}{1 + 1.5 \, \mu_0 \, \frac{h}{w}} \qquad \textbf{(4-b)}$$

with *h* and *w* the height and length of the block/ or (brick), respectively.

Diagonal tension. Diagonal tension failure occurs when the principal tension stress induced by a combination of higher shear and compressive force reaches to the tensile strength of the wall (Li et al. 2005; Silva et al. 2008; Petersen 2009). Diagonal tension shear capacity is calculated in accordance with **Equation 5**:

$$V_{dt} = \frac{tan\theta + \sqrt{21.16 + tan\theta^2}}{10.58} f_t' A_n \quad (5)$$

where f'_t is the masonry tensile strength assumed $0.5\sqrt{f'_m}$ (MPa) and $0.67\sqrt{f'_m}$ (MPa) for CMU and clay brick URM walls, respectively (Silva et al. 2008). This failure takes place in case of weak block/or (brick) and strong mortar, and cracks pass through the block/or (brick).

Toe crushing. A wall fails by toe crushing when the stress generated at the loading end reaches the compressive masonry strength (Li et al. 2005; Silva et al. 2008; Petersen 2009). Shear capacity controlled by compression is shown by **Equation 6**:

$$V_c = \frac{2wf'_m}{3h + 2w\ tan\theta} A_m \quad (6)$$

where A_m in diagonal compression tests is defined as the horizontal interface loading area between steel shoe and masonry walls.

Equations (3) to **(6)** completely represent the failure envelope for the shear strength of masonry plotted in **Figure 16** as a function of the compressive stress applied to the wall that varies from zero to the full compressive strength of the masonry.

A numerical example on how to calculate V_m is given in appendix A for the case of the CMU wall tested under compressive force in this research program.

FRCM Contribution (V_f)

The contribution of FRCM reinforcement is computed as per ACI 549 (2013). The ultimate tensile strain of FRCM, ε_{fu}, is the average minus one standard deviation derived from tensile tests conducted as per AC434 (2013). The tensile strain in the FRCM shear reinforcement, ε_{fv}, is calculated in accordance with **Equation 7**.

$$\varepsilon_{fv} = \varepsilon_{fu} \leq 0.004 \quad (7)$$

The tensile strength in the FRCM shear reinforcement, f_{fv}, is calculated in accordance with **Equation 8**:

$$f_{fv} = E_f \varepsilon_{fv} \quad (8)$$

where E_f is the tensile modulus of elasticity of the cracked FRCM.

V_f is calculated in accordance with **Equation 9**:

$$V_f = 2nA_f \, L f_{fv} \quad (9)$$

where A_f, n, L are the area of the fabric reinforcement by unit width (Both horizontal and vertical directions), the number of layers of fabric, and the length of the masonry, respectively.

Appendix A shows how to compute V_f for the case of 1-ply FRCM CMU wall tested in this research program.

The nominal shear capacity, V_n, is computed as the sum of masonry and FRCM contributions.

Analytical results in terms of maximum load, $P_{n,An.}$, and failure modes in each set of walls are presented in **Table 3** Columns (4), and (5), while Column (6) presents the ratio of experimental to analytical capacity. **Figure 17** compares experimental and analytical shear capacity of masonry walls retrofitted with FRCM. The analysis according to well established formulations of ACI 549 (2013) predicts the shear capacity and failure modes of strengthened walls with a good accuracy. However, predicted shear capacity for control clay wall is higher than the experimental values. This is because of the shear friction capacity (**Equation 4**) assumes the step-shape failure always through the wall diagonal; but, in the case of the three clay walls tested in this program (see **Figure 13** d), the crack pattern ran through smaller surface.

The analysis predicts that substrate toe compression controls the failure mode in the masonry wall strengthened with 4-ply FRCM; therefore, adding more reinforcement is ineffective. Analytical load capacities and failure modes are presented in **Table 3** Columns (4) and (5) and **Figure 14** (horizontal dash lines)).

Design Provisions

ACI 549 (2013) establishes design provisions by limiting the increase in shear capacity of strengthened walls provided by the FRCM reinforcement not to exceed 50 percent of the un-strengthened wall capacity in order to limit the total force per unit width transferred to the substrate of the masonry. Additionally, the strength reduction factor for shear, ϕ_v, is equal 0.75. It can be observed that these design provisions are conservative (Columns (7) and (8) in **Table 3** and **Figure 14** (horizontal solid lines)). In the case of CMU and clay brick wall strengthened with 4-ply FRCM, the difference between experimental and design values is more noticeable. **Figure 18** compares experimental and design values.

CONCLUSIONS

The in-plane shear testing of CMU and clay brick masonry walls strengthened with FRCM system was conducted in this research program. The following observations and conclusions are drawn from the experimental results:

1. The experimental results proved the technical feasibility of FRCM shear strengthening of existing URM walls. Proportional to the amount of FRCM, an increment in terms of ultimate in-plane load ranged between 2.0 and 2.4 times of concrete control wall, and 2.4 and 4.7 times that of clay brick control wall, using 1-ply and 4-ply carbon FRCM, respectively.

2. Based on the results obtained from shear stress-shear strain diagrams, it can be observed that FRCM strengthening is effective in increasing the stiffness and pseudo-ductility; however, when 1-ply FRCM is applied on both wall faces, higher pseudo-ductility is achieved compared to 4-ply FRCM. It can be inferred that pseudo-ductility of 4-ply strengthened masonry wall is limited by toe crushing failure occurring prior to FRCM failure. Test results clearly showed that the failure modes of the strengthened walls were directly influenced by the strengthening schemes.

3. An analysis using the methodology proposed by ACI 549 (2013) based on the classical formulation of shear strength showed that calculated shear strength well predicts the experimental results. Similarly, design shear strength values are conservative when applying limitations of maximum 50% increase and reduction factor, ϕ_v, as per ACI 549 (2013).

NOTATIONS

A_f = area of mesh reinforcement by unit width, mm^2/mm (in^2/in)

A_m = interface loading area between steel shoe and wall, mm^2/mm (in^2/in)

A_n = cross-sectional net area of masonry wall, mm^2/mm (in^2/in)

E^*_f = tensile modulus of elasticity of the un-cracked FRCM specimen, MPa (ksi)

E_f = tensile modulus of elasticity of the cracked FRCM specimen and other strengthening system, MPa (ksi)

E_m = modulus of elasticity of masonry wall, MPa (ksi)

f_{ft} = transition stress corresponding to the transition point, MPa (psi)

f_{fu} = ultimate tensile strength of FRCM, MPa (psi)

f_{fv} = tensile strength of FRCM shear reinforcement, MPa (psi)

f'_m = specified compressive strength of masonry, MPa (psi)

f'_t = tensile strength of masonry, MPa (psi)

G = shear modulus of rigidity of masonry wall, GPa (ksi)

h = height of concrete block/ or (brick), mm (in)

L = length of masonry wall in the direction of applied shear force, mm (in)

n = number of layers of mesh reinforcement

P = applied load which is geometrically 1.4 times of shear strength of the wall, kN (kip)

t = thickness of the wall, mm (in)

V_c = masonry wall shear capacity due to compression failure, kN (kip)

V_{dt} = masonry wall shear capacity due to diagonal tension failure, kN (kip)

V_f = contribution of FRCM to nominal shear strength of the wall, kN (kip)

V_m = contribution of masonry to nominal shear strength of the wall, kN (kip)

V_n = nominal shear strength, kN (kip)

V_{sf} = masonry wall shear friction capacity, kN (kip)

V_{ss} = masonry wall shear sliding capacity, kN (kip)

w = width of clay brick, mm (in)

θ = inclined angle between horizontal and main diagonal of wall, deg

μ = pseudo-ductility of masonry wall

μ_0 = coefficient of internal shear friction in mortar joint

μ_m = modified coefficient of internal shear friction in mortar joint

γ_{cr} = shear strain at cracking, mm/mm (in/in)

γ_u = shear strain of the masonry at ultimate, mm/mm (in/in)

ε_{ft} = transition strain corresponding to the transition point, mm/mm (in/in)

ε_{fu} = ultimate tensile strain of the FRCM, mm/mm (in/in)

ε_{fv} = tensile strain of FRCM shear reinforcement, mm/mm (in/in)

τ_0 = bond strength of the mortar joint, MPa (psi)

$\tau_{0,m}$ = modified shear bond strength of mortar joint, MPa (psi)

τ_{cr} = shear stress at cracking, MPa (psi)

τ_u = shear stress of the masonry at ultimate, MPa (psi)

ϕ_v = strength reduction factor for shear

ρ = the ratio between area of FRCM/FRP reinforcement and net area of URM walls

Table 1– In-plane test matrix

Specimen Code (1)	**Strengthening Material (2)**	**Masonry Type (3)**	**Repetitions (4)**
CMU-Control	None	Concrete Block	3
CMU-1	1-ply of FRCM		
CMU-4	4-ply of FRCM		
CL-Control	None	Clay Brick	3
CL-1	1-ply of FRCM		
CL-4	4-ply of FRCM		

Table 2– Mechanical properties of carbon FRCM coupons

FRCM Property (1)	**Symbol (2)**	**Units (3)**	**Mean (4)**	**Standard Deviation (5)**	**COV [%] (6)**
Modulus of elasticity (un-cracked)	E_f*	GPa	813	212	26
Modulus of elasticity (cracked)	E_f	GPa	80	18	23
Ultimate tensile strength	f_{fu}	MPa	1031	54	5
Ultimate tensile strain	ε_{fu}	mm/mm	0.0100	0.0014	14
Fiber area by unit width (One direction)	A_f	mm^2/mm	0.05	-	-

(Note: 1.0 GPa =145.03 ksi; 1.0 MPa = 0.145 ksi; 1.0 mm/mm = 1.0 in/in; 1.0 mm^2/mm = 0.039 in^2/in)

Table 3– Experimental, analytical, and design results

Specimen ID	Experimental Results			Analytical Results		Exp./An. Ratio	Design results*	Exp. /Des. Ratio
	Max. Load P_u kN (1)	Ave. Max. Load $P_{u,avg}$ kN (2)	Failure Mode - (3)	Max. Load $P_{n,An.}$ kN (4)	Failure Mode - (5)	$P_{u,avg}/P_{n,An.}$ - (6)	Max. Load $\phi_v P_{n,Des}$ kN (7)	$P_{u,avg}/\phi_v P_{n,Des}$ kN (8)
CMU-Control-1	116.7	109.4	Diagonal tensile cracking	65.5	Joint Sliding	1.7	49.1	2.2
CMU-Control-2	115.6							
CMU-Control-3	95.8							
CMU-1 ply-1	237.5	212.9	Toe Crushing	161.5	Toe Crushing	1.3	73.7	2.9
CMU-1 ply-2	197.6							
CMU-1 ply-3	203.7							
CMU-4 ply-1	261.6	257.6	Toe Crushing	161.5	Toe Crushing	1.6	73.7	3.5
CMU-4 ply-2	255.1							
CMU-4 ply-3	256.2							
CL-Control-1	72.9	69.7	Joint Sliding	99.1	Joint Sliding	0.7	74.3	0.9
CL-Control-2	70.4							
CL-Control-3	65.8							
CL-1 ply-1	153.9	169.7	FRCM Failure	189.3	FRCM Failure	0.9	111.5	1.5
CL-1 ply-2	188.4							
CL-1 ply-3	166.9							
CL-4 ply-1	348.9	329.7	Toe Crushing	310.5	Toe Crushing	1.06	111.5	3.0
CL-4 ply-2	315.5							
CL-4 ply-3	324.7							

(Note: 1.0 kN = 0.23 kips; *ϕ factor and maximum 50% increase limits apply)

Table 4– Test results: pseudo-ductility

Specimen ID	τ_u MPa (1)	γ_u mm/mm (2)	τ_{cr} MPa (3)	γ_{cr} mm/mm (4)	G GPa (5)	μ - (6)
CMU-Control-1	1.13	0.0004	1.13	0.0004	3.14	1.0
CMU-Control-2	1.12	0.0003	1.12	0.0003	3.22	1.0
CMU-Control-3	0.93	0.0003	0.93	0.0003	2.83	1.0
CMU-1 ply-1	2.30	0.0013	1.61	0.0004	3.82	3.2
CMU-1 ply-2	1.91	0.0011	1.34	0.0003	3.88	3.3
CMU-1 ply-3	1.97	0.0012	1.38	0.0004	3.54	3.1
CMU-4 ply-1	2.53	0.0004	1.77	0.0004	4.81	1.3
CMU-4 ply-2	2.47	0.0005	1.73	0.0004	4.74	1.4
CMU-4 ply-3	2.48	0.0004	1.74	0.0003	5.27	1.2
CL-Control-1	0.63	0.0007	0.63	0.0007	0.90	1.0
CL-Control-2	0.61	0.0007	0.61	0.0007	0.87	1.0
CL-Control-3	0.57	0.0008	0.57	0.0008	0.71	1.0
CL-1 ply-1	1.33	0.0134	0.93	0.0007	1.33	19.1
CL-1 ply-2	1.48	0.0128	1.14	0.0007	1.63	18.2
CL-1 ply-3	1.16	0.0109	1.01	0.0006	1.60	17.4
CL-4 ply-1	3.02	0.0031	2.11	0.0007	2.83	4.2
CL-4 ply-2	2.74	0.0040	1.92	0.0009	2.13	4.4
CL-4 ply-3	2.82	0.0028	1.97	0.0007	3.02	4.3

(Note: 1.0 GPa =145.03 ksi; 1.0 MPa = 0.145 ksi; 1.0 mm/mm = 1.0 in/in)

(a)

(b)

Figure 2- In-plane failures of load-bearing walls

Umbria, Italy, September 1997

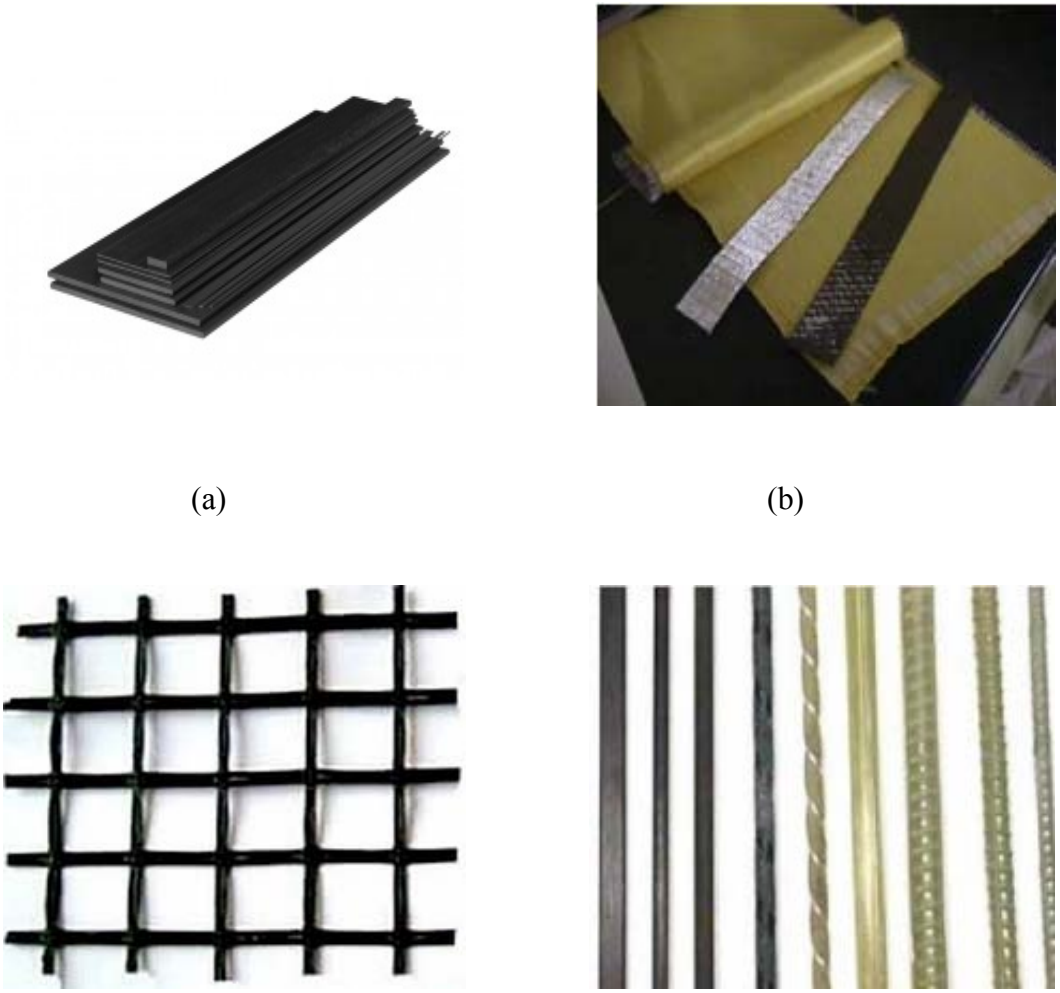

(a) (b)

(c) (d)

Figure 3- Representative different types of FRP:

Laminates (a); sheets (b); grids (c); bars (d)

Figure 4- Representative of applied pre-cut fabric

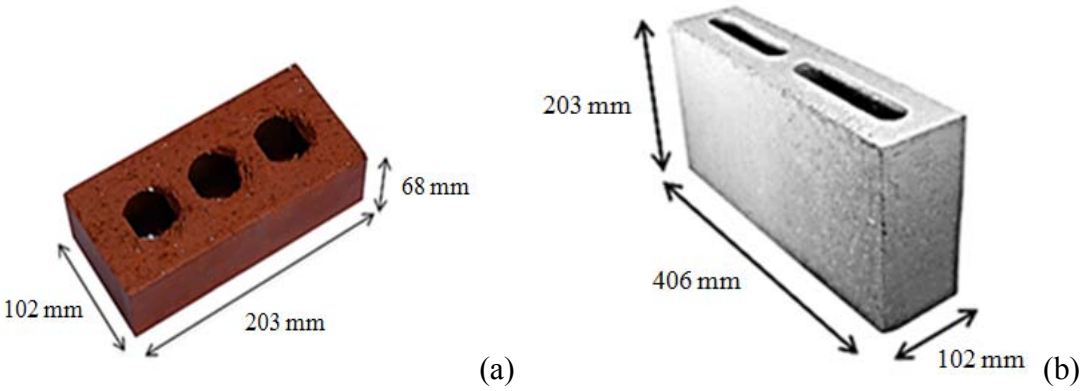

Figure 5- Representative details of:

Clay brick (a); CMU block (b)

Figure 6- Representative failure of a compressive strength cube mortar

(a)

(b)

Figure 7- Representative failures during the compressive strength tests of masonry prisms, a) CMU block; and b) clay brick

(a)

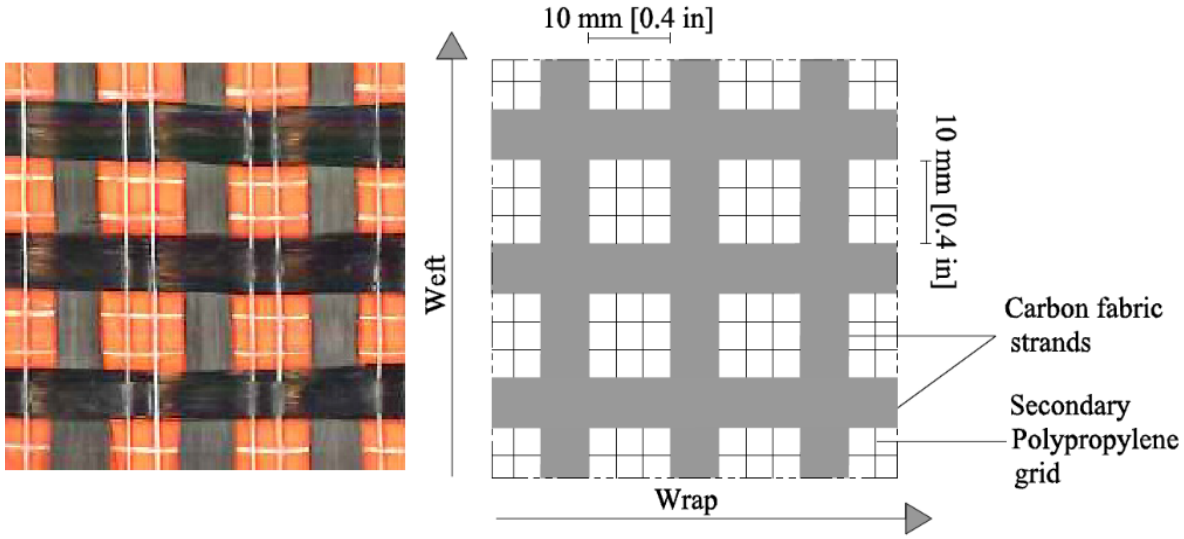

(b)

Figure 8- Dry matrix powder (a), Carbon fabric architecture (b)

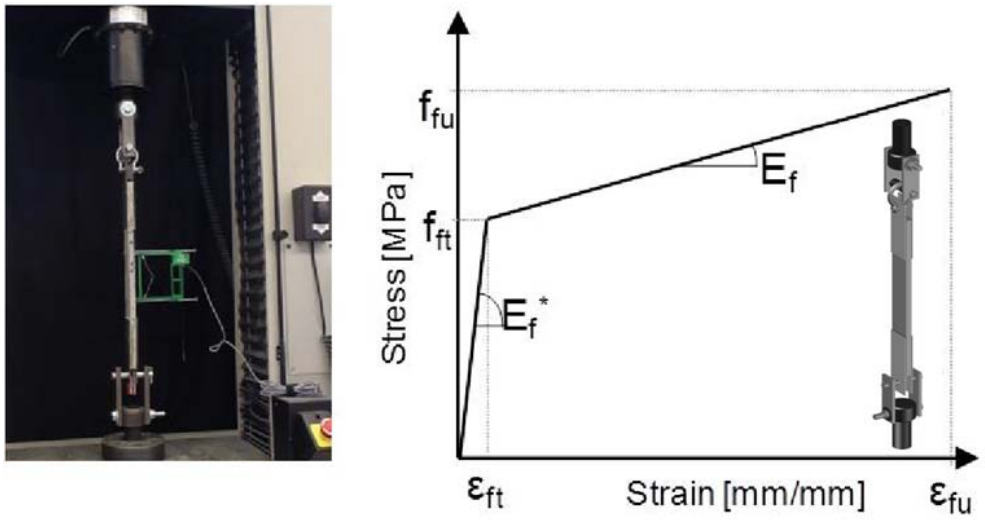

(a) (b)

Figure 9- (a) Test setup for direct tensile testing of flat FRCM coupons; (b) Idealized tensile stress-strain curve for a FRCM coupon

Figure 10- Representative failure of tensile FRCM coupon (Crack line enhanced)

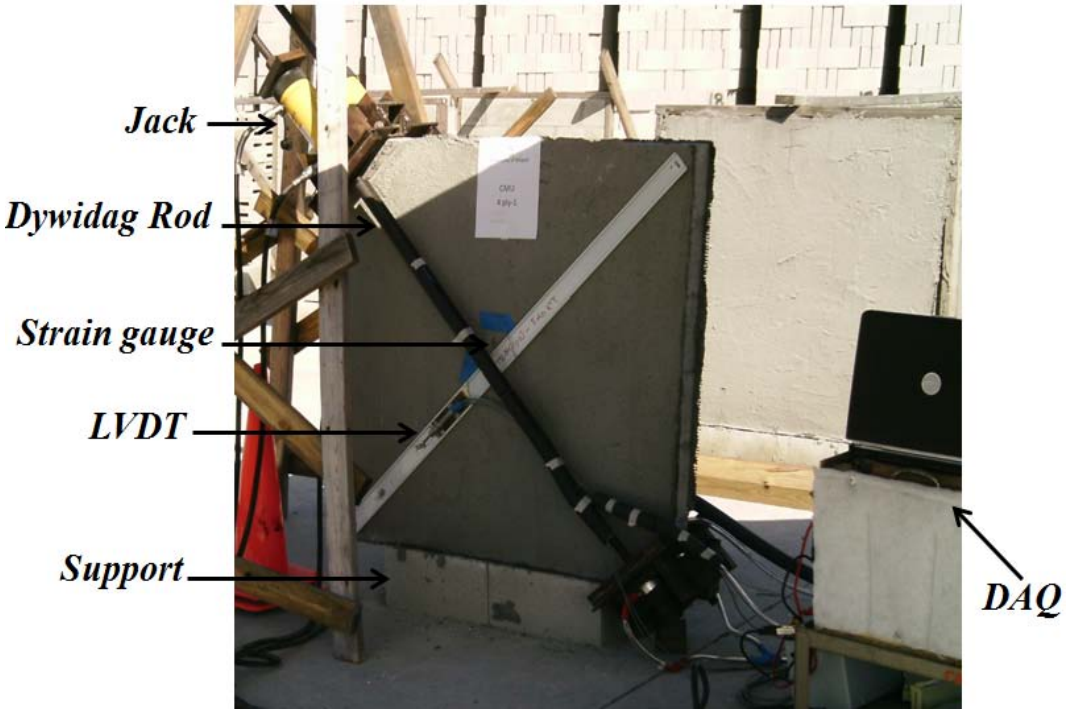

Figure 11- In-plane test setup

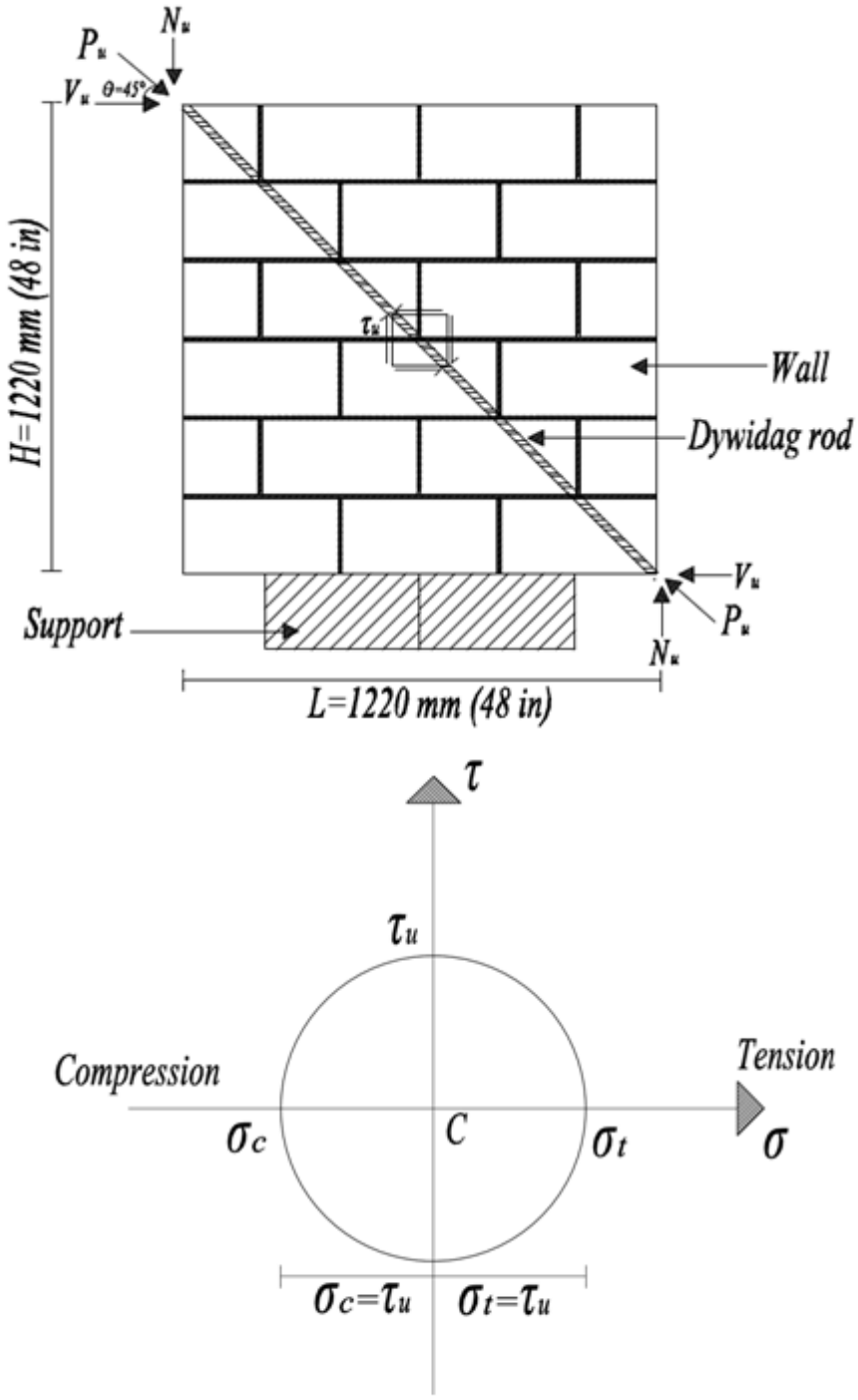

Figure 12- Schematic of in-plane load test of the wall

(a)

(b)

(Crack line enhanced)

(c)

(d)

(e)

(f)

Figure 13- Failure mode of wall specimens:

CMU-Control (a); CMU-1 ply (b); CMU-4 ply (c)

CL-Control (d); CL-1 ply (e); CL-4 ply (f)

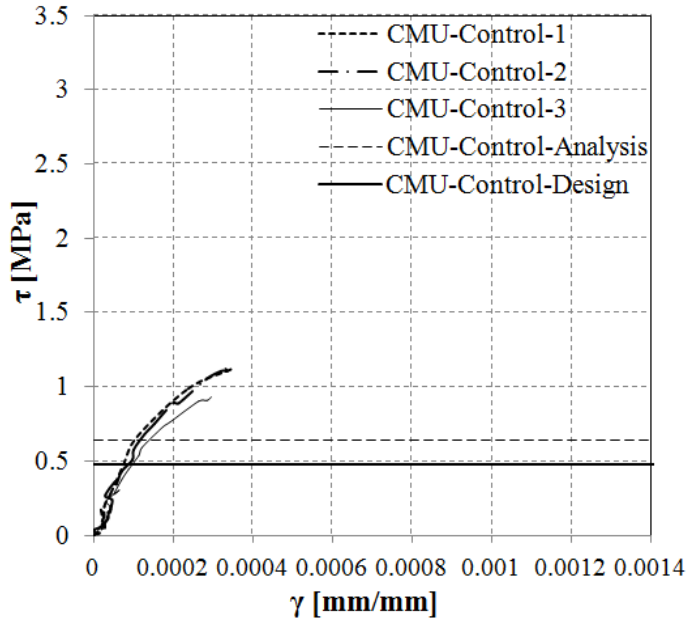
CMU-Control-1
CMU-Control-2
CMU-Control-3
CMU-Control-Analysis
CMU-Control-Design
τ [MPa]
γ [mm/mm]
0
0.5
1
1.5
2
2.5
3
3.5
0.0002
0.0004
0.0006
0.0008
0.001
0.0012
0.0014

(a)

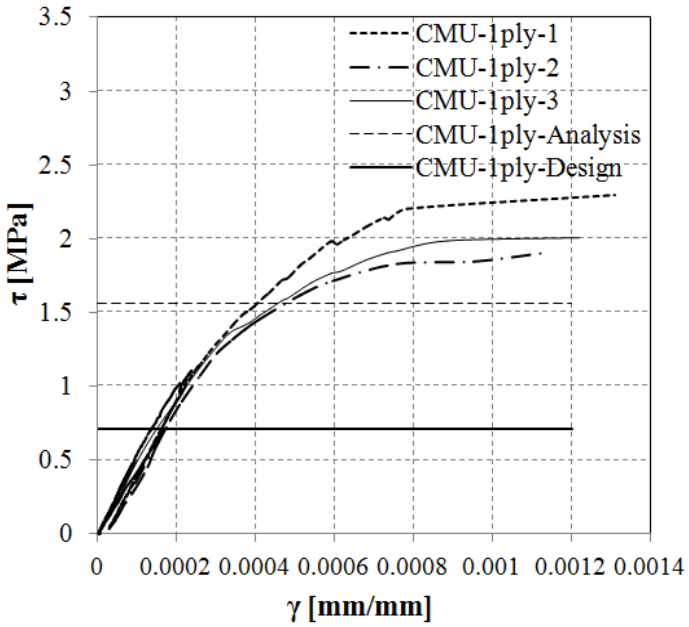
CMU-1ply-1
CMU-1ply-2
CMU-1ply-3
CMU-1ply-Analysis
CMU-1ply-Design
τ [MPa]
γ [mm/mm]
0
0.5
1
1.5
2
2.5
3
3.5
0.0002
0.0004
0.0006
0.0008
0.001
0.0012
0.0014

(b)

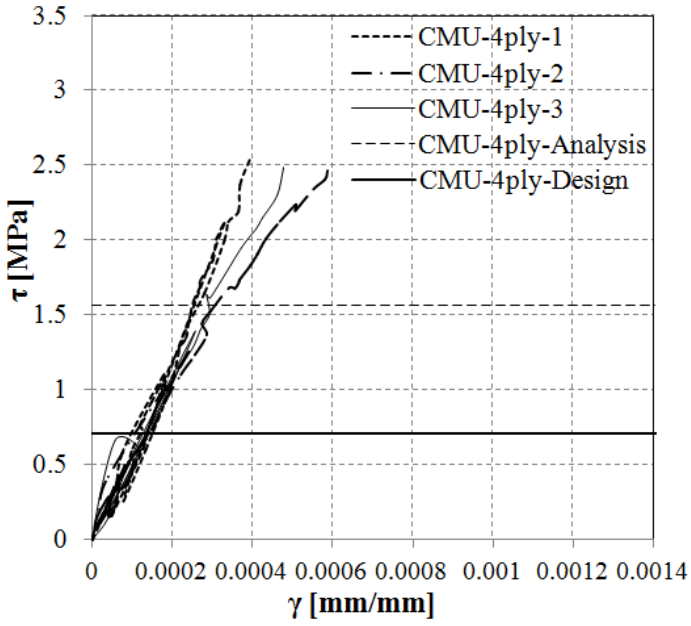
CMU-4ply-1
CMU-4ply-2
CMU-4ply-3
CMU-4ply-Analysis
CMU-4ply-Design
τ [MPa]
γ [mm/mm]
0
0.5
1
1.5
2
2.5
3
3.5
0.0002
0.0004
0.0006
0.0008
0.001
0.0012
0.0014

(c)

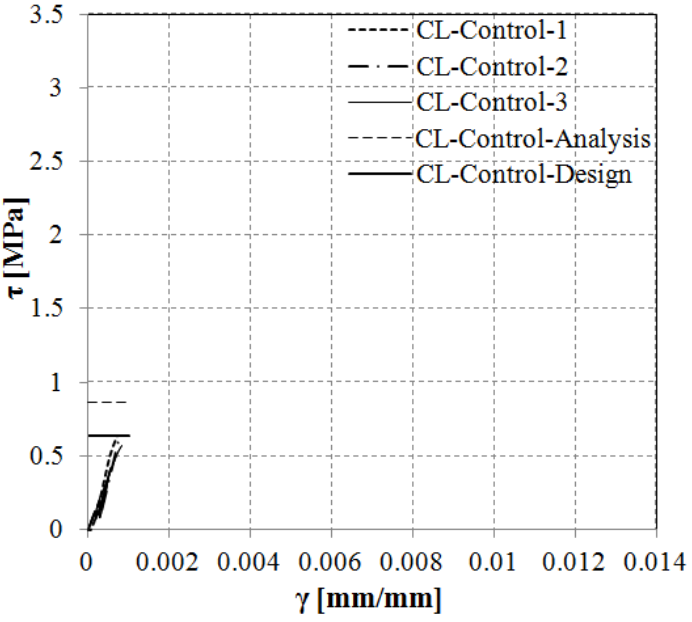
CL-Control-1
CL-Control-2
CL-Control-3
CL-Control-Analysis
CL-Control-Design
τ [MPa]
γ [mm/mm]
0
0.5
1
1.5
2
2.5
3
3.5
0.002
0.004
0.006
0.008
0.01
0.012
0.014

(d)

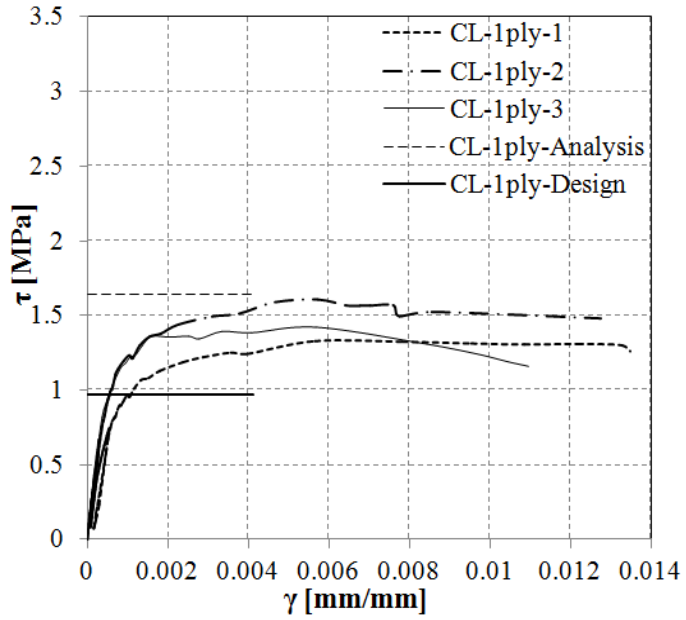

(e)

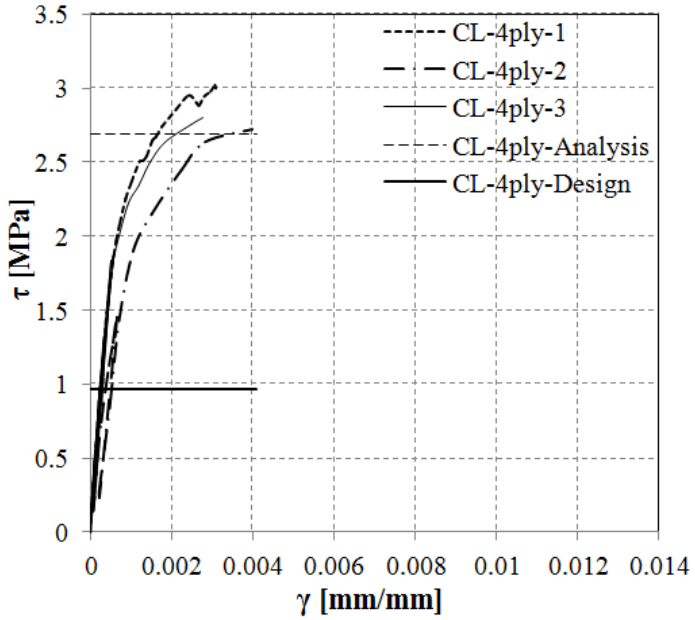

(f)

Figure 14- Shear stress-shear strain diagrams of wall specimens:

CMU-Control (a); CMU-1 ply (b); CMU-4 ply (c)

CL-Control (d); CL-1 ply (e); CL-4 ply (f)

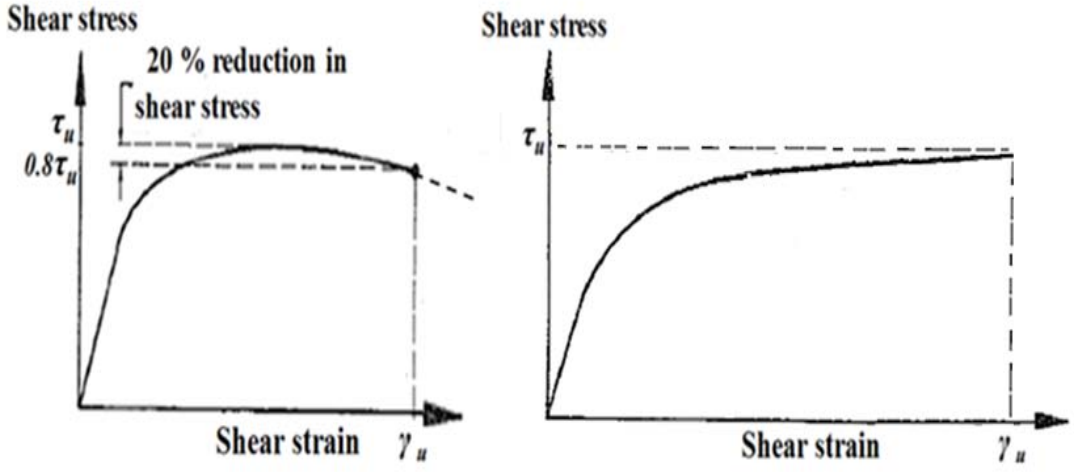

Figure 15- Definitions of ultimate shear strain

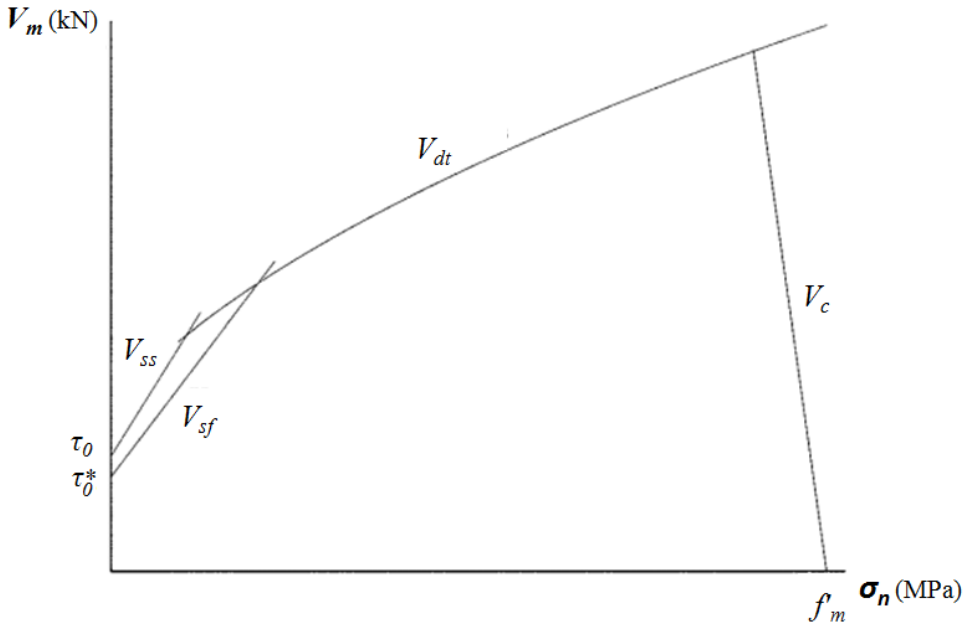

Figure 16- Failure envelope of URM wall

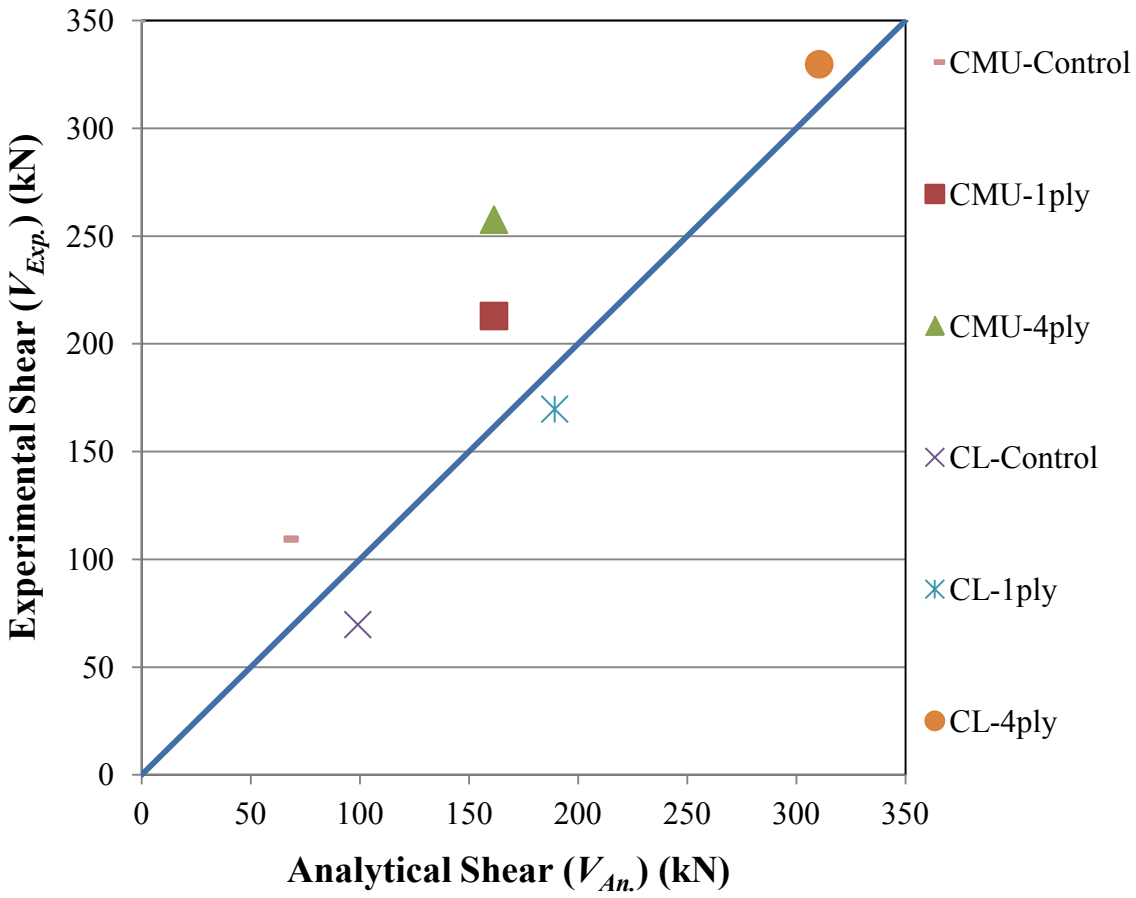

Figure 17- Comparison between experimental and analytical results

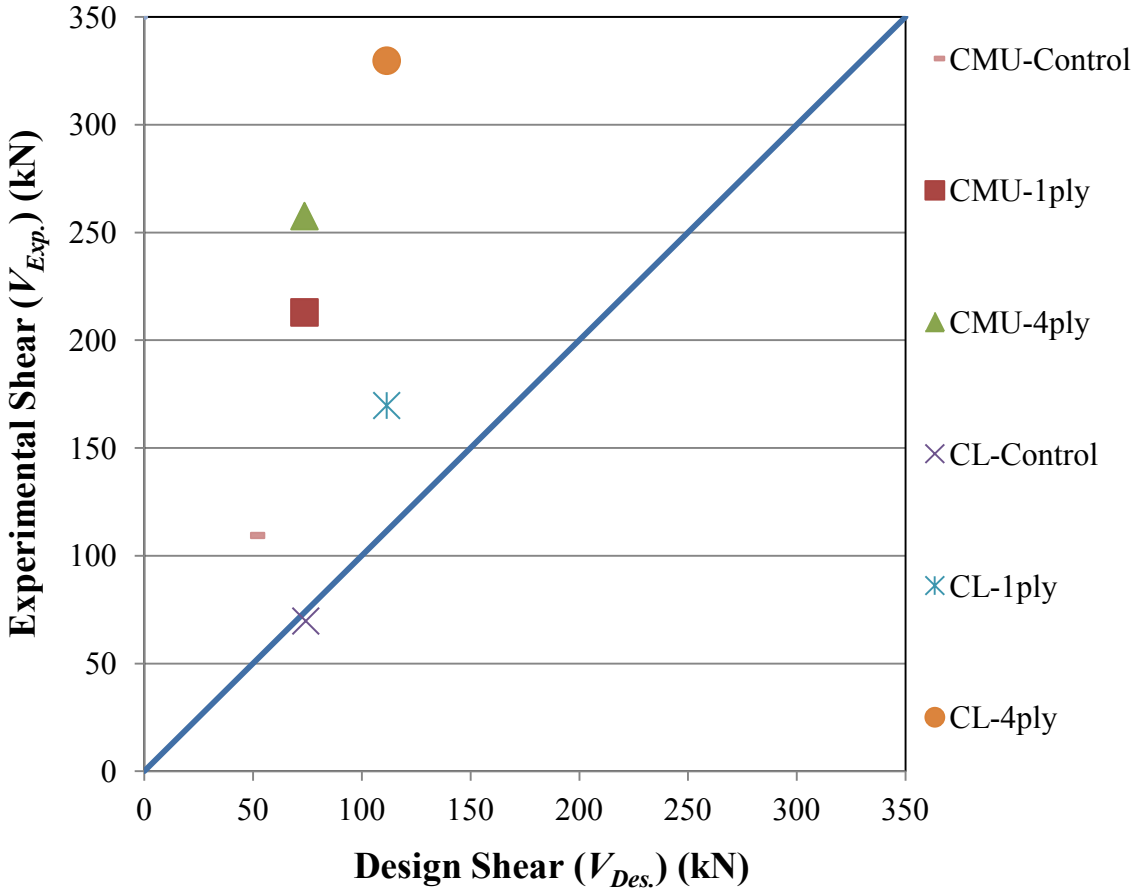

Figure 18- Comparison between experimental and design results

CHAPTER III

*STUDY 2*_ OUT-OF-PLANE BEHAVIOR OF URM WALLS STRENGTHENED WITH FRCM

Study 2 evaluates the feasibility of using FRCM systems as an alternative external strengthening technology to improve out-of-plane behavior of URM walls. This study reports experimental results on flexural capacity of 18 CMU and clay brick walls strengthened with two different amounts of FRCM reinforcement, namely: one and four reinforcement fabrics, subjected to out-of-plane loading. Experimental evidence shows a significant improvement in the structural performance in terms of flexural capacity and stiffness of the strengthened walls. An analysis according to ACI 549 (2013) and MSJC (2011), disregarding arching effect, is conducted to calculate the flexural capacity of strengthened walls and compare its results with the experimental database.

BACKGROUND

Seismic loadings induce out-of-plane bending of walls between the restraining floors. Analysis of the failure modes must take into account many different factors, such as boundary conditions, wall compressive strengths, joint tensile strengths, wall stiffness, and applied loadings (Tumialan 2001; Morbin 2002; Secondin 2003).

Most existing exterior masonry walls, particularly unreinforced masonry (URM) walls, have insufficient strength to withstand out-of-plane loads and are in need to repair. Their failure is prone to be sudden and brittle and is aggravated by the production of fragments. **Figure 19** shows out-of-plane failures of load-bearing walls resulted from an earthquake in Umbria, Italy on September 1997.

The building evaluation showed that 96% of the URM buildings in California needed to be retrofitted (Tumialan 2001;Morbin 2002; Secondin 2003). To date, it has been estimated that only half of the owners have taken remedial actions, which may be attribute to the retrofitting cost. Thereby, the development of effective and affordable retrofitting techniques for masonry elements is an urgent need. Retrofitting of URM walls has proven to increase flexural capacity, stiffness, and energy absorption and reduce fragmentation. Conventional retrofitting techniques can be classified according to the problem to be addressed: damage repair or structure upgrading. For strengthening or upgrading of structures, some of the available conventional methods are:

- Grout injection of hollow masonry units with non-shrink portland cement grout or epoxy grout to strengthen or stiffen the wall. This method often requires disruptive activities such as drilling of holes and utilization of relatively heavy equipment, which could increase the cost.

- Construction of an additional masonry wythe to increase the flexural strength. This method will cause the loss of valuable space. In addition, the normal operations of the building area being strengthened are affected during construction, which could require the relocation of building inhabitants. These factors could increase the cost of the project.

- Post-tensioning of an existing construction. This method is particularly effective to increase the flexural capacity of masonry elements. In addition, post-tensioning does not affect the masonry aesthetics. However, it demands high-skilled labor, which increases the cost.

- External reinforcement with steel plates and angles. This is a relatively simple method to implement; however, one of the main disadvantages is that it can affect the aesthetics of the building. This fact can increase the intangible costs. In addition, additional costs can be incurred due to maintenance.

In the past two decades, numerous research studies have addressed the use of FRP composites in both forms of laminates and near-surface mounted (NSM) bars to

strengthen URM walls which resulted in a significant increase in the out-of-plane flexural capacity (Tumialan et al. 2003; Galati et al. 2005; Hrynyk et al. 2007). These researchers have proposed computational procedures to predict the load-carrying capacity of FRP-strengthened walls and a recent design guideline (ACI 440.7R 2010) has provided simplified analytical models to calculate the contribution of FRP to out-of-plane strength. Tumialan et al. (2003) carried out an experimental testing on concrete block and clay brick masonry walls strengthened with externally-bonded glass FRP (GFRP) and aramid FRP (AFRP) laminates subjected to out-of-plane loads. Experimental results showed remarkable enhancement in flexural capacity. Galati et al. (2005) performed an experimental program applying out-of-plane loading to concrete block and clay brick walls retrofitted with NSM rectangular GFRP bars. This strengthening system resulted in significantly improved out-of-plane behavior in terms of flexural capacity and stiffness.

Previous studies have investigated FRCM to retrofit reinforced-concrete (RC) members as well as masonry to improve their structural behavior in terms of strength and pseudo-ductility (Faella et al. 2004; Prota et al. 2006; Papanicolaou et al. 2008; D'Ambrisi and Focacci 2011; Ombres 2011; Al-Salloum et al. 2012; Parisi et al. 2012; Babaeidarabad et al. 2013; Loreto et al. 2013). For example, Papanicolaou et al. (2008) tested under out-of-plane cyclic loading perforated clay brick and solid stone block walls strengthened with carbon-FRCM. Test results showed that FRCM provided a remarkable gain in strength and pseudo-ductility.

Study 2 presents an experimental program on 18 masonry walls made of CMU and clay brick externally strengthened with different levels of fabric-reinforced cementitious matrix (FRCM). This study also presents an analysis in accordance to ACI 549 (2013) and MSJC (2011) to predict flexural capacity of URM walls retrofitted with FRCM.

EXPERIMENTAL PROGRAM

Test Matrix

Eighteen URM walls with dimension of 1422 by 1220 by 92 mm (56 by 48 by 3.63 in) were constructed by a professional mason to ensure compliance to building codes and good construction practices. All walls were made of concrete block and clay brick units and were built in a running bond pattern to be tested under out-of-plane loading. Three were control specimens, three were strengthened with 1-ply FRCM completely covering the tension face of the wall, and three were strengthened with 4-ply FRCM in the same fashion. **Figure 20** shows the area where the walls were fabricated, reinforced and tested. The strengthening system installation procedure involved the following steps: a first layer of mortar with the thickness of 5 mm (0.2 in) was applied to the masonry, 1-ply of pre-cut carbon fabric was laid next, and the second layer of mortar with the same thickness was applied and finished. The 3-part installation process is depicted in the three pictures of **Figure 21**. This procedure of alternate fabric and mortar layer was repeated in the case of multi-ply strengthening. The application of the strengthening system was limited to a single face since specimens were tested without reversal of the applied lateral pressure. For field applications, strengthening is typically necessary on both faces. An outline of

test matrix is summarized in **Table 5**. Test specimens were identified using the "A-B" format where: "A" identifies the masonry substrate material: CMU for concrete masonry block and CL for clay brick; while "B" identifies the number of carbon fabric plies (0, 1 or 4). **Table 5** consists of four columns: Column (1) and (2) represent the specimen code and the strengthening material, respectively, while Columns (3) and (4) represent the masonry type and the number of repetitions used for each set of walls.

Material Characterization

Material properties (CMU, clay bricks, a type M mortar, prisms, and FRCM) are given in *Study 1*. The mechanical properties of the masonry prisms and the FRCM coupons were used as the basis of the analytical work to calculate flexural capacity of the FRCM strengthened walls.

Test setup

Test setup used in this experimental program is shown in **Figure 22**. The walls were loaded horizontally by means of a uniformly distributed pressure generated by an air bag capable of applying a maximum pressure of 0.14 MPa (20 psi). The air bag was placed between the test specimens and a reaction wall. Static pressure of an approximate rate of 700 Pa/min (0.1 psi/min) was applied in three cycles of loading and unloading, where the last half-cycle was carried until failure. URM walls were tested in a single half-cycle due to their low strength. A ply-wood sheet 6-mm (0.25 in) thick was placed between the airbag and both test and reaction walls to protect the air bag. Four Dywidag rods and steel channel/tube box sections on the top and bottom of the wall were used to anchor the

specimen to the reaction wall, creating a close-loop system. In the strengthened walls, FRCM was cut just below the supports. These cuts were made to prevent the continuity and the restraint of the fabric reinforcement. This condition is representative of field applications where FRCM cannot be continued passed the slabs (or beams) below and above the wall. However, in order to capture the full flexural capacity of the strengthened walls and avoid pre-mature shear failure at the supports, steel rods with a nominal diameter of 6.35 mm (0.25 in) and length of 406 mm (16 in) were embedded at a depth of 6.35 mm (0.25 in) within the masonry substrate to increase shear capacity without affecting on the flexural capacity. Out-of-plane displacements of the wall specimens were measured using three string-type wire displacement transducers (WDT) located at the supports and at mid-height. In the strengthened walls, strain was measured in the vertical direction with strain gauges at mid-height. Applied pressure was measured with a pressure transducer connected to the air bag outflow. Simultaneously, the support reaction provided by the four Dywidag rods was measured with two 111-kN (25-kip) load cells at the top and with two 222-kN (50-kip) load cells at the bottom. Data were collected at a frequency of 10 Hz using National Instruments data acquisition system operating LabVIEW™ software.

TEST RESULT AND DISCUSSION

Experimental results in terms of maximum moment, average maximum moment for each set, and failure mode are presented in Columns (1), (2) and (3) of **Table 6**, while in Columns (1), (2) of **Table 7** and **Table 8**, results are presented in terms of maximum and average mid-height deflection, and maximum and average FRCM strain. It can be

observed that depending to the amount of the externally-bonded FRCM, higher moment capacity is achieved. Flexural strength enhancement is defined as the ratio between the average maximum moment capacity for each set and the control one. Strength enhancements are found to be 2.7 and 7.8 for concrete block and 2.8 and 7.5 for clay walls, using 1-ply and 4-ply FRCM, respectively.

Crack Pattern and Failure Modes

Un-reinforced masonry — The three URM concrete block and clay brick masonry walls failed in flexure by developing cracks in the mortar joint at mid-height which opened uncontrollably as the load increased (**Figure 23** (a) and (d)). Column (2) in **Table 6** shows that the average maximum moment capacity at failure was 2.37 kN.m (1745.9 lb.ft) and 2.32 kN.m (1713.9 lb.ft) for CMU and clay control walls, respectively. Column (2) in **Table 7** and **Table 8** shows that average maximum mid-height deflection was 0.9 mm (0.03 in) for both CMU and clay brick un-strengthened masonry walls, respectively.

Masonry wall strengthened with 1-ply FRCM— The flexural failure in the three CMU and clay brick walls strengthened with 1-ply FRCM was controlled by fabric slippage within the matrix at the location of the cracks. Eventually, rupture of the fabric occurred with the wall collapse (**Figure 23** (b) and (e)). The average peak moment for three 1-ply FRCM CMU walls was 6.48 kN.m (4777.1 lb.ft) which was about three times that of the control walls; while for the three 1-ply clay walls, the average peak moment was 6.39 kN.m (4715.4 lb.ft) about three times higher that of control clay ones (see

Column (2) in **Table 6**). Column (2) in **Table 7** and **Table 8** shows that average maximum mid-height deflection and strain in the FRCM were 14.7 mm (0.6 in) and 0.0082 mm/mm (0.0082 in/in) for three 1-ply CMU and were 15.9 mm (0.6 in) and 0.0084 mm/mm (0.0084 in/in) for three 1-ply clay brick, respectively.

Masonry wall strengthened with 4-ply FRCM— The three 4-ply FRCM CMU walls reached the maximum loading capacity of the air bag and ultimate failure of the wall was not reached (**Figure 23** (c)). The three clay walls strengthened with 4-ply FRCM experienced shear failure due to large amount of FRCM reinforcement. Shear failure was identified by development of fine vertical cracks in the masonry substrate near the supports that progressed at a slope of approximately 45°, as shown in **Figure 23** (f) with enhanced crack lines. Column (2) in **Table 6** shows average maximum moment capacity of 18.49 kN.m (13640.6 lb.ft) for the case of 4-ply FRCM CMU wall about three times that of 1-ply ones and 17.46 kN.m (12874.8 lb.ft) for the case of clay walls strengthened with 4-ply FRCM also about three times that of 1-ply FRCM clay wall. The average maximum mid-height deflection and strain in the FRCM were found to be 4.7 mm (0.2 in) and 0.0045 mm/mm (0.0045 in/in) for the case of three CMU walls strengthened with 4-ply FRCM; while for the case of 4-ply FRCM clay brick walls, those were found to be 6.6 mm (0.3 in) and 0.0048 mm/mm (0.0048 in/in), respectively (see Column (2) in **Table 7** and **Table 8)**.

Moment-Deflection

Figure 24 (a) to (f) presents the moment versus deflection curves for three sets of walls, respectively. Each diagram displays three curves representing the three replications (all figures are plotted to the same scale for ease of comparison). The horizontal lines correspond to the values obtained by analysis and design according to ACI 549 (2013).

It can be observed that depending on FRCM amount, the moment capacity and stiffness increased drastically. The test outcomes show a clear and consistent pattern and the moment-deflection curves in the strengthened walls present two distinct phases, namely: cracking and ultimate. The first phase is the result of the masonry mortar reaching the tensile capacity and is almost linear up to cracking. Initial cracking was delayed due to the presence of FRCM in both 1- ply and 4-ply cases. The second phase can be approximated by a straight line representing the tensile contribution of the FRCM reinforcement with slope obviously function of the FRCM amount. FRCM increases pseudo-ductility; however, the wall strengthened with 1-ply FRCM achieved more pseudo-ductility than the 4-ply one (also because in this instance, shear controls the failure).

Analytical Approach

According to the Masonry Standards Joint Committee (MSJC) (2011), nominal flexural strength of un-reinforced walls is equal to the cracking moment calculated based on the moment modulus of rupture in accordance with **Equation 10**:

$$\phi_m M_n = \phi_m M_{cr} \quad \textbf{(10)}$$

where:

$$M_{cr} = S f_r \quad \textbf{(10-a)}$$

where M_n, M_{cr}, ϕ_m, S, and f_r are the nominal flexural strength, cracking flexural strength, flexural strength reduction factor, section modulus of the un-cracked wall, and modulus of rupture, respectively. Following the recommendations of the MSJC (2011), the allowable modulus of rupture, f_r, for clay masonry with a type M mortar is taken as 0.43 MPa (63 psi).

To predict nominal flexural strength of FRCM strengthened walls, analytical calculations are developed based on the procedure as per ACI 549 (2013): a) plane sections remain plane; b) the bond between the FRCM and the substrate as well as the fabric within the matrix is perfect; c) a parabolic distribution is used for compressive stresses of the masonry. The stress block parameters, β_1 and γ, associated with such a parabolic distribution are expressed in **Equation 11** (a) and (b) (Tumialan et al. 2003; Turco et al. 2003; Galati et al. 2005):

$$\gamma\beta_1 = \frac{\varepsilon_m}{\varepsilon_m'} - \frac{1}{3}\left(\frac{\varepsilon_m}{\varepsilon_m'}\right)^2 \quad \textbf{(11-a)}$$

$$\gamma\beta_1\left(1 - \frac{1}{2}\beta_1\right) = \frac{2}{3}\left(\frac{\varepsilon_m}{\varepsilon_m'}\right) - \frac{1}{4}\left(\frac{\varepsilon_m}{\varepsilon_m'}\right)^2 \quad \textbf{(11-b)}$$

where β_1 is the ratio of depth of equivalent rectangular stress block to depth to neutral axis, and γ is multiplier of f'_m to determine intensity of the equivalent block stress for masonry. β_1 and γ are assumed equal to 0.7 for simplicity (Tumialan et al. 2003; ACI 549 2013). ε_m and ε'_m are compressive strain in masonry and maximum compressive strain in masonry associated to peak f'_m, respectively. d) failure modes are controlled either by slipping in the FRCM or crushing of the masonry (ACI 549 2013); e) the maximum compressive strain, ε'_m, for concrete and clay masonry is considered to be 0.0025 mm/mm (in/in) and 0.0035 mm/mm (in/in) (Tumialan et al. 2003; Galati et al. 2005; MSJC 2011); f) the tensile strength of the masonry is neglected (Tumialan et al. 2003; Galati et al. 2005; MSJC 2011; ACI 549 2013); and, g) FRCM has a bi-linear elastic behavior up to failure controlled by slip. As per ACI 549 (2013), the ultimate tensile strain for FRCM design considerations, ε_{fu}, is the average minus one standard deviation derived from tensile test conducted as per AC434 (2013).

The effective tensile strain level in FRCM at failure, ε_{fe}, is limited to the ultimate tensile strain, ε_{fu}, shown in **Equation 12**.

$$\varepsilon_{fe} = \varepsilon_{fu} \leq 0.012 \qquad (\mathbf{12})$$

The effective tensile stress level in the FRCM reinforcement attained at failure, f_{fe}, is calculated in accordance with **Equation 13**:

$$f_{fe} = E_f \varepsilon_{fe} \quad \textbf{(13)}$$

where E_f is the tensile modulus of elasticity of the cracked FRCM.

The analytical flexural capacity of an FRCM strengthened wall is determined based on strain compatibility, internal force equilibrium and the controlling mode of failure, calculated in accordance with **Equation (14)** to (**16)**:

$$\phi_m M_n = \phi_m M_f \quad \textbf{(14)}$$

where M_n is the nominal flexural strength, and M_f is the contribution of FRCM. M_f is expressed in accordance with **Equation 15**:

$$M_f = A_f f_{fe}(t_m - \frac{\beta_1 c}{2}) \quad \textbf{(15)}$$

where:

$$T = A_f f_{fe} = \gamma f_m^{'}(\beta_1 c) b_m = C \quad \textbf{(15-a)}$$

where T, A_f, t_m, c, b_m , f'_m, and C are the tension provided by FRCM, area of the fabric reinforcement per unit width, thickness of the wall, distance from extreme compression fiber to neutral axis, width of masonry wall considered in flexural analysis, compressive strength of masonry, and compression force provided by masonry, respectively.

The effective tensile strain level in FRCM, ε_{fe}, and the compressive strain in the masonry, ε_m, are related in accordance with **Equation 16**:

$$\frac{\varepsilon_m}{c} = \frac{\varepsilon_{fe}}{t_m - c} \quad \textbf{(16)}$$

In the analysis, the wall is assumed to behave as a simply supported element and the arching effect is neglected. An analytical mid-height deflection, δ_u, for un-reinforced and strengthened masonry walls is calculated in accordance with **Equations 17** and **18**, respectively (MSJC 2011; Brandow et al. 2009):

$$\delta_u = \frac{5M_{cr}h_{eff}^2}{48E_m I_n} \quad \textbf{(17)}$$

where h_{eff}, E_m, I_n are the clear height of the wall, modulus of elasticity of the masonry, and un-cracked moment of inertia of the wall, respectively.

$$\delta_u = \frac{5M_{cr}h_{eff}^2}{48E_m I_n} + \frac{5(M_n - M_{cr})h_{eff}^2}{48E_m I_{cr}} < 0.007h_{eff} \quad \textbf{(18)}$$

where I_{cr} is the cracked moment of inertia of the strengthened wall. The cracked moment of inertia is the summation of the moment of inertia of the masonry and transformed area of FRCM about the neutral axis, expressed in accordance with **Equation 18-a**:

$$I_{cr} = \frac{b_m c^3}{3} + \frac{E_f}{E_m} A_f (t_m - c)^2 \quad \textbf{(18-a)}$$

where E_f and E_m are the modulus elasticity of FRCM and masonry, respectively.

In the analysis, the flexural strength reduction factor is assumed equal to be 1.0. The appendix B demonstrates the procedure used for calculation of moment capacity (analytical and design) for clay wall strengthened with 1-ply FRCM using actual geometry and properties obtained from prism and coupon testing. The analytical model underestimates the flexural capacity of strengthened walls, since arching is disregarded. This approach predicts that flexural failure is the controlling mode for both masonry walls strengthened with 1 and 4-ply FRCM. Analytical flexural capacities and failure modes are presented in columns (4) and (5) in **Table 6** and **Figure 24** (a) to (f) (horizontal dash lines). **Figure 25** compares experimental and analytical flexural moment capacity of masonry walls retrofitted with FRCM.

Design Provisions

ACI 549 (2013) establishes design provisions by limiting the maximum force transferred by the FRCM to 87.6 kN/m (6,000 lbf/ft) in strengthened URM walls subjected to out-of-plane loading as expressed in **Equation 19**:

$$T = A_f E_f \varepsilon_{fe} < 87.6 \frac{kN}{m} (6000 \frac{lbf}{ft}) \quad (\mathbf{19})$$

Additionally, the flexural strength reduction factor, ϕ_m, is equal to 0.6, which is similar to the reduction factor recommended by the MSJC (2011) for URM walls subjected to flexural loads. The conservative reduction factor is in recognition of a section with low ductility that requires a higher reserve of strength. Following the recommendation of

MSJC (2011), the shear strength reduction factor, ϕ_v, is considered equal to be 0.8. It can be observed that applying the flexural strength reduction factor in the design provisions makes the difference between experimental and design values more profounded (column (7) of **Table 6** and **Figure 24** (a) to (f) (horizontal solid lines)). **Figure 26** compares experimental and design moment values for FRCM walls.

CONCLUSIONS

Experimental testing on CMU and clay brick masonry walls retrofitted with FRCM resulted in the following conclusions:

1. The experimental results proved the technical feasibility of FRCM strengthening of concrete block and clay brick URM walls. In terms of ultimate out-of-plane moment capacity, depending on the amount of FRCM, flexural strength can be significantly increased. The flexural enhancement was calculated to be 2.7 and 7.8 for CMU masonry and 2.8 and 7.5 for clay brick wall, using 1-ply and 4-ply carbon FRCM, respectively.

2. Two basic modes of failure were observed: cracking of the masonry at the mid-height with FRCM slippage, and shear failure in the substrate at the supports depending on FRCM amount.

3. Based on the results obtained from moment-deflection diagrams, it can be observed that FRCM is effective in increasing stiffness and pseudo-ductility; however, pseudo-ductility is higher for lower FRCM amounts (i.e., pseudo-ductility of 4-ply strengthened wall is limited by shear failure).

4. A sectional analysis according to the methods proposed by MSJC (2011) and ACI 549 (2013) is used to predict flexural capacity. Analytical results underestimate the experimental database, since arching mechanism is disregarded. Similarly, design flexural capacity values are very conservative when applying limitations and the flexural strength reduction factor, ϕ_m, as per ACI 549 (2013).

NOTATIONS

A_f = area of fabric reinforcement by unit width, mm^2/mm (in^2/in)

b_m = width of masonry wall considered in flexural analysis, mm (in)

c = distance from extreme compression fiber to neutral axis, mm (in)

C = compression force provided by masonry, kN (kip)

E^*_f = tensile modulus of elasticity of the un-cracked FRCM specimen, MPa (ksi)

E_f = tensile modulus of elasticity of the cracked FRCM specimen, MPa (ksi)

E_m = modulus of elasticity of masonry wall, MPa (ksi)

f'_m = compressive strength of masonry, MPa (psi)

f_{fe} = effective tensile stress level in FRCM attained at failure, MPa (ksi)

f_{ft} = transition stress corresponding to the transition point, MPa (psi)

f_{fu} = ultimate tensile strength of FRCM, MPa (ksi)

f_r = modulus of the rupture, kPa (psi)

H = height of the wall, mm (in)

h_{eff} = clear height of the wall, mm (in)

I_{cr} = cracked moment of inertia of the strengthened wall, mm^4 (in^4)

I_n = un-cracked moment of inertia of the wall, mm^4 (in^4)

L = length of the wall, mm (in)

M_{cr} = cracking flexural strength, kN-m (lb-ft)

M_f = contribution of FRCM, kN-m (lb-ft)

M_n = nominal flexural strength, kN-m (lb-ft)

p_u = ultimate lateral uniform pressure, kPa (psf)

S = sectional modulus of un-cracked wall, cm^3 (in^3)

T = tension force provided by FRCM, kN (kip)

t_m = thickness of the wall, mm (in)

T_{max} = maximum force in the FRCM transferred to the masonry per unit width, kN/m (lbf/ft)

W_u = ultimate lateral unit load, kN/m (lbf/ft)

β_1 = ratio of depth of equivalent rectangular stress block to depth to neutral axis

γ = multiplier of f'_m to determine intensity of the equivalent block stress for masonry

δ_u = mid-height deflection for un-reinforced and strengthened wall, mm (in)

ε'_m = maximum compressive strain in masonry associated to peak f'_m, mm/mm (in/in)

ε_{fe} = effective tensile strain level in FRCM composite material attained at failure, mm/mm (in/in)

ε_{ft} = transition strain corresponding to the transition point, mm/mm (in/in)

ε_{fu} = ultimate tensile strain level in FRCM, mm/mm (in/in)

ε_{m} = compressive strain in masonry, mm/mm (in/in)

ϕ_{m} = flexural strength reduction factor

Table 5 – Out-of-plane test matrix

Specimen Code (1)	**Strengthening Material (2)**	**Masonry Type (3)**	**Repetitions (4)**
CMU-Control	None	Concrete Block	3
CMU-1	1-ply of FRCM		
CMU-4	4-ply of FRCM		
CL-Control	None	Clay Brick	3
CL-1	1-ply of FRCM		
CL-4	4-ply of FRCM		

Table 6– Test results: experimental, analytical, and design

Specimen ID	Experimental Results			Analytical Results		Exp./An. Ratio	Design Results*	Exp./Des. Ratio
	Moment			Moment			Moment	
	Max. M_u kN.m (1)	Ave. $M_{u,ave}$ kN.m (2)	Failure Mode (3)	Max. $M_{n,An}$ kN.m (4)	Failure Mode (5)	$M_{u,avg}$ /$M_{n,An.}$ - (6)	Max. ϕ_m $M_{n,Des}$ kN.m (7)	$M_{n,avg}$ / ϕ_m $M_{n,Des.}$ - (8)
CMU-Control-1	2.15		F					
CMU-Control-2	2.32	2.37	F	0.75	F	3.2	0.5	5.3
CMU-Control-3	2.63		F					
CMU-1 ply-1	6.09		F					
CMU-1 ply-2	6.35	6.48	F	3.86	F	1.7	2.3	2.8
CMU-1 ply-3	6.99		F					
CMU-4 ply-1	18.49		N/A**					
CMU-4 ply-2	18.49	18.49	N/A**	14.79	F	1.3	5.7	3.2
CMU-4 ply-3	18.49		N/A**					
CL-Control-1	2.14		F					
CL-Control-2	2.57	2.32	F	0.75	F	3.1	0.5	5.2
CL-Control-3	2.27		F					
CL-1 ply-1	6.57		F					
CL-1 ply-2	6.2	6.39	F	3.87	F	1.7	2.3	2.8
CL-1 ply-3	6.4		F					
CL-4 ply-1	17.62		S					
CL-4 ply-2	16.94	17.46	S	14.95	F	1.2	5.7	3.0
CL-4 ply-3	17.81		S					

(Note: 1.0 kN.m = 737.56 lb.ft; 1.0 kN = 0.23 kip; Slenderness ration (h/t) = 13.2; Strengthening material: C-FRCM on tension side; F = Flexural failure; S = Shear failure; *ϕ factors and other limits apply; **The shear failure expected, exceeded equipment capacity)

Table 7– Test results: maximum mid-height deflection

Specimen ID	Experimental Results		Analytical Results
	Max. Displacement δ_u **mm** **(1)**	**Ave. Displacement** $\delta_{u,ave}$ **mm** **(2)**	**Max. Displacement** $\delta_{u,An.}$ **mm** **(3)**
CMU-Control-1	1.1	0.9	0.1
CMU-Control-2	0.8		
CMU-Control-3	0.9		
CMU-1 ply-1	13.9	14.7	8.5
CMU-1 ply-2	14.1		
CMU-1 ply-3	16.0		
CMU-4 ply-1	4.3	4.7	8.5
CMU-4 ply-2	4.8		
CMU-4 ply-3	5.0		
CL-Control-1	1.0	0.9	0.1
CL-Control-2	0.9		
CL-Control-3	0.7		
CL-1 ply-1	16.9	15.9	8.5
CL-1 ply-2	15.8		
CL-1 ply-3	14.9		
CL-4 ply-1	5.2	6.6	8.5
CL-4 ply-2	7.0		
CL-4 ply-3	7.7		

(Note: 1.0 mm=0.039 in)

Table 8– Test results: maximum mid-height strain

Specimen ID	Experimental Results		Analytical Results
	Max. Strain ε_{FRCM} **mm/mm (1)**	**Ave. Strain** $\varepsilon_{FRCM,ave}$ **mm/mm (2)**	**Max. Strain** $\varepsilon_{FRCM,An.}$ **mm/mm (3)**
CMU-Control-1 CMU-Control-2 CMU-Control-3	-	-	-
CMU-1 ply-1 CMU-1 ply-2 CMU-1 ply-3	0.0082 0.0084 0.0080	0.0082	0.0086
CMU-4 ply-1 CMU-4 ply-2 CMU-4 ply-3	0.0045 0.0045 0.0045	0.0045	0.0086
CL-Control-1 CL-Control-2 CL-Control-3	-	-	-
CL-1 ply-1 CL-1 ply-2 CL-1 ply-3	0.0084 0.0080 0.0087	0.0084	0.0086
CL-4 ply-1 CL-4 ply-2 CL-4 ply-3	0.0048 0.0048 0.0049	0.0048	0.0086

(Note: 1.0 mm/mm=1.0in/in)

(a)

(b)

Figure 19- Out-of-plane failures of load-bearing walls

Umbria, Italy, 1997

Figure 20- Masonry walls fabrication and test site

(a) (b) (c)

Figure 21- FRCM installation: first layer of mortar (a); pre-cut carbon fabric (b); second layer of mortar (c)

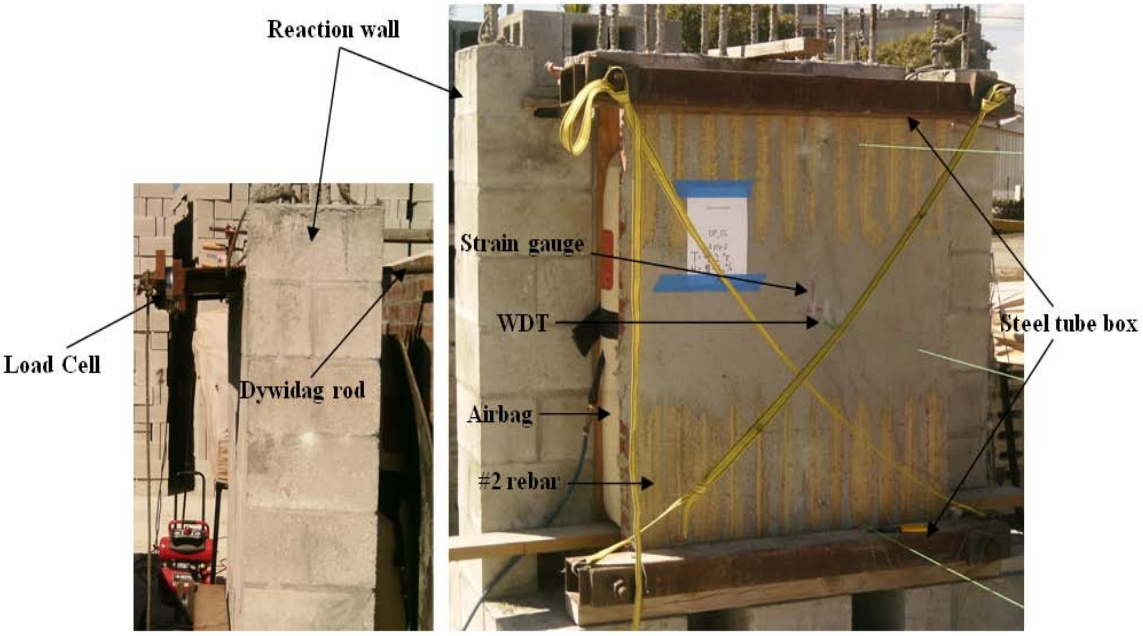

Figure 22- Out-of-plane test setup

(a)

(b) (Fabric breaks because of collapse)

(c)

(d)

(e) (Fabric breaks because of collapse)

(f) (Enhanced crack lines)

Figure 23- Failure mode of wall specimens:

CMU-Control (a); CMU-1 ply (b); CMU-4 ply (c)

CL-Control (d); CL-1 ply (e); CL-4 ply (f)

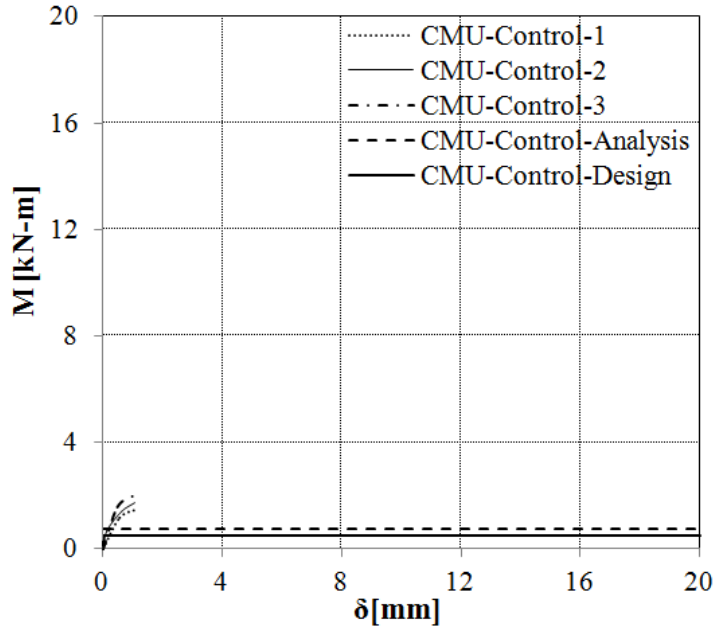
CMU-Control-1
CMU-Control-2
CMU-Control-3
CMU-Control-Analysis
CMU-Control-Design
M [kN-m]
δ[mm]
0
4
8
12
16
20

(a)

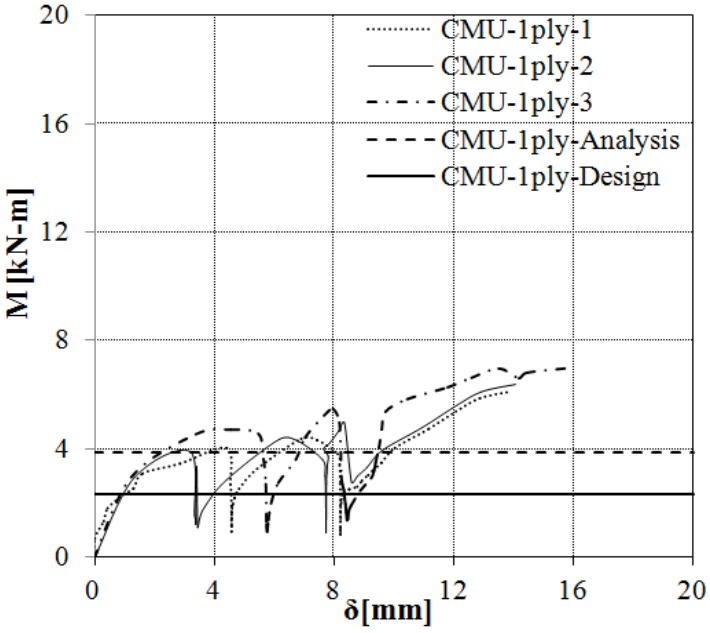
CMU-1ply-1
CMU-1ply-2
CMU-1ply-3
CMU-1ply-Analysis
CMU-1ply-Design
M [kN-m]
δ[mm]
0
4
8
12
16
20

(b)

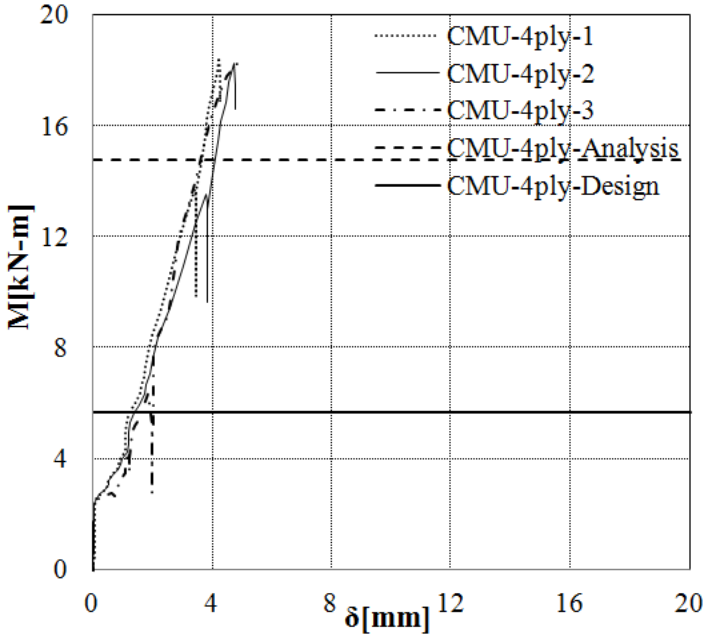
CMU-4ply-1
CMU-4ply-2
CMU-4ply-3
CMU-4ply-Analysis
CMU-4ply-Design
M[kN-m]
δ[mm]
0
4
8
12
16
20

(c)

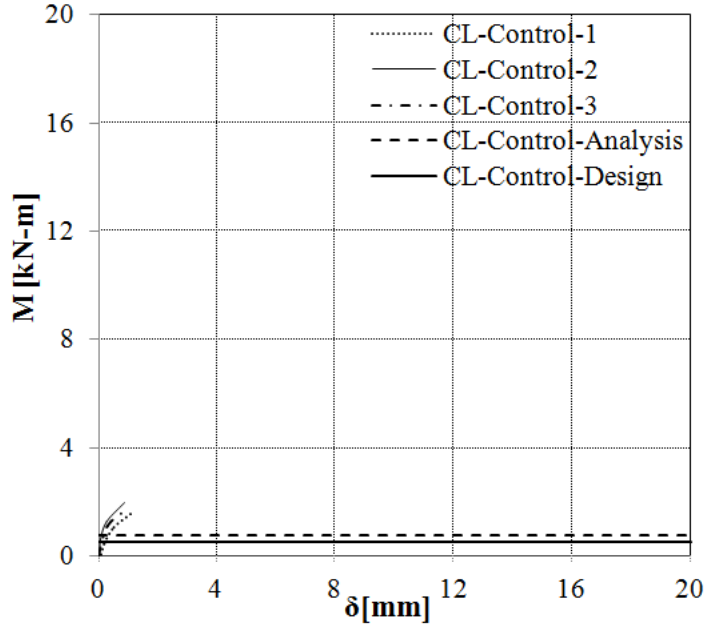
CL-Control-1
CL-Control-2
CL-Control-3
CL-Control-Analysis
CL-Control-Design
M [kN-m]
δ[mm]
0
4
8
12
16
20

(d)

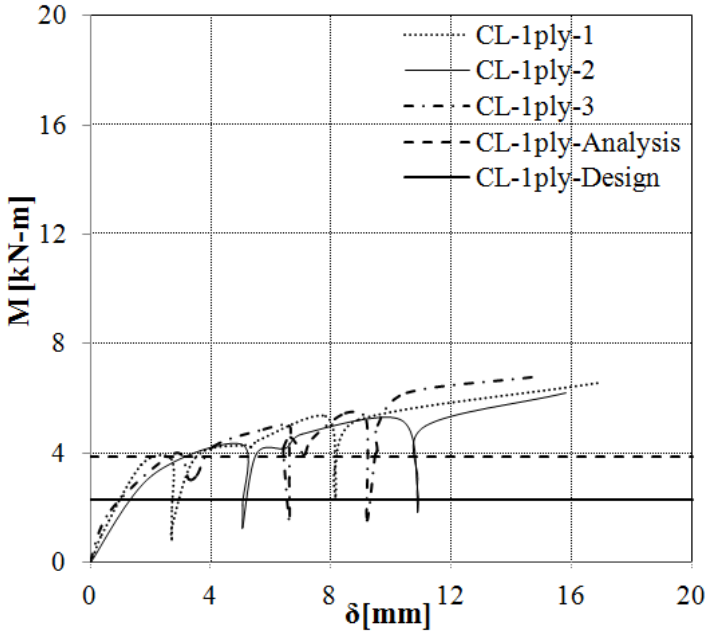

(e)

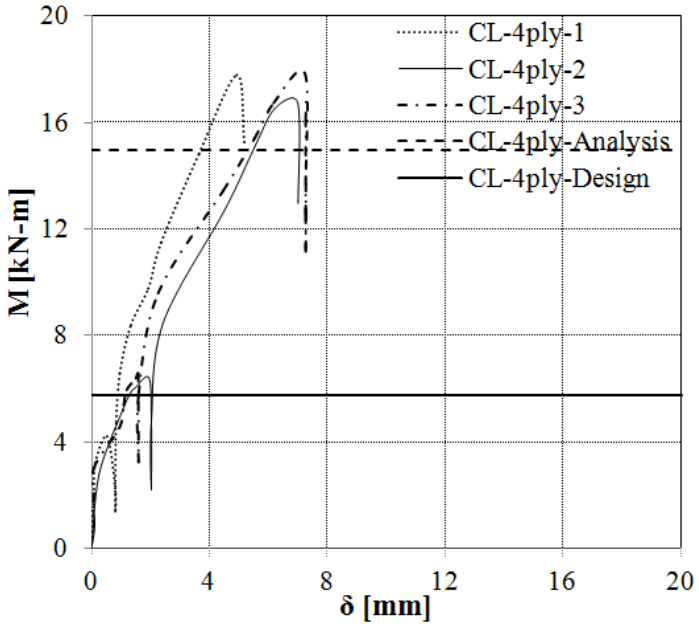

(f)

Figure 24- Moment-deflection diagrams of wall specimens:

CMU-Control (a); CMU-1 ply (b); CMU-4 ply (c)

CL-Control (d); CL-1 ply (e); CL-4 ply (f)

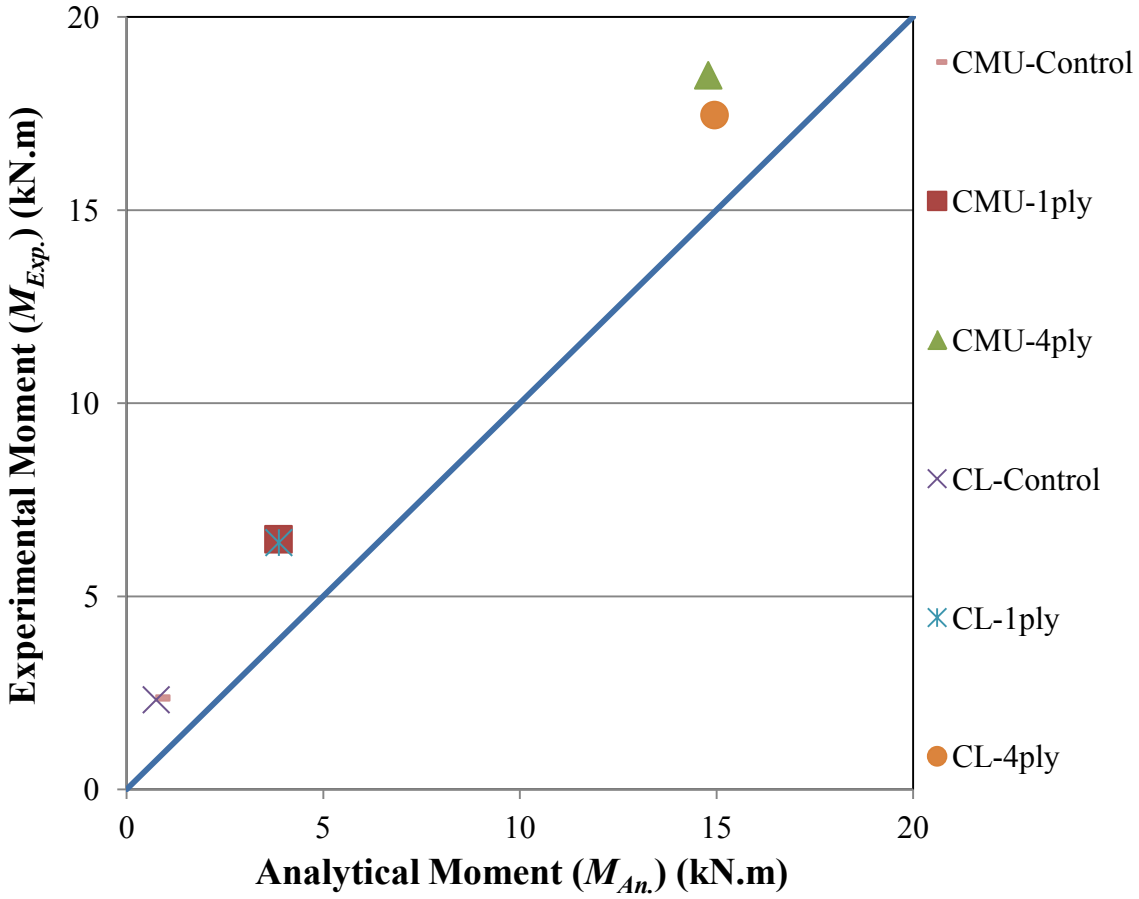

Figure 25- Comparison between experimental and analytical results

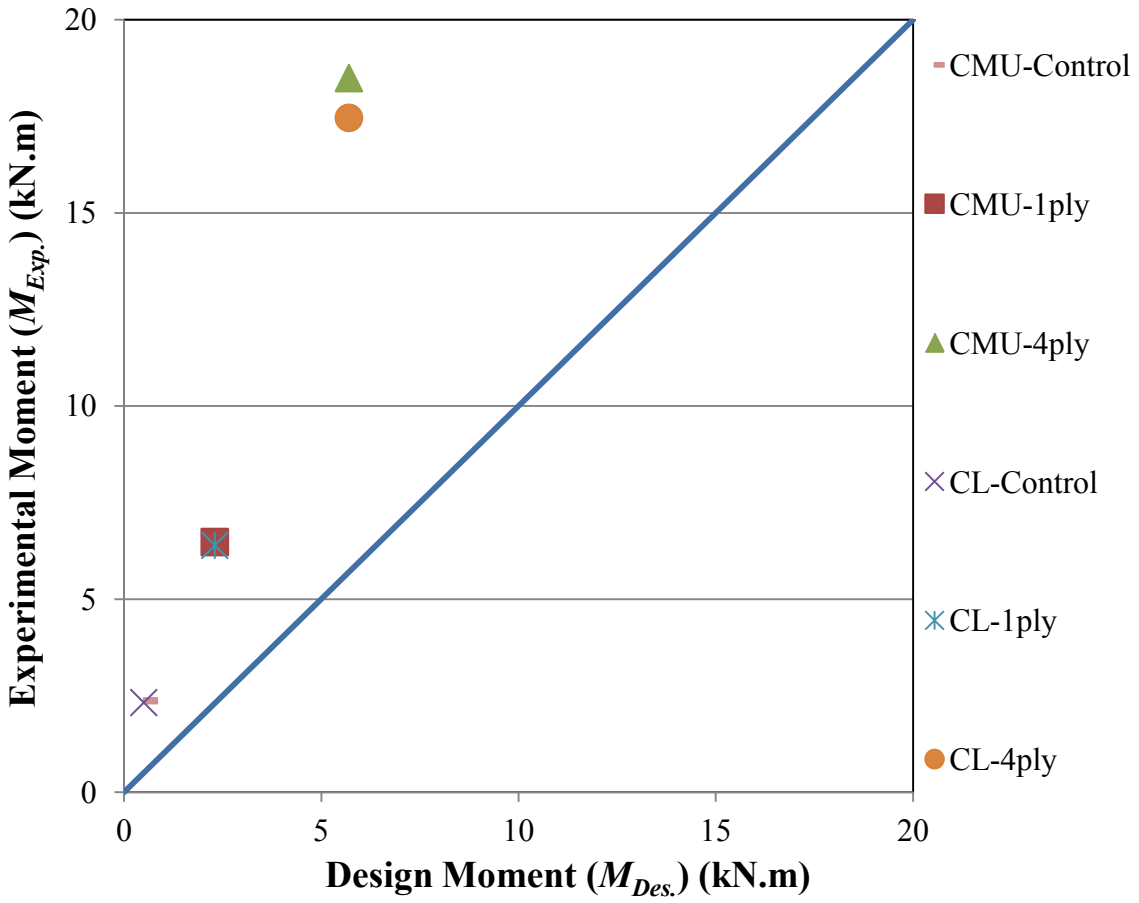

Figure 26- Comparison between experimental and design results

CHAPTER IV

*STUDY 3*_ COMPARISON BETWEEN FRCM AND FRP STRENGHENED WALLS

In *study 3*, experimental results under in-plane diagonal compression and flexural loading on CMU and clay brick masonry walls retrofitted with FRP system are reported from other research programs. It is shown that after normalizing the shear and flexural capacity according to a calibrated reinforcement ratio, the two strengthening technologies are comparable and provide similar enhancements. All tests conducted in the laboratory by various researchers were performed on newly constructed masonry walls with new brick and CMU; therefore, the quality of the bond among different research program is not affected by the substrate. In particular application, when strengthening is done on the wall, the quality affect bond and performance of the substrate.

BACKGROUND

Sixteen CMU and 18 clay brick walls were strengthened with FRP system and tested to failure under diagonal force (Tinazzi 2000; Tumialan 2001; Morbin 2002; Grando et al. 2003; Li et al. 2005; Yu et al. 2007).

Tumialan et al. (2003) and Galati et al. (2005) conducted under out-of-plane loading a total of 19 CMU concrete block walls and 12 clay brick walls strengthened with FRP with different strengthening schemes.

COMPARISON OF TEST RESULTS FOR IN-PLANE LOAD

Table 9 and **Table 10** presents the shear strengthening schemes of 16 concrete block and 18 clay brick masonry walls tested under diagonal in-plane compression in other research programs. The original specimen labels are maintained and the last name of the first author is presented (Columns (1) and (2)). The strengthening methods included horizontal and vertical NSM GFRP bars, GFRP and CFRP laminates, and GFRP grid reinforced polyurea (Columns (3)) (Tinazzi 2000; Tumialan 2001; Morbin 2002; Grando et al. 2003; Li et al. 2005; Yu et al. 2007).

Experimental results obtained from this research program using FRCM system are compared to those derived from other research programs using FRP after normalizing shear capacity (see **Table 11** and **Table 12**).

The wall calibrated reinforcement ratio, ω_s, is defined as $\rho E_f/E_m$ (see Column (5) of **Table 11** and **Table 12**); where ρ is the ratio between the FRCM or (FRP) reinforcement area (in both horizontal and vertical directions) (Column (1)) and the net masonry area (Column (2)), E_f and E_m are the moduli elasticity of FRCM or (FRP) (Column (3)) and masonry (Column (4)), respectively.

The calibrated reinforcement ratio is an index that includes the main parameters affecting the shear capacity and failure mode. This index represents the axial stiffness ratio. The shear capacity of each wall is normalized as shear strength by dividing the shear force by the cross-sectional area.

Table 11, **Table 12**, **Figure 27**, and **Figure 28** illustrate the shear strength (Column (7)) as a function of the calibrated reinforcement ratio. It can be observed that the shear strength increases proportionally to the calibrated reinforcement ratio, and for the same calibrated reinforcement ratio, results achieved in this test program match well with FRP. Accordingly, there is no substantial difference between FRCM and FRP strengthening technologies if normalized to the calibrated reinforcement ratio. When the calibrated reinforcement ratio index exceeds 1.5%, for the concrete and 4% for the clay brick walls, substrate toe compression controls the failure mode; therefore, adding more reinforcement may be ineffective.

COMPARISON OF TESTS RESULTS FOR OUT-OF-PLANE LOAD

Table 13 and **Table 14** summarize the retrofitting layout of 19 concrete block and 12 clay brick masonry wall specimens tested under out-of-plane loading in other research project strengthened with FRP. The original specimen identification including the last name of the first author and year of publication is presented in Columns (1) and (2) of

Table 13 and **Table 14,** while Column (3) presents the strengthening schemes including externally-bonded GFRP and AFRP laminates and vertical NSM rectangular GFRP bars (Tumialan et al. 2003; Galati et al. 2005).

Experimental data base reported from other research program using FRP system are compared with this research program after normalizing the results. The calibrated reinforcement ratio, ω_f, is defined as $\rho E_f / f'_m(h_{eff}/t_m)$ (Columns (5) of **Table 15** and **Table 16**); where ρ is the ratio between area of FRCM (or FRP) reinforcement and net area of un-cracked URM wall (Columns (1)), E_f is the modulus elasticity of FRCM/FRP ((Columns (3)), f'_m is the compressive strength of masonry (Columns (4)), and (h_{eff}/t_m) is wall slenderness ratio ((Columns (2))). The calibrated reinforcement ratio is an index that intends to capture the key parameters that influence the flexural capacity. This index represents the ratio of axial stiffness for FRCM and masonry ($A_f E_f / A_n E_m$), but since the E_m is directly proportional to f'_m, the latter can replace E_m (Tumialan et al. 2003; Turco et al. 2003; Galati et al. 2005). The inclusion of the slenderness ratio h_{eff}/t_m has been recognized as a key factor in the out-of-plane behavior of masonry, and accounts for the ability of the wall behavior to be controlled by flexural failure rather than shear failure. The slenderness ratios and the out-of-plane capacity are inversely proportional: as the slenderness ratio decreases, the out-of-plane strength becomes larger (Angel et al. 1994; Tumialan et al. 2003; Turco et al. 2003; Galati et al. 2005).

In order to find normalized flexural capacity (Columns (7) **Table 15** and **Table 16**), **Equation 13** is substituted into **Equation 15**. By dividing both terms by the factor, $b_m t^2{}_m f'_m (h_{eff}/t_m)$, and considering ϕ_m equal to 1.0, **Equation 20** is obtained:

$$\frac{M_n}{b_m t_m^2 f_m^{'}(^{h_{eff}}/_{t_m})} = \frac{\rho E_f}{f_m^{'}\left(^{h_{eff}}/_{t_m}\right)} \varepsilon_{fe}\left(1 - \frac{\beta_1 c}{2t_m}\right) \qquad \textbf{(20)}$$

Finally, replacing **Equation 13** and **Equation 15-a** into **Equation 20** with using ω_f definition and manipulating mathematically, explicit relation between normalized flexural capacity and calibrated reinforcement ratio is derived in accordance with **Equation 21**:

$$\frac{M_n}{b_m t_m^2 f_m^{'}(^{h_{eff}}/_{t_m})} = \omega_f \varepsilon_{fe}\left(1 - \frac{\omega_f \varepsilon_{fe}}{2} \frac{(^{h_{eff}}/_{t_m})}{\gamma}\right) \qquad \textbf{(21)}$$

Table 15, **Table 16**, **Figure 29**, and **Figure 30** show the normalized experimental flexural moment capacity in the strengthened walls as a function of the calibrated reinforcement ratio. It can be observed that the flexural capacity increases proportionally to the calibrated reinforcement ratio, and for the same level of ω_f, test results achieved in this project are in good agreement with the FRP experimental results. It is understood that there is not significant difference between FRCM and FRP strengthening systems if flexural capacity is normalized according to the calibrated reinforcement ratio. Additionally, when the calibrated reinforcement ratio index, ω_f, is higher than 0.8 for the

concrete and 0.6 for the clay brick walls, shear failure is the controlling mode; therefore, adding more reinforcement may be unproductive.

CONCLUSIONS

The objectives of this study are to compare the FRCM and FRP retrofitted CMU and clay brick masonry walls. The following conclusions are drawn:

1. Experimental evidence showed that shear capacity of the strengthened walls well correlates to the calibrated reinforcement ratio, ω_S, derived as the ratio of axial stiffness of FRCM and masonry $A_f E_f / A_n E_m$. For the same level of ω_S, FRCM and FRP provide comparable enhancements in shear capacity. The substrate toe crushing failure occurs in the strengthened walls with the calibrated reinforcement ratio higher than 1.5% for the concrete and 4% for the clay brick walls. Consequently, increment of FRCM/ (or FRP) beyond these values may be unproductive.

2. Based on the out-of-plane loading test results, for the same level of ω_f, FRCM and FRP strengthening methods are comparable and provide similar increments in flexural capacity if normalized according to calibrated reinforcement ratio. For ω_f larger than 0.8 for the concrete and 0.6 for the clay brick walls, shear controls the failure mode. Increments of FRCM/ (or FRP) beyond this value may be unproductive.

NOTATIONS

A_f = area of mesh reinforcement by unit width, mm^2/mm (in^2/in)

A_n = cross-sectional net area of masonry wall, mm^2/mm (in^2/in)

b_m = width of masonry wall considered in flexural analysis, mm (in)

c = distance from extreme compression fiber to neutral axis, mm (in)

E_f = tensile modulus of elasticity of the cracked FRCM specimen and other strengthening system, MPa (ksi)

E_m = modulus of elasticity of masonry wall, MPa (ksi)

f'_m = specified compressive strength of masonry, MPa (psi)

h_{eff} = clear height of masonry wall, mm (in)

M_n = nominal flexural strength, kN-m (lb-ft)

t_m = thickness of masonry wall, mm (in)

V_n = nominal shear, kN (kip)

β_1 = ratio of depth of equivalent rectangular stress block to depth to neutral axis

γ = multiplier of f'_m to determine intensity of the equivalent block stress

ε_{fe} = effective tensile strain of the FRCM, mm/mm (in/in)

τ_u = shear stress of the masonry at ultimate, MPa (psi)

ω_f = calibrated reinforcement ratio

ρ = the ratio between area of reinforcement and net area of URM walls

Table 9– Shear strengthening schemes of concrete block walls with FRP

Resources (1)	Specimen ID (2)	Strengthening Schemes (3)
Yu et al. 2007	WC1	Four 114 mm wide horizontal GFRP grid -polyurea strip at 305 mm on centers
	WC2	
	WC3	Four 114 mm wide vertical GFRP grid -polyurea strip at 305 mm on centers
	WC4	
Li et al. 2005	COW 2	Seven 6.4 mm diameter GFRP bars at every bed joint
	COW 3	Four 6.4 mm diameter GFRP bars at every other bed joint (front) and three 6.4 mm diameter GFRP bars at every other bed joint (back)
	COW 8	Seven 6.4 mm diameter GFRP bars at every bed joint
	COW 9	Seven 6.4 mm diameter GFRP bars every bed joint and four vertical GFRP strips
	COW 10	Seven 6.4 mm diameter GFRP bars at every bed joint
	COW 11	Four 6.4 mm diameter GFRP bars at every second bed joint
	COW 12	Three 6.4 mm diameter GFRP bars at every second bed joint
Grando et al. 2003	WL 2	GFRP laminates with the thickness of 51 mm at every joint
	WL 3	GFRP laminates with the thickness of 76 mm at every two joints
Tumialan 2001	Wall IL2	Seven 6.4 mm GFRP bars at every horizontal joint
	Wall IL3	Seven 6.4 mm GFRP bars at every horizontal and three 6.4 mm GFRP bars at every vertical joints
	Wall IL4	Seven 6.4 mm GFRP bars at every horizontal joints (front) and three 6.4 mm GFRP bars at vertical joints (back)

(Note: 1 mm=0.039 in)

Table 10– Shear strengthening schemes of clay brick walls with FRP

Resources (1)	**Specimen ID (2)**	**Strengthening Schemes (3)**
Yu et al. 2007	WK1	Four 114 mm. wide horizontal GFRP grid reinforced polyurea strip at 305 mm. on centers
	WK2	
	WK3	Four 114 mm. wide vertical GFRP grid reinforced polyurea strip at 305 mm. on centers
	WK4	
Grando et al. 2003	CL B1	Seven 6.4 mm. GFRP circular bars, one for second mortar joint
	CL B2	
	CL 1	Five 76 mm. wide CFRP laminates strips every 152 mm.
	CL 2	
Morbin 2002	CLW 3	Twelve 6.4 mm. GFRP bars, one for every fourth mortar joint
Tinazzi 2000	Wall 1	Four 6.4 mm. GFRP circular bars, one for every second mortar joint
	Wall 2	Eight 6.4 mm. GFRP circular bars, one for every mortar joint
	Wall 3	
	Wall 4	Eight 6.4 mm. vertical GFRP circular bars
	Wall 5	Four 100 mm. wide vertical GFRP laminates strips
	Wall 6	Four 100 mm. wide horizontal GFRP laminates strips ,and four 100 mm. wide vertical GFRP laminates strips
	Wall 7	Eight 6.4 mm. GFRP circular bars, one for every mortar joint in one face, and eight 6.4 mm. vertical GFRP circular bars in the other face
	Wall 8	Eight 6.4 mm. GFRP circular bars, one for every mortar joint in one face, and four 100 mm. wide vertical GFRP laminates strips in the other face
	Wall 9	Eight 6.4 mm. GFRP circular bars, one for every mortar joint in one face, and four 100 mm. wide vertical GFRP laminates strips and two 6.4 mm. GFRP circular bars in the other face

(Note: 1 mm=0.039 in)

Table 11– FRCM and FRP reinforced CMU walls subjected to in-plane load

Specimen ID		Area of FRCM or FRP A_f mm^2 (1)	Net Area of URM Wall A_n mm^2 (2)	Elastic Modulus of FRCM/FRP E_f MPa (3)	Elastic Modulus of URM wall E_m MPa (4)	Calibrated Reinf. Ratio $\rho E_f / E_m$ % (5)	Exp. Shear Force $V_{u,exp}$ kN (6)	Exp. Shear strength $\tau_{u,exp}$ MPa (7)
CMU-1 ply-1	IP-CMU-FRCM	248	72903	79726	17513	1.55	168.0	2.3
CMU-1 ply-2							139.7	1.9
CMU-1 ply-3							144.1	2.0
CMU-4 ply-1		991				6.19	185.0	2.5
CMU-4 ply-2							180.4	2.5
CMU-4 ply-3							181.2	2.5
WC1	IP-CMU-FRP	154	141935	36584	13590	0.29	135.2	1.0
WC2		307				0.58	168.1	1.2
WC3		154				0.29	109.4	0.8
WC4		307				0.58	159.2	1.1
COW 2		230		50166	15079	0.54	141.5	1.0
COW 3							137.9	1.0
COW 8							130.3	0.9
COW 9		266		54636		0.68	134.8	0.9
COW 10		230		50166		0.54	170.4	1.2
COW 11		132				0.31	98.3	0.7
COW 12		99		50166		0.23	134.8	0.9
WL 2		126		83123	14893	0.50	111.2	0.8
WL 3		108				0.65	208.2	1.5
Wall IL2		230		40679	12969	0.51	161.6	1.1
Wall IL3		329				0.73	178.9	1.3
Wall IL4							168.2	1.2

(Note: 1.0 mm^2 = 0.0016 in^2; 1.0 MPa = 145 psi; 1.0 kN = 0.23 kips)

Table 12– FRCM and FRP reinforced clay brick walls subjected to in-plane load

Specimen ID		Area of FRCM or FRP A_f mm^2 (1)	Net Area of URM Wall A_n mm^2 (2)	Elastic Modulus of FRCM/FRP E_f MPa (3)	Elastic Modulus of URM wall E_m MPa (4)	Reinf. Ratio $\rho\, E_f / E_m$ % (5)	Exp. Shear $V_{u,th}$ kN (6)	Exp. Shear Strength τ MPa (7)
CL-1 ply-1	IP-CL-FRCM	232	81290	79726	17147	1.33	108.8	1.34
CL-1 ply-2							133.2	1.64
CL-1 ply-3							118	1.45
CL-4 ply-1		929				5.31	246.7	3.03
CL-4 ply-2							223.1	2.74
CL-4 ply-3							229.6	2.82
WK1	IP-CL-FRP	154	112258	36584	11245	0.44	105.4	0.94
WK2		307				0.89	114.3	1.02
WK3		154				0.44	93.9	0.84
WK4		307				0.89	105.0	0.94
CLW 4		395	330322	40651	10269	0.47	255.0	0.77
CL B1		230	123871	50162	11045	0.84	115.7	0.93
CL B2		461				1.69	173.6	1.40
CL 1		135		83129		0.82	91.8	0.74
CL 2		271				1.65	159.1	1.8
Wall 1		139	54200	40800	11032	0.95	50.9	0.94
Wall 2		279				1.90	79.3	1.46
Wall 3						1.90	65.5	1.21
Wall 4						1.90	73.3	1.35
Wall 5		144		72400		1.74	82.2	1.52
Wall 6		287				3.48	90.2	1.66
Wall 7		557		40800		3.80	110.1	2.03
Wall 8		422		51653		3.65	123.3	2.27
Wall 9		422		46384		3.28	112.7	2.08

(Note: 1.0 mm^2 = 0.0016 in^2; 1.0 MPa = 145 psi; 1.0 kN = 0.23 kips)

Table 13– Flexural strengthening schemes of concrete block walls with FRP

Resources (1)	**Specimen ID (2)**	**Strengthening Schemes (3)**
Tumialan et al. 2003	COG3	One 75 mm wide vertical GFRP laminate strip
	COG3R	
	COG5	One 125 mm wide vertical GFRP laminate strip
	COG9	One 225 mm wide vertical GFRP laminate strip
	COG12	One 300 mm wide vertical GFRP laminate strip
	COA3	One 75 mm wide vertical AFRP laminate strip
	COA5	One 125 mm wide vertical AFRP laminate strip
	COA7	One 175 mm wide vertical AFRP laminate strip
	COA9	One 225 mm wide vertical AFRP laminate strip
	COA12	One 300 mm wide vertical AFRP laminate strip
Galati et al. 2005	CO1-GTE1	One vertical GFRP (2x15 mm) rectangular bar
	CO2-GRE21	One vertical 6.35 mm GFRP circular bar
	CO2-GRE22	Two vertical 6.35 mm GFRP circular bar
	CO2-GRE23	Three vertical 6.35 mm GFRP circular bar
	CO2-GRC31	One vertical 9.53 mm GFRP circular bar
	CO2-GRC33	Three vertical 9.53 mm GFRP circular bar
	CO2-GRE22-SJ	Two vertical 6.35 mm GFRP circular bar in the vertical joint
	CO2-GRE21-S	One vertical 6.35 mm GFRP circular bar crossing the blocks
	CO2-GRE22-S	Two vertical 6.35 mm GFRP circular bar crossing the blocks

(Note: 1 mm=0.039 in)

Table 14– Flexural strengthening schemes of clay brick walls with FRP

Resources (1)	**Specimen ID (2)**	**Strengthening Schemes (3)**
Tumialan et al. 2003	CLG3	One 75 mm wide vertical GFRP laminate strip
	CLG3R	
	CLG5	One 125 mm wide vertical GFRP laminate strip
	CLG5R	
	CLG7	One 175 mm wide vertical GFRP laminate strip
	CLG9	One 225 mm wide vertical GFRP laminate strip
	CLG12	One 300 mm wide vertical GFRP laminate strip
	CLA3	One 75 mm wide vertical AFRP laminate strip
	CLA5	One 125 mm wide vertical AFRP laminate strip
	CLA7	One 175 mm wide vertical AFRP laminate strip
Galati et al. 2005	CL1-GTE1	One vertical GFRP (2x15 mm) rectangular bar
	CL1-GTE2	Two vertical GFRP (2x15 mm) rectangular bar

(Note: 1 mm=0.039 in)

Table 15– FRCM and FRP reinforced CMU walls under out-plane load

Specimen ID		Amount of FRCM /FRP ρ - (1)	Slenderness Ratio h/t_m - (2)	Elastic Modulus of FRCM/ FRP E_f GPa (3)	Comp. strength of Masonry f'_m MPa (4)	Calibrated Reinf. Ratio $(\rho E_f) / ((h/t)x f'_m)$ - (5)	Exp. Moment $M_{u,exp}$ kN-m (6)	Normalized Exp. Moment Capacity $M_{u,exp}/(b_m t_m^2 f'_m(h/t))$ - (7)
1 ply-1	OP-CMU-FRCM	0.0007	13.2	79.7	19.5	0.23	6.09	0.0023
1 ply-2							6.35	0.0024
1 ply-3							6.99	0.0027
4 ply-1		0.0029				0.91	18.49	0.0071
4 ply-2							18.49	0.0071
4 ply-3							18.49	0.0071
COG3	OP-CMU-FRP	0.0005	12.3	92.9	10.5	0.36	2.05	0.0029
COG3R		0.0005				0.36	3.22	0.0046
COG5		0.0008				0.58	3.33	0.0048
COG9		0.0014				1.01	5.23	0.0075
COG12		0.0019				1.37	6.06	0.0080
COA3		0.0004				0.29	2.54	0.0036
COA5		0.0006		115.2		0.54	3.57	0.0051
COA7		0.0009				0.80	4.66	0.0067
COA9		0.0011				0.98	5.25	0.0075
COA12		0.0015				1.34	5.33	0.0076
CO1-GTE1		0.0003	8.5	44.0	11.4	0.15	3.35	0.0028
CO2-GRE21		0.0005	13.2	50.2	10.5	0.19	2.52	0.0036
CO2-GRE22		0.0011				0.39	2.64	0.0037
CO2-GRE23		0.0019				0.68	4.94	0.0066
CO2-GRC31		0.0014		40.8		0.40	2.99	0.0042
CO2-GRC33		0.0041				1.20	6.07	0.0081
CO2-GRE22-SJ		0.0001		50.2		0.04	3.43	0.0049
CO2-GRE21-S		0.0005				0.18	1.91	0.0027
CO2-GRE22-S		0.0010				0.36	3.60	0.0051

(Note: 1.0 kN.m = 737.56 lb.ft; 1.0 MPa = 0.145 ksi; 1.0 GPa =145.03 ksi)

Table 16– FRCM and FRP reinforced clay walls under out-plane load

Specimen ID		Reinf. Ratio ρ - (1)	Slenderness Ratio h/t_m - (2)	Elastic Modulus of FRCM/ FRP E_f GPa (3)	Comp. strength of Masonry f'_m MPa (4)	Calibrated Reinf. Ratio $(\rho E_f) / ((h/t)x f'_m)$ - (5)	Exp. Moment Capacity $M_{u,exp}$ kN-m (6)	Normalized Exp. Moment Capacity $M_{u,exp}/(b_m t_m^2 f'_m (h/t))$ - (7)
1 ply-1	OP-CL-FRCM	0.0007	13.2	79.7	24.0	0.18	6.57	0.0020
1 ply-2							6.20	0.0019
1 ply-3							6.40	0.0020
4 ply-1		0.0029				0.74	17.62	0.0055
4 ply-2							16.94	0.0052
4 ply-3							17.81	0.0055
CLG3	OP-CL-FRP	0.0005	12.3	92.9	17.1	0.22	3.23	0.0028
CLG3R							3.88	0.0034
CLG5		0.0008				0.35	4.89	0.0043
CLG5R							5.37	0.0047
CLG7		0.0011				0.49	6.58	0.0058
CLG9		0.0014				0.62	6.94	0.0061
CLG12		0.0019				0.84	6.16	0.0054
CLA3		0.0004		115.2		0.22	2.94	0.0026
CLA5		0.0006				0.33	5.23	0.0046
CLA7		0.0009				0.49	6.13	0.0054
CL1-GTE1		0.0005	12.8	44.0	19.4	0.09	2.16	0.0016
CL1-GTE2		0.0010				0.18	3.66	0.0027

(Note: 1.0 kN.m = 737.56 lb.ft; 1.0 MPa = 0.145 ksi; 1.0 GPa =145.03 ksi)

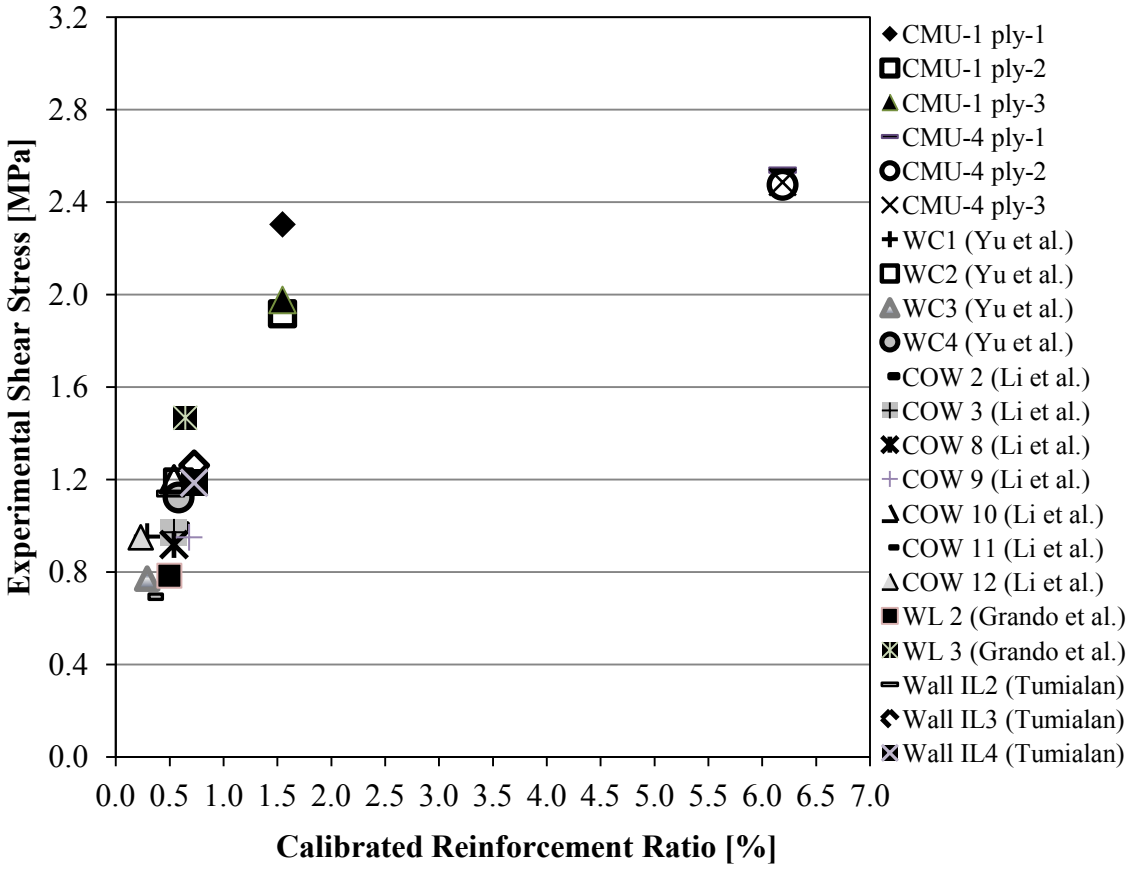

Figure 27- Shear strength of FRCM and FRP strengthened concrete block walls vs. calibrated reinforcement ratio

(Note: 1.0 MPa = 145 psi)

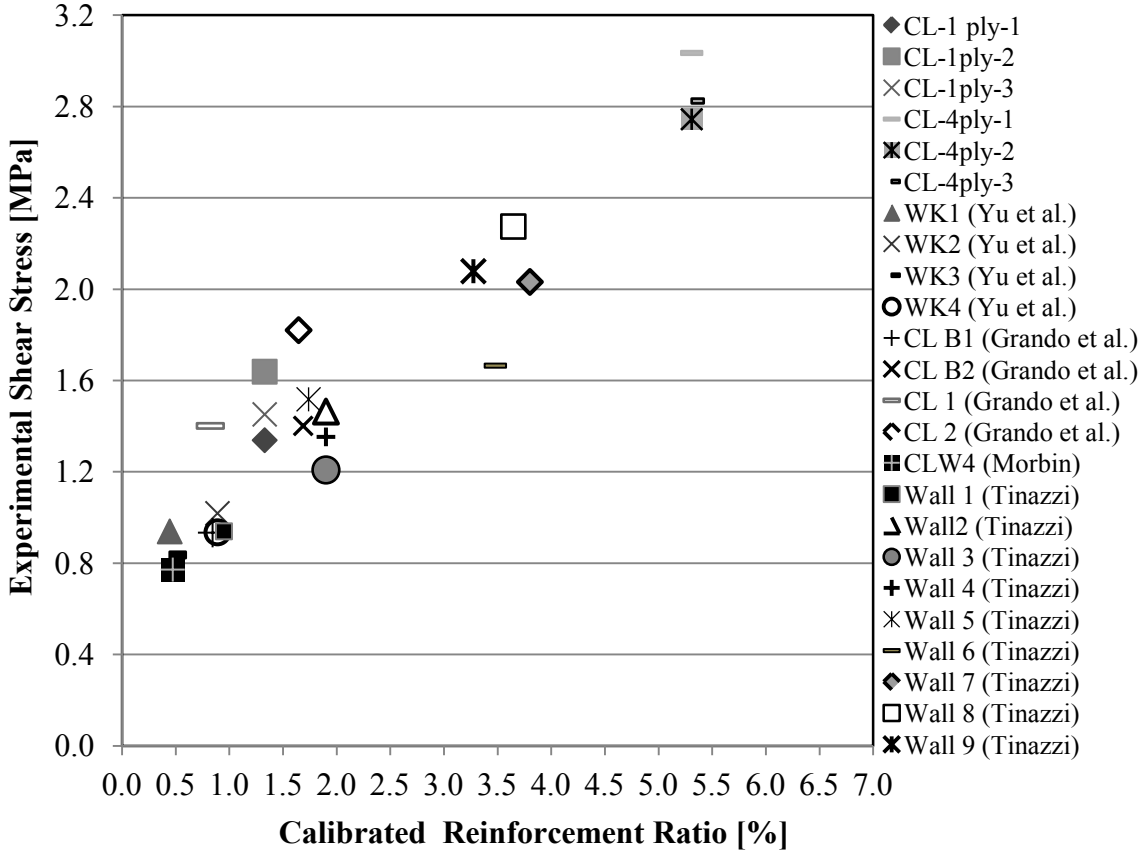

Figure 28- Shear strength of FRCM and FRP strengthened clay brick walls vs. calibrated reinforcement ratio

(Note: 1.0 MPa = 145 psi)

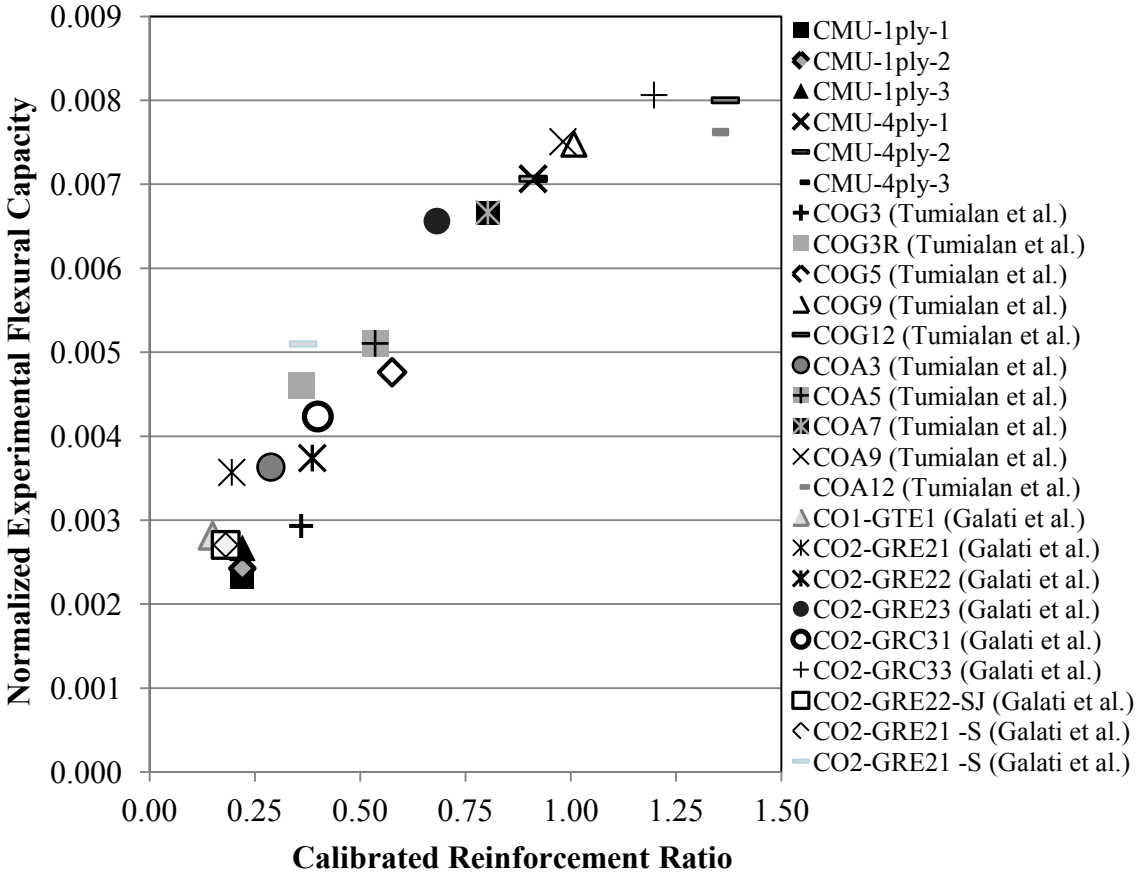

Figure 29- Normalized experimental flexural capacity of FRCM and FRP strengthened concrete block walls vs. calibrated reinforcement ratio

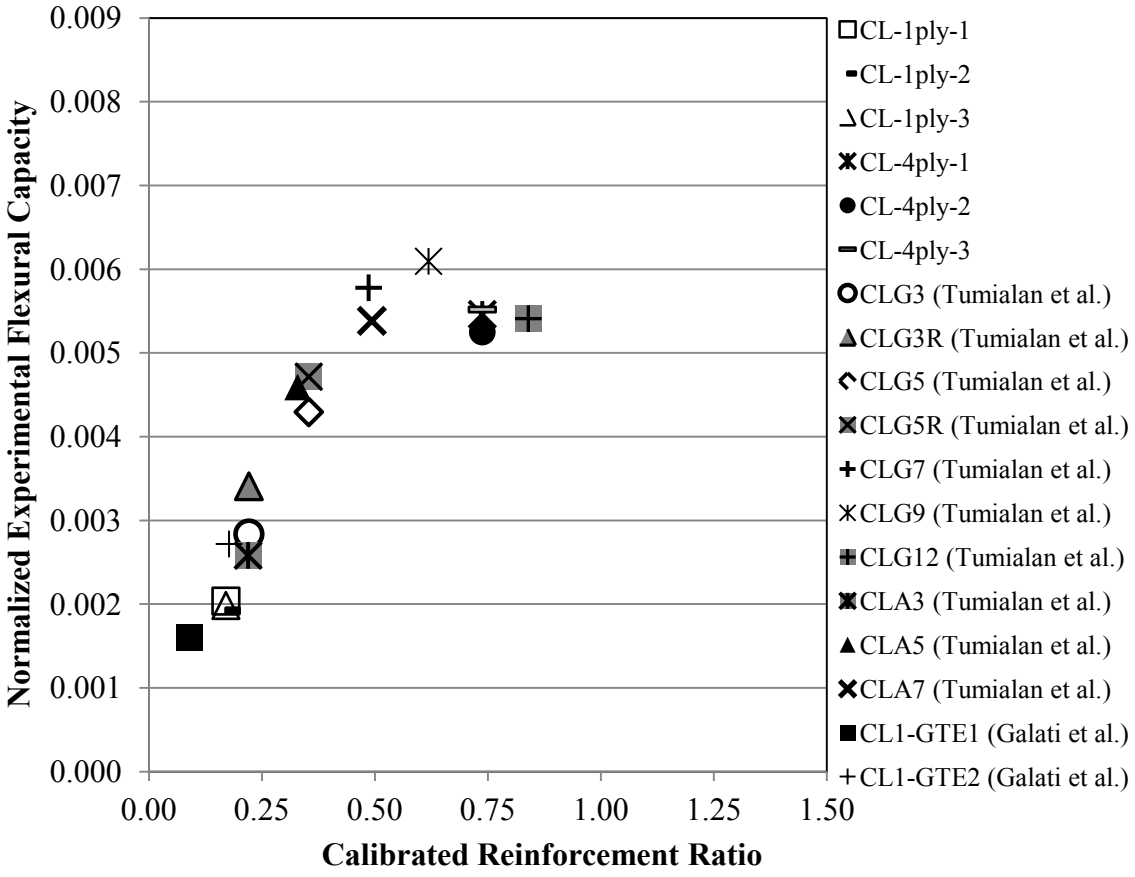

Figure 30- Normalized experimental flexural capacity of FRCM and FRP strengthened clay brick walls vs. calibrated reinforcement ratio

CHAPTER V

CONCLUSIONS

This dissertation is articulated in three studies. The experimental programs presented in *Study 1* and *Study 2* are unique activities to advance knowledge of effectiveness of FRCM composite systems as a novel strengthening technique for masonry retrofitting.

Study 1 conducted an extensive experimental and analytical program under diagonal compression on CMU and clay brick masonry walls strengthened with FRCM (one and four plies fabric). The study showed the feasibility of FRCM on improving the structural performance of masonry walls in terms of shear strength and pseudo-ductility. *Study 2* presents a pilot research including experimental tests and analytical methods as per ACI 549 (2013) on retrofitted masonry walls with two amounts of FRCM reinforcement (one and four fabrics) under out-of-plane loading. The second study showed enhancement in the flexural capacity of masonry walls.

Study 3 compares experimental results from this research using FRCM and other programs using FRP composites on masonry walls. This study compares FRCM and FRP

strengthened walls under different loading conditions: diagonal compression (shear) and out-of-plane load (flexure) after normalizing the data against the calibrated reinforcement ratio.

The following conclusions can be drawn based upon *Study 1* and *Study 3*:

1. The test results proved the technical viability of FRCM strengthening of URM walls when subjected to diagonal compression. Depending to the amount of FRCM, increment in terms of ultimate in-plane load ranged between 2.4 and 4.7 times that of clay brick control wall, and 2.0 and 2.4 times of concrete control wall using 1-ply and 4-ply carbon FRCM, respectively.
2. Experimental evidence and analysis showed that the key parameter affecting shear capacity and failure mode of FRCM strengthened walls is the calibrated reinforcement ratio. It is understood that FRCM and FRP strengthening methods provide similar increments in shear capacity if normalized according to the calibrated reinforcement ratio derived as the ratio of axial stiffness of the composite and masonry ($A_f E_f / A_n E_m$). The substrate toe crushing controlled failure in the strengthened walls with the calibrated reinforcement ratio more than 1.5% (e.g., 1-ply FRCM) for the case of CMU walls and 4% (e.g., 4-ply FRCM) for the case of clay brick walls. Consequently, increment of FRCM beyond these values is unproductive.
3. Based on the results obtained from shear stress and strain, it is observed that FRCM strengthening is effective in increasing the stiffness and pseudo-ductility of URM walls. For the case of CMU walls, pseudo-ductility gain is limited due to toe crushing

failure in both cases of 1-ply and 4-ply (with the former showing higher values). Pseudo-ductility of 4-ply clay brick walls is also limited by toe crushing failure.

4. Analysis as per ACI 549 (2013) showed good agreement with the experimental results. Similarly, design values are conservative when applying the limits of 50% maximum increase due to strengthening and reduction factor, ϕ_v.

Based upon *Study 2* and *Study 3*, the following observations and conclusions are drawn:

- Ultimate out-of-plane moment capacity increases depending to the amount of FRCM. The flexural enhancement was calculated to be 2.7 and 7.8 for CMU masonry and 2.8 and 7.5 for clay brick wall, using 1-ply and 4-ply carbon FRCM, respectively.
- Two basic modes of failure were observed: cracking of the masonry at the mid-height with FRCM slippage, and shear failure in the substrate at the supports depending on FRCM amount.
- Based on the moment-deflection results, it can be observed that FRCM is effective in increasing flexural strength, stiffness, and pseudo-ductility; however, pseudo-ductility is higher for lower FRCM amounts since flexure controls the failure mode.
- For the same level of the calibrated reinforcement ratio, ω_f, FRCM and FRP strengthening methods are comparable and provide similar increments in flexural capacity. For ω_f larger than 0.8 for the CMU and 0.6 for clay brick walls, shear

controls the failure mode. Increments of FRCM beyond this value may be unproductive.

- A sectional analysis according to the methods proposed by MSJC (2011) and ACI 549 (2013) is used to predict flexural capacity. Analytical results underestimate the experimental database, since arching mechanism is disregarded. Similarly, design flexural capacity values are very conservative when applying limitations and the flexural strength reduction factor, ϕ_m, as per ACI 549 (2013).

RECOMMENDATIONS FOR FUTURE RESEARCH

To allow for the inclusion of FRCM composites with various types of fabrics and cementitious mortars for strengthening masonry, further research and more experimental tests are needed.

More experimental data are also necessary for a complete validation of the design methodology discussed in *Study 1* and *Study 2*. More experimental data would allow corroborating the methodology described in *Study 3* to compare different strengthening schemes. Further research is needed to extend validity to different types of FRCM.

Experimental in-plane tests were performed only on one-wythe masonry walls, while double-wythe wall with headers can be further investigated. Research is also needed to investigate the behavior of FRCM-reinforced masonry subjected to cyclic lateral loads. In the flexural analysis in this research project, arching mechanism effect was disregarded.

This phenomenon should be further investigated. Since slenderness ratio is a major factor influencing flexural capacity, masonry walls with different slenderness ratio should be tested and provide more experimental evidence and validate more sophisticated models.

BIIBLIOGRAPHY

AC434 (2013). "Proposed acceptance criteria for masonry and concrete strengthening using fiber-reinforced cementitious matrix (frcm) composite systems." ICC-Evaluation Service, Whittier, CA.

Al-Salloum, Y.A., Elsanadedy, H.M., Alsayed, S.H., and Iqbal, R.A. (2012). "Experimental and numerical study for the shear strengthening of reinforced concrete beams using textile-reinforced mortar." Journal of Composites for Construction, 16(1), 74–90.

American Concrete Institute (ACI). (2010). "Guide for the design and construction of externally bonded fiber-reinforced polymer systems for strengthening unreinforced masonry structures." ACI 440.7R, Farmington Hills, MI.

American Concrete Institute (ACI). (2013). "Design and construction guide of externally bonded FRCM systems for concrete and masonry repair and strengthening." ACI 549, Farmington Hills, MI.

Arboleda, D., Loreto, G., De Luca, A., and Nanni, A. (2012). "Material characterization of fiber reinforced cementitious matrix (FRCM) composite laminates." Proc., 10th International Symposium on Ferrocement and Thin Reinforced Cement Composite, Editor: Rivas, H.W., Seoane, L.P., and Castro, I.G., October 12-17, Havana, Cuba, 29-37.

Arduini, M. and Nanni, A. (1997). "Behavior of pre-cracked RC beams strengthened with carbon FRP sheets." Journal of Composite for Construction, 1(2), 63–70.

ASTM. (2010). "Standard test methods for diagonal tension (shear) in masonry assemblages." ASTM E519/ E519M, West Conshohocken, PA.

ASTM. (2012). "Standard test method for compressive strength of hydraulic cement mortars (using 2-in. or [50-mm] cube specimens)." ASTM C109, West Conshohocken, PA.

ASTM. (2012). "Standard test methods for compressive strength of masonry prisms." ASTM C1314, West Conshohocken, PA.

Babaeidarabad, S., De Caso, F., and Nanni, A. (2013). "URM walls strengthened with fabric-reinforced cementitious matrix (FRCM) composite subjected to diagonal compression." Journal of Composites for Construction, Accepted. DOI: 10.1061/ (ASCE) CC.1943-5614.0000441.

Babaeidarabad, S., Arboleda, D., Loreto, G., Nanni, A. (2013). "Shear strengthening of concrete masonry with fabric-reinforced-cementitious-matrix." Construction and Building Materials, Elsevier, September 2013, Under Review.

Babaeidarabad, S., Nanni, A. (2013). "In-plane behavior of unreinforced masonry walls strengthened with fabric-reinforced cementitious matrix (FRCM)." ACI, Special Publication, October, 2013, Submitted.

Babaeidarabad, S., De Caso, F., and Nanni, A. (2013). "Out-of-plane behavior of URM walls strengthened with fabric-reinforced cementitious matrix (FRCM) Composite." Journal of Composites for Construction, Accepted. DOI: 10.1061/(ASCE)CC.1943-5614.0000457.

Babaeidarabad, S., Nanni, A. (2013). "Out-of-plane strengthening of URM walls with fabric-reinforced-cementitious-matrix (FRCM)." ACI, Special Publication, October, 2013, Submitted.

Babaeidarabad, S., De Caso, F., and Nanni, A. (2013). "Out-of-plane behavior of unreinforced masonry wall strengthened with fabric-reinforced-cementitious matrix (FRCM)." Zero Energy Mass Customization Housing, ZEMCH, International conference, October 2013, University of Miami, Miami, 2013.

Bakis, C., Bank, L., Brown, V., Cosenza, E., Davalos, J., Lesko, J., Machida, A., Rizkalla, S., and Triantafillou, T. (2002). "Fiber-reinforced polymer composites for construction—state-of-the-art review." Journal of Composite for Construction, 6(2), 73–87.

Banholzer, B., Brockmann, T., and Brameshuber, W. (2006). "Material and bonding characteristics for dimensioning and modeling of textile reinforced concrete (TRC) elements." Materials and Structures, 39 (8), 749–763.

Bisby,L.A., Roy, E. C., Ward, M., and Straford, T.J. (2009). "Fibre reinforced cementitious matrix systems for fire-safe flexural strengthening of concrete: Pilot testing at ambient temperature." Proc., Advanced Composite in Construction, Network Group for Composites in Construction, Chesterfield, U.K.

Blanksvärd, T., Täljsten, B., and Carolin, A. (2009). "Shear strengthening of concrete structures with the use of mineral-based composites." Journal of Composite for Construction, 13(1), 25–34.

Brückner, A., Ortlepp, R., and Curbach, M. (2006). "Textile reinforced concrete for strengthening in bending and shear." Mater. Struct., 39, 741–748.

Crisafulli, F. J., Carr, A. J., and Park, R. (1995). "Shear strength of unreinforced masonry panels." Proc., Pacific Conference on Earthquake Engineering, Melbourne, Australia, Nov.20-22, 77–86.

D'Ambrisi, A. and Focacci, F. (2011). "Flexural strengthening of RC beams with cement based composites." Journal of Composites for Construction, 15(5), 707-720.

Dizhur, D., Griffith, M. C., and Ingham, J.M. (2013). "In-plane shear improvement of unreinforced masonry wall panels using NSM CFRP strips." Journal of Composites for Construction, posted ahead of print. DOI: 10. 1061/ (ASCE) CC.1943-5614.0000400.

Dizhur, D. and Ingham, J.M. (2013). "Diagonal tension strength of vintage unreinforced clay brick masonry wall panels." Construction and Building Materials, 43(6), 418–427.

Ehsani, M. R., and Saadatmanesh, H. (1994). "Out-of-plane strength of unreinforced brickwork retrofitted with fiber composites." Proceedings, NCEER Workshop on Seismic Response of Masonry Infills, San Francisco, Calif.

El-Hacha, R. and Rizkalla, S. H. (2004). "Near-surface-mounted fiber-reinforced polymer reinforcements for flexural strengthening of concrete structures." ACI Structural Journal, 101 (5), 717–726.

El-Mihilmy, M., and Tedesco, J. W. (2000). "Deflection of reinforced-concrete beams strengthened with fiber -reinforced polymer (FRP) plates." ACI Struct. J., 975, 679–688.

Essaway, A. M. (1986). "Strength of hallow concrete block masonry walls subjected to lateral (out-of-plane) loading." Ph.D. thesis, McMaster University, Canada.

Faella, C., Martinelli, E., Nigro, E., Paciello, S. (2004). "Experimental tests on masonry walls strengthened with an innovative C-FRP sheet." Proceedings of the First International Conference on Innovative Materials and Technologies for Construction and Restoration, Lecce, V. 2, June 6-9, pp. 458-474.

fib bulletin 14 (2001). "Externally bonded FRP reinforcement for RC structures." Technical Report, International Federation for Structural Concrete, Lausanne, Switzerland.

Grando, S., Valluzzi, M.R., Modena, C., and Tumialan, J.G. (2003). "Shear strengthening of URM clay walls with FRP systems." Advancing with Composites, Ed. I. Crivelli-Visconti, May 7–9, Milan, Italy.

Hartig, J., Häußler-Combe, U., and Schicktanz, K. (2008). "Influence of bond properties on the tensile behaviour of textile reinforced concrete." Cem. Concr. Compos., 30, 898–906.

Hegger, J., Will, N., Bruckermann, O., and Voss, S. (2006). "Load-bearing behavior and simulation of textile reinforced concrete." Mater. Struct.,39, 765–776.

Hrynyk, T. and Myers, J.J. (2006). "Comparative study on the out-of-plane behavior of retrofitted wall systems with arching action." 10th North American Masonry Conference, St. Louis.

Loreto, G., Leardini, L., Arboleda, D., and Nanni, A. (2013). "Performance of RC slab-type elements strengthened with fabric-reinforced-cementitious-matrix (FRCM) composites." Journal of Composites for Construction, posted ahead of print. DOI: 10.1061/ (ASCE) CC.1943-5614.0000415.

Li, T., Galati, N., Tumialan, J.G., and Nanni, A. (2005). "Analysis of unreinforced masonry concrete walls strengthened with glass fiber-reinforced polymer bars." ACI Structural Journal, V.102, No.4, 569–577.

Mann, W., and Müller, H. (1982). "Failure of shear-stressed masonry—An enlarged theory, tests and application to shear walls." Proceeding of the British Ceramic Society, V.30, 223–235.

Morbin, A. (2002). "Strengthening of masonry elements with FRP composites." CIES Research Report, 02-23, University of Missouri – Rolla.

Myers, J.J. (2011). "Strengthening unreinforced masonry structures using externally bonded fiber-reinforced polymer systems: An overview of the American Concrete Institute 440.7R design approach." 9th Australasian Masonry Conference, Queenstown, New Zealand, 15–18.

Nanni, A., Galati, N., Tumialan, J.G. (2003) "Outline of provisional design protocols and field applications of strengthening of URM walls." Advancing with Composites, 187–197.

Ombres, L. (2011). "Flexural analysis of reinforced concrete beams strengthened with a cement based high strength composite material." Composite Structure, 94(1), 143-155.

Papanicolaou, C. G., Triantafillou, T. C., Karlos, K., and Papathanasiou, M. (2007). "Textile reinforced mortar (TRM) versus FRP as strengthening material of URM walls: in-plane cyclic loading." Materials and Structures, RILEM, 40(10), 1081-1097.

Papanicolaou, C. G., Triantafillou, T. C., Papathanasiou, M., and Karlos, K. (2008). "Textile reinforced mortar (TRM) versus FRP as strengthening material of URM walls: out-of-plane cyclic loading." Materials and Structures, RILEM, 41(1), 143-157.

Parisi, F., Iovinella, A., Balsamo, A., Augenti, N., and Prota, A. (2012). "In-plane behavior of tuff masonry strengthened with inorganic matrix–grid composites." Elsevier, Composites: Part B, Volume 45, Issue 1, 1657–1666.

Park, R. (1989). "Evaluation of ductility of structures and structural assemblages from laboratory testing." Bulletin of the New Zealand National Society for Earthquake Engineering, 22(3):155–166.

Paulay, T. and Priestley, M. J. N. (1992). "Seismic design of reinforced concrete and masonry buildings." Wiley, New York.

Peled, A. (2007). "Confinement of damaged and non damaged structural concrete with FRP and TRC sleeves." Journal of Composite for Construction, 11(5), 514–522.

Petersen, R. (2009). "In-plane shear behavior of unreinforced masonry panels strengthened with fiber reinforced polymer strips." Ph.D. thesis, School of Engineering, The Univ. of Newcastle, Newcastle, New South Wales.

Prota, A., Marcari, G., Fabbrocino, G., Manfredi, G., and Aldea, C. (2006). "Experimental in-plane behavior of tuff masonry strengthened with cementitious matrix-grid composites." Journal of Composite for Construction, 10(3), 223-233.

Secondin, S. (2003). "Masonry reinforced with FRP systems." CIES Research Report, 03-43, University of Missouri – Rolla.

Sharif, A., Al-Sulaimani, G. J., Basunbul, I. A., Baluch, M. H., and Ghaleb, B. N. (1994). "Strengthening of initially loaded reinforced concrete beams using FRP plates." ACI Structural Journal, 91 (2), 160–168.

Silva, P.F., Yu, P., and Nanni, A. (2008). "Monte carlo simulation for validating the in-plane shear capacity of URM walls strengthened with GFRP grid reinforced polyurea." Journal of Composites for Construction, Vol. 12, No. 4, 405–415.

Spadea, G., Bencardino, F., and Swamy, R. (1998). "Structural behavior of composite RC beams with externally bonded CFRP." Journal of Composite for Construction, 2(3), 132–137.

Tinazzi, D. (2000). "Assessment of technologies of masonry retrofitting with FRP." Ph.D. thesis, CIES Research Report, University of Missouri – Rolla.

Toutanji,H. and Deng, Y. (2007). "Comparison between organic and inorganic matrices for RC beams strengthened with carbon fiber sheets." Journal of Composite for Construction, 11(5), 507–13.

Triantafillou, T.C. and Papanicolaou, C.G. (2006). "Shear strengthening of reinforced concrete members with textile reinforced mortar (TRM)." Materials and Structures, 39(1), 93–103.

Tumialan, J.G., Morbin, A., Nanni, A., and Modena, C. (2001). "Shear strengthening of masonry walls with FRP composites." Convention and Trade Show, Composites Fabricators Association, Tampa, FL, October 3–6, 6 pp. CD-ROM.

Velazquez-Dimas, J. I.; Ehsani, M. R.; and Saadatmanesh, H., 1998, Cyclic Behavior of Retrofitted URM Walls, Proceedings ICCI-98, Tucson, Ariz., pp. 328-340

Velazquez-Dimas, J. I., 1998, Out-of-Plane Cyclic Behavior of URM Walls Retrofitted with Fiber Composites, Ph.D. dissertation, University of Arizona.

Wiberg, A. (2003). "Strengthening of concrete beams using cementitious carbon fibre composites." Ph.D. thesis, Royal Institute of Technology, Stockholm, Sweden.

Wu, H. C., and Sun, P. (2005). "Fiber reinforced cement based composite sheets for structural retrofit." Proc., Int. Symposium on Bond Behavior of FRP in Structures (BBFS 2005), International Institute for FRP in Construction, Manitoba, Canada.

Yu, P., Silva, P.F., and Nanni, A. (2007). "In-plane response of URM walls strengthened with GFRP reinforced polyurea." North America Masonry Conference, June 3–5, St. Louis, MO.

Zastrau, B., Lepenies, I., and Richter, M. (2008). "On the multi scale modeling of textile reinforced concrete." Technische Mechanik, 28(1), 53–63.

APPENDIX A
STUDY 1- DESIGN EXAMPLE

Design of Concrete Masonry Wall Strengthened with 1-Ply FRCM

Calculate the analytical and design shear capacity of a concrete masonry wall strengthened with 1-ply FRCM according to ACI 549 (2013), using actual geometry and material properties obtained from coupon and prism tests. The shear capacity of a strengthened wall is computed in three steps: 1) calculate the shear capacity of the URM wall; 2) calculate the contribution of FRCM reinforcement; 3) calculate overall shear capacity:

Masonry Properties

Height of the wall	H=1220 mm (48 in)
Thickness of the wall	t_m=92 mm (3.63 in)
Length of the wall	L=1220 mm (48 in)
Height of the block	h=194 mm (7.63 in)
Length of the block	w=397 mm (15.63 in)
Net cross-sectional area	A_n= 72903 mm^2 (113 in^2)
Compressive strength of masonry	f'_m=19.46 MPa (2,823 psi)
Compressive strength of mortar	f_c =22.01 MPa (3,193psi)

Tensile strength of masonry	f'_t=2.21 Mpa (320 psi)
Masonry elastic modulus	E_m=900 f'_m =17513 MPa (2540 ksi)
Shear bond strength in mortar joint	τ_0=0.58 MPa (84.7 psi)
Coefficient of internal shear friction	μ_0=0.3

FRCM Properties

Area of fabric per unit width (Both directions)	A_f=0.10 mm^2/mm (0.004 in^2/in)
Tensile modulus of elasticity	E_f=80 GPa (11563 ksi)
Ult. tensile strain (Ave. minus one St.dev)	ε_{fu}=0.0086 mm/mm (in/in)

Masonry Contribution (V_m)

- Shear capacity due to shear sliding failure calculated according to **Equation 3**:

$$V_{ss} = \frac{\tau_0}{1 - \mu_0 \, tan\theta} \, A_n$$

$$= \frac{0.58\text{x}1000}{1 - 0.3\text{xtan}45^\text{o}}\text{x}0.0729 = 60.8 \text{ kN (13.7 kips)}$$

- Shear capacity due to shear friction failure calculated according to **Equation 4**:

$$V_{sf} = \frac{\tau_{0,m}}{1 - \mu_m \, tan\theta} \, A_n = \frac{\tau_0}{1 + 1.5\mu_0 \frac{h}{w} - \mu_0 tan\theta}$$

$$= \frac{0.58\text{x}1000}{1 + 1.5\text{x}0.3\text{x}\frac{0.194}{0.397}\text{xtan}45^\text{o} - 0.3\text{xan}45^\text{o}}\text{x}0.0729 = 46.3 \text{ kN (10.4 kips)}$$

- Shear capacity due to diagonal tension failure is calculated according to **Equation 5**:

$$V_{dt} = \frac{tan\theta + \sqrt{21.16 + tan\theta^2}}{10.58} f_t^{'} A_n \left(\frac{L}{H}\right)$$

$$= \frac{\tan 45^o + \sqrt{21.16 + \tan 45^{o\,2}}}{10.58} \text{x2.206x1000x0.0729x} \left(\frac{1220}{1220}\right)$$

$$= 86.7 \text{ kN (19.5 kips)}$$

- Shear capacity due to toe crushing failure at the loading end is calculated according to **Equation 6**:

$$V_c = \frac{2wf_m^{'}}{3h + 2w\ tan\theta} A_m$$

$$= \frac{2\text{x}0.397\text{x}19.46\text{x}1000}{3\text{x}0.194 + 2\text{x}0.397} \text{x}(0.17\text{x}0.092\text{x}0.65) = 114.2 \text{ kN (25.7 kips)}$$

- URM shear capacity is calculated according to **Equation 2**:

$$V_m = Min\{V_{ss}; V_{sf}; V_{dt}; V_c\} = 46.3 \text{ kN (10.4 kips)}$$

FRCM Contribution (V_f)

- Effective tensile strain of FRCM is calculated according to **Equation 7**:

$$\varepsilon_{fv} = 0.004 \text{ mm/mm (0.004 in/in)}$$

- Effective stress level in the FRCM at failure is calculated according to **Equation 8**:

$$f_{fv} = E_f \varepsilon_{fv} = 79726\text{x}0.004 = 318.9 \text{ MPa (46.25 ksi)}$$

- FRCM contribution, V_f, is calculated according to **Equation 9**:

$$V_f = 2nA_f\, Lf_{fv}$$

$$= \frac{2\text{x}1\text{x}0.10\text{x}1220\text{x}318.9\text{x}1000}{1000\text{x}1000} = 79.1 \text{ kN (17.8 kips)}$$

Shear capacity of 1-ply strengthened wall (V_n)

- 1-ply FRCM wall shear capacity is calculated according to **Equation 1** considering ϕ_v is equal to 1.0:

$V_n = V_m + V_f = 46.3 + 79.1 = 125.4$ kN (28.2 kips)

Limitation:

As per ACI 549 (2013), the summation of the masonry and FRCM shear contributions according to Equation 1 should be checked against the substrate toe crushing capacity computed according to **Equation 6**:

$V_n = Min\{V_m + V_f; V_c\} = 114.2$ kN (25.7 kips)

Design Provisions

According to ACI 549 (2013) design provisions, maximum force transferred to substrate should not exceed 50% of un-strengthened wall capacity.

$V_f = Min\{2nA_f\, Lf_{fv}; 50\%\, V_m\} = 23.2$ kN (5.2 kips)

$V_n = V_m + V_f = 46.3 + 23.2 = 69.5$ kN (15.6 kips)

Limitation:

Following ACI 549 (2013) design provisions, the summation of the masonry and FRCM shear contributions before strength reduction factors are applied (**Equation 1**) should be checked against the substrate toe crushing capacity computed according to (**Equation 6**).

$V_n = Min\{V_m + V_f; V_c\} = 69.5$ kN (15.6 kips)

Shear strength reduction factor ϕ_v=0.75

$\phi_v V_n = 0.75\text{x}69.5 = 52.1$ kN (11.7 kips)

The experimental shear value for this wall was:

$V_u = 150.5$ kN (33.8 kips)

The failure mode for this wall was toe crushing.

APPENDIX B
STUDY 2- DESIGN EXAMPLE

Design of Clay Brick Masonry Strengthened with 1-Ply FRCM

Using actual geometry and material properties, calculate the analytical and design moment capacity of a clay brick masonry wall strengthened with 1-ply FRCM in accordance to ACI 549 (2013).The wall is assumed to behave as a simply supported element and arching mechanism is ignored. The flexural capacity of a strengthened wall is computed at two stages: 1) ***cracking***; and 2) ***ultimate***.

Masonry Properties

Height of the wall	H=1422 mm (56 in)
Thickness of the wall	t_m=92 mm (3.625 in)
Length of the wall	L=1220 mm (48 in)
Clear height	h_{eff}=1220 mm (48 in)
Net section area per unit length	A_n= 841.8 cm^2 (130.5 in^2)
Nominal compressive strength of masonry	f'_m=24.5 MPa (3,553 psi)
Maximum compressive strain of masonry	ε'_m =0.0035 mm/mm (in/in)
Masonry elastic modulus	E_m=700 f'_m =17150 MPa (2487 ksi)

Modulus of the rupture f_r=434.4 kPa (63 psi)

Slenderness ratio h_{eff}/t_m=13.24

FRCM Properties

Area of fabric (One direction perpendicular to crack)A_f=0.05 mm^2/mm (0.0020 in^2/in)

Tensile modulus of elasticity E_f=80 GPa (11563ksi)

Ult. tensile strain (Ave. minus one St.dev) ε_{fu}=0.0086 mm/mm (in/in)

1. **Cracking Moment (M_{cr})**

- Un-cracked moment of inertia and sectional modulus are calculated as:

$$I_g = \frac{bh^3}{12} = \frac{1}{10^4}\text{x}\frac{1220\text{x}92^3}{12} = 7930.8 \text{ cm}^4 \ (190.5 \text{ in}^4)$$

$$S = \frac{I_g}{t_m/_2} = \frac{1}{10}\text{x}\frac{7930.8}{92/_2} = 1722.3 \text{ cm}^3 \ (105.1 \text{ in}^3)$$

- Cracking moment is computed according to **Equation 10-a**:

$$M_{cr} = f_r\, S = \frac{1}{10^6}\text{x}434.4\text{x}1722.3 = 0.8 \text{ kN. m } (553.4 \text{ lbf. ft})$$

- Cracking displacement is computed according to **Equation 18**:

$$\delta_{cr} = \frac{5M_{cr}h_{eff}^2}{48E_m I_g} = \frac{10^{-6}\text{x}10^3}{10^3\text{x}10^{-8}}\text{x}\frac{5\text{x}0.75\text{x}\ 1220^2}{48\text{x}17150\text{x}7930.8} = 0.1 \text{ mm } (0.004 \text{ in})$$

2. **Ultimate Moment capacity (M_n)**

It is assumed that the failure mode is governed by FRCM failure (slippage). This assumption is verified by checking that the compressive strain in the masonry does not exceed ε'_m. If it is assumed that the failure mode is governed by masonry crushing, it

should then be verified that the tensile strain in the FRCM reinforcement does not exceed the FRCM effective tensile strain.

- Effective tensile strain of FRCM according to **Equation 12**:

$\varepsilon_{fe} = \varepsilon_{fu} = 0.0086$ mm/mm (0.0086 in/in)

- Effective stress level in the FRCM at failure according to **Equation 13**:

$f_{fe} = E_f \varepsilon_{fe} = 79726\text{x}0.0086 = 685.6$ MPa (99.4 ksi)

When FRCM slippage governs the failure mode, the stress block factors, β_1 and γ, is be assumed to be 0.7.

- Compute the depth of the neutral axis according to **Equation 15-a**:

$$c = \frac{nA_f f_{fe}}{\gamma f'_m \beta_1 b_m} = \frac{10^{-3}}{10^{-3}}\text{x}\frac{1\text{x}0.051\text{x}685.6\text{x}1220}{0.7\text{x}24.5\text{x}0.7\text{x}1220} = 2.9 \text{ mm } (0.11 \text{ in})$$

- Compute the flexural capacity according to **Equation 15:**

$$M_n = A_f f_{fe}\left(t_m - \frac{\beta_1 c}{2}\right) = 10^{-3}\text{x}10^{-3}\text{x}1\text{x}0.051\text{x}685.6\text{x}1220\text{x}(92 - \frac{0.7\text{x}2.9}{2})$$

$= 3.87$ kN. m (2852.1 lbf. ft)

Verify Failure Mode

- Compressive strain in the masonry, ε_m, should be checked not to exceed maximum compressive strain of masonry, ε'_m according to **Equation 16**:

$$\frac{\varepsilon_m}{c} = \frac{\varepsilon_{fe}}{t_m - c}$$

$\varepsilon_m = 0.0003$ mm/mm (0.0003 in/in) $< \varepsilon'_m = 0.0035$ mm/mm

Maximum Displacement at Mid-Height

- Cracked moment of inertia of the wall is calculated according to **Equations18-a**:

$$I_{cr} = \frac{b_m c^3}{3} + \frac{E_f}{E_m} A_f (t_m - c)^2 = 10^{-4}\text{x}\frac{1220\text{x}(2.9^3)}{3} + \frac{79726}{17150}\text{x}1220\text{x}0.051\text{x}(92 - c)^2$$

$$= 10^{-4}\text{x}[\frac{1220\text{x}(2.9^3)}{3} + \frac{79726}{17150}\text{x}1220\text{x}0.051\text{x}(92 - 2.9)^2] = 230.6 \text{ cm}^4 \text{ (5.54 in}^4\text{)}$$

- Ultimate displacement is computed according to **Equation 18**:

$$\delta_u = Min\{\frac{5M_{cr}h_{eff}^2}{48E_m I_n} + \frac{5(M_n - M_{cr})h_{eff}^2}{48E_m I_{cr}}; 0.007h_{eff}\}$$

$$\delta_u = 0.1 + \frac{10^{-6}\text{x}10^3}{10^3\text{x}10^{-8}}\text{x}\frac{5\text{x}(3.87 - 0.75)\text{x}1220^2}{48\text{x}17150\text{x}231} =$$

$$= 12.3 \text{ mm (0.48 in)}$$

$$\delta_{max} = 0.007h_{eff} = 8.5 \text{ mm (0.34 in)}$$

$$\delta_u = 8.5 \text{ mm (0.34 in)}$$

Note: Maximum displacement limitation, 0.007 h_{eff}, is required by MSJC (2011).

Maximum force transferred from FRCM reinforcement to substrate

According to ACI 549 (2013), the maximum force transferred by the FRCM to substrate should be limited to 87.6 kN/m (6,000 lbf/ft) in strengthened walls subjected to out-of-plane loading as expressed in **Equation 19**:

$$T = nA_f E_f \varepsilon_{fe} = \frac{10^{-3}}{10^{-3}}\text{x}1\text{x}0.051\text{x}79726\text{x}0.0086 =$$

$$= 34.8 \text{ kN/m (2387 lbf/ft)} < 87.6 \text{ kN/m (6000 lbf/ft)}$$

Design Provisions

In design provisions, strength reduction factor for flexure is applied according to **Equations 14**.

Flexural strength reduction factor ϕ_m=0.6

$\phi_m M_n = \phi_m M_f = 2.3$ kN. m (1711.2 lbf. ft)

Lateral pressure

- Ultimate lateral unit load

$$W_u = \frac{8M_n}{h_{eff}^2} = 10^6 \text{x} \frac{8\text{x}2.3}{1220^2} = 12.5 \text{ kN/m (856 lbf/ft)}$$

- Ultimate lateral uniform pressure

$$p_u = \frac{W_u}{L} = 10^3 \text{x} \frac{12.4}{1220} = 10.2 \text{ kPa (213.9 psf)}$$

The experimental pressure and deflection values for this wall were:

$p_u = 28.2$ kPa (588.9 psf)

$\delta_u = 15.9$ mm (0.6 in)

The failure mode for this wall was flexure controlled by fabric slippage within the matrix.

APPENDIX C
COST ANALYSIS

When initially considering an URM structures for potential structural retrofit, the stakeholders (i.e. owners, contractors, and consultants) need to consider demolishing the deficient URM walls and re-constructing new walls, or performing structural retrofitting.

Demolition and Reconstruction

This option requires the substitution of a deficient wall by a new one complying with new specifications. This option can generate large expenditures associated to disruption of activities, removal of debris and transportation of new materials within the site. In the case of a historical building, this is not a viable option since it would alter its historical value. If the "demolition and reconstruction" alternative is a possibility, then it should be compared against the retrofitting option such as conventional, FRP, or FRCM materials.

Structural Retrofitting

This alternative determines whether to use conventional method, FRP, or FRCM materials to retrofit the structure. URM buildings located in regions susceptible to potential earthquake or high wind pressures may need to be retrofitted. In those areas, the expected cost of not retrofitting an URM building could be extensive.

Comparison of Alternatives

In this section a method to analyze the alternatives dealing with the reconstruction and retrofitting of masonry members is presented. It is based on comparisons that include both direct and indirect costs. These comparisons also include up-front costs as well as follow-on costs and are consistent with a life-cycle cost (LCC) approach. LCC is useful method to make effective decision in the projects considering the maintenance costs and expected life of the structure. The procedure of the life-cycle cost method for building economics is performed according to ASTM E917.

The reality of retrofitting operations is that the costs and benefits of any of these alternatives change significantly. Consequently, it is not possible to determine exact costs for any of the activities being considered. Appropriate estimates must take into account the specific conditions for each case. However, general guidelines can be provided to allow a comparison between different cases.

Direct Costs

The direct costs include the initial costs related to the design process, material used and, construction activities. The direct costs also include maintenance costs.

1. ***Design***: A thorough assessment of a masonry wall and adjacent regions before retrofitting is extremely important before deciding an appropriate method. The reconstruction alternative will represent the most economic alternative since new and different design ideas are not considered. Design is the engineering process conducted to determine the strengthening strategy.

- Masonry typology: Construction practices vary from region to region. Furthermore, masonry typologies vary by years. For instance, masonry construction practices are different in the Western and the Eastern regions of the United States. Similarly current practices are different than they were 30 years ago. This is due to loading requirements (wind and earthquake), construction practices, and material availability. As a consequence different kind of masonry typologies can be observed. These differences include masonry units (e.g. clay bricks, concrete blocks, and tuff stone), type of mortar, and wall arrangement (number of wythes).

- Seismic requirements: In the Western region, especially in California, seismic criteria prevail when developing a strengthening strategy. The use of conventional materials to retrofit an URM walls in a building can increase the mass. As a

consequence larger seismic forces will be attracted which can have effects on the overall structural systems (i.e. beams, slabs, columns, and foundation). Due to their reduced thickness and light weight, the use of FRCM or FRP in terms of laminates and rods has the advantage of not increasing significantly the building mass as other strengthening methods.

- Environment: Since masonry walls are subjected to water infiltration from rain, conventional reinforcing materials such as steel can be corroded. In contrast, FRCM or FRP composites are non-corrosive and can be used in harsh environments.

2. ***Material***: FRP or FRCM materials are generally more expensive than traditional materials used for retrofitting. Materials used for wall reconstruction include masonry units (bricks or blocks), mortar and steel rebars. Therefore, reconstruction sometimes offers the lowest cost of all the alternatives.

3. ***Construction***: Cost estimates and schedules of potential strengthening strategies should be analyzed. In general, labor is the most important factor that influence significantly to the total cost; therefore, considerable use of labor have a cost disadvantage. FRP retrofit system requires large amount of surface preparation prior to installation that increase the labor cost considerably. However, application of FRCM system does not need any surface preparation; therefore, the project's duration is much shorter and labor cost is much less than FRP case.

4. ***Maintenance and Repair***: The maintenance of a new wall and a wall retrofitted with FRCM or FRP materials exhibit the lowest costs. Traditional strengthening methods may need larger maintenance efforts, which can slightly lead to increasing future costs. Some of these methods involve the use of steel plates, which can be subject to corrosion. In addition, since FRP system using epoxy does not have resistance to heat; therefore, application of this material under high amount of temperature can be hazardous.

Indirect Costs

The indirect costs are those that are harder to identify and quantify. They are related to aesthetics, occupants' relocation and loss of business.

1. ***Aesthetics***: In some special cases, it is crucial that the retrofit project should be carried out with the least possible irrevocable alteration to the building's appearance. Many URM buildings are part of the cultural heritage of the city or country. Therefore, to preserve their aesthetic and architecture is critical. Since the use of external reinforcing overlays of steel or FRP/FRCM can change the aesthetics of masonry, "FRP structural repointing" can be a valuable alternative. Since the reinforcing rods are placed in the mortar joints, this method has the advantage of maintaining the original appearance of the masonry surface.

2. ***Occupants Relocation:*** Retrofitting involves some disruption activities to the building occupants. Conventional strengthening may require the use of relatively heavy equipment such as welding machines, saws, etc, which can produce dust

and noise which disrupt the normal activities for the building occupants. Also, for FRP strengthening method, surface preparation is required prior to the FRP installation which can be also disruptive. However, retrofitting with FRCM significantly lessen these effects.

3. ***Lost Business***: During the retrofit work, shutdown of the building operations should be considered.

SUMMARY

A method to analyze reconstruction and retrofitting alternatives is based on comparison of direct and indirect costs that include up-front and follow-on costs.

The most important characteristic in the retrofit work influencing the cost is the labor and shutdown costs as opposed to material costs and long-term durability. Advantages of FRCM composites versus conventional materials and FRP for strengthening of structural elements include lower installation costs and improved corrosion resistance. In addition, disturbance to the occupants of the facility being retrofitted is minimized.

It should be recognized that each retrofitting project is unique, and depending on the project's characteristics. However, the use of FRCM materials can offer a significant total cost reduction.